Characterisation and Role of Sugarcane Invertase with Special Reference to Neutral Invertase

by

Darren James Vorster

Submitted in fulfilment of the academic
requirements for the degree of

Doctor of Philosophy

in the
School of Life and Environmental Sciences
University of Natal, Durban
South Africa
November 2000

Abstract

The relationship between extractable invertase activities and sucrose accumulation in the sugarcane (*Saccharum* spp. hybrids) culm and *in vivo* invertase mediated sucrose hydrolysis was investigated to determine the significance of invertases in sucrose utilisation and turnover. *In vitro* activities were determined by assaying the soluble acid invertase (SAI), cell wall bound acid invertase (CWA) and neutral invertase (NI) from internodes three to ten in mature sugarcane plants of cultivar NCo376. Extractable activities were verified by immunoblotting. *In vivo* invertase mediated sucrose hydrolysis was investigated in tissue discs prepared from mature culm tissue of the same cultivar. Sugarcane NI had a higher specific activity than SAI (apoplastic and vacuolar) in the sucrose accumulating region of the sugarcane culm. CWA was also present in significant quantities in both immature and mature tissue.

Sugarcane NI was partially purified from mature sugarcane culm tissue to remove any potential competing activity. The enzyme is non-glycosylated and exhibits catalytic activity as a monomer, dimer and tetramer. Most of the activity elutes as a monomer of native M_r *ca* 60 kDa. The enzyme displays typical hyperbolic saturation kinetics for sucrose hydrolysis. It has a K_m of 9.8 mM for sucrose and a pH optimum of 7.2. An Arrhenius plot shows the energy of activation of the enzyme for sucrose to be 62.5 $kJ.mol^{-1}$ below 30°C and -11.6 $kJ.mol^{-1}$ above 30°C. Sugarcane NI is inhibited by its products, with fructose being a more effective inhibitor than glucose. Sugarcane NI is significantly inhibited by $HgCl_2$, $AgNO_3$, $ZnCl_2$, $CuSO_4$ and $CoCl_2$ but not by $CaCl_2$, $MgCl_2$ or $MnCl_2$. Sugarcane NI showed no significant hydrolysis of cellobiose or trehalose.

When radiolabelled fructose was fed to sugarcane internodal tissue, label appeared in glucose which demonstrates that invertase mediated hydrolysis of sucrose occurs. A combination of continuous feeding and pulse chase

experiments was used to investigate the *in vivo* contribution of the invertases and the compartmentation of sugars.

Sucrose is synthesised at a rate greater than the rate of breakdown at all stages of maturity in sugarcane culm tissue. The turnover time of the total cytosolic label pool is longer for internode three than internode six. A higher vacuolar:cytosolic sugar molar ratio than previously assumed is indicated. Developmentally, the greatest change in carbon allocation occurs from internodes three to six. The main competing pools are the insoluble and neutral fractions. As the tissue matures, less carbon is allocated to the insoluble and more to the neutral fraction. The neutral fraction consists mainly of sucrose, glucose and fructose.

The compartmented nature of sugarcane storage parenchyma carbohydrate metabolism results in a system that is complex and difficult to investigate. A computer based metabolic flux model was developed to aid in the interpretation of timecourse labelling studies. A significant obstacle was the global optimization of the model, while maintaining physiologically meaningful flux parameters. Once the vacuolar:cytosolic molar ratio was increased, the model was able to describe the internode three and six labelling profiles. The model results were in agreement with experimental observation. An increase in the rate of sucrose accumulation was observed with tissue maturation.

Only the internode three glucokinase activity was greater than the experimentally determined limit. The rate was however physiologically feasible and may reflect the underestimation of the *in vivo* rate. SAI and NI contributed to sucrose hydrolysis in internode three but not in internode six. The rates in internode six were set to fixed low values to enable the model to fit the experimental data. This does not however preclude low levels of *in vivo* SAI and NI activity, which would prove significant over a longer time period. The flow of label through the individual pools, which comprise the experimentally measured composite pools could be observed. This provides insight into the sucrose moiety label ratio, SPS:SuSy sucrose synthesis ratio, and the rate of $^{14}CO_2$ release. The model provides a framework for the investigation and interpretation of timecourse labelling studies of sugarcane storage parenchyma.

Preface

The experimental work described in this thesis was supervised primarily by Professor FC Botha and Dr B Huckett. Research was conducted in the Biotechnology Department at the South African Sugar Association Experiment Station (SASEX) and the Institute for Plant Biotechnology, University of Stellenbosch, South Africa

The results presented are original and have not been submitted in any form to another University. Where use was made of the work of others, it is duly acknowledged in the text.

Acknowledgements

The support of my supervisors, Professor FC Botha and Dr B Huckett is gratefully acknowledged. Their guidance, encouragement and understanding is much appreciated.

Thank you to SASEX, directed by Dr PH Hewitt, for financial support in the form of a SASA bursary and for the facilities in which the majority of the research was conducted.

I thank the Foundation for Research and Development (FRD) for financial support in the form of a bursary.

Thank you to Dr. Kenneth Holmström, Research Director, Applied Optimization and Modelling (TOM), Center for Mathematical Modelling (CMM), Dept of Mathematics and Physics (IMa), Malardalen University, Vasteras, Sweden. The advice on the model optimization and the use of the algorithm 'DIRECT' implemented in gclsolve.m was invaluable.

Thanks to Dr H. Murrell of the University of Natal, Computer Science Department and Prof. V. Bajik of the Natal Technikon, Electronic Engineering Department, for valuable initial discussions regarding the flux model implementation.

The polyclonal antibodies were generous gifts from Dr H. Davies from the Scottish Crop Research Institute, Dundee, UK.

Thank you to Dr Derek Watt for valuable commentary on the thesis.

The support of colleagues in the Biotechnology Department during the course of this study.

Finally, thanks to my mother for her never ending and unconditional support.

List of Contents

List of Abbreviations

A	absorbance
ADP	adenosine 5'-diphosphate
AMP	adenosine 5'-monophosphate
Apo	apoplast
ATP	adenosine 5'-triphosphate
Bq	Becquerel
BSA	bovine serum albumin
CWA	cell wall bound acid invertase
Cyt	cytosol
Da	Dalton
DEAE	diethylaminoethyl
DTT	dithiothreitol
EDTA	ethylenediaminetetraacetic acid
Ext	external
f	flux
FBPase	Fru-1,6-bisphosphatase
Fru	fructose
Glc	glucose
HEPES	N-2-hydroxyethylpiperazine-N'-2-ethanesulfonic acid
HPLC	high performance liquid chromatography
Keq	equilibrium constant
Km	concentration of substrate that produces half maximal activity
NAD	oxidised nicotinamide-adenine dinucleotide (NAD^+)
NADH	reduced nicotinamide-adenine dinucleotide ($NAD+H^+$)
NI	neutral invertase
PAGE	polyacrylamide gel electrophoresis
PFK	ATP-dependent phosphofructokinase
PFP	PPi-dependent phosphofructokinase
PMSF	phenylmethylsulfonyl flouride

Ponceau-S	3-hydroxy-4-[2-sulfo 4-(4 sulfophenylazo) phenylazo]-2,7-napthalenedisulfonic acid
ppt.	precipitate
SAI	soluble acid invertase
s.d.	standard deviation
SDS	sodium dodecyl sulphate
SPP	sucrose phosphatase
SPS	sucrose phosphate synthase
SuSy	sucrose synthase
Suc	sucrose
Synth	synthesis
TBS	tris-buffered saline
TBST	tris-buffered saline containing Tween 20
TCA	tricarboxylic acid
TEMED	N,N,N',N'-tetramethylethylenediamine
Tris	2-amino-2-(hydroxymethyl)-1,3-propanediol
Tween 20	polyoxyethylene sorbitan monolaurate
UDP	uridine 5'-diphosphate
UDPGlc	uridine 5'-diphosphate Glc
Vac	vacuole
Vmax	maximum rate under substrate saturating conditions

List of Figures

List of Tables

Chapter 1

General Introduction

Sugarcane (*Saccharum spp. hybrids*) and sugar beet (*Beta vulgaris*) are the main commercial sources of sucrose for mankind. Sugarcane accounts for more than 60 percent of global sucrose production (Hawker, 1985). A total of 121 million tons of sucrose was consumed in 1996/1997 of which 87 million tons was consumed in the countries in which it was produced (Anon, 1998). Sucrose forms a large part of the energy intake of humans. In developing countries up to 40% and globally 10% of the total food energy requirement of the human population is provided in the form of sucrose (Anon, 1998). The need for a cheap energy rich foodstuff in developing countries is reflected by the high percentage intake of sucrose.

South Africa ranks as the 13th largest sugar producer out of 121 countries and the 10th highest exporter of sucrose. The South African sugar industry produced 2.4 million tons of sucrose in the 1997/1998 season with a total of 131 000 employees in the growing and milling sectors combined (Anon, 1998). Sugarcane is a crop characterised by an unusually high efficiency of product yield relative to other commercially important crops. A yield plateau has been reached in sugarcane sucrose production due to the successful exploitation of the sugarcane gene pool (Anon, 1998). The development of sugarcane biotechnology is an option that will provide an increase in yield that may not be possible using conventional approaches. Due to the importance and volume of sucrose produced, even a small gain in the efficiency of this crop will result in large gains in revenue.

Sugarcane sucrose metabolism has been an active area of research since the mid 1950s. This long history is reflected in the large body of literature on this topic relative to other commercial crops (for review see Moore, 1995). Hatch and co-workers made early inroads into the understanding of sugarcane sucrose

metabolism in the 1960s. This resulted in a model of sucrose accumulation in sugarcane (Hawker, 1972) that was thought to represent a clear understanding of the mechanisms by which sugarcane accumulated sucrose. Although the major pathways had been described, more recent investigations have revealed weaknesses in the model (for review see Moore, 1995). A simple schematic representation of sucrose transport and metabolism in sugarcane storage parenchyma is depicted in Fig. 1.1.

Sucrose is a non-reducing disaccharide and is the product of photosynthetic activity in plants. It is the main form of photosynthate transported from the leaves to the storage tissue of most plants. Many reasons for its ubiquitous presence have been postulated (Hawker, 1985). In sugarcane, the photosynthate is stored as sucrose, unlike many other plants, which store carbohydrate as starch. In plants, there are two routes for sucrose synthesis and two for sucrose breakdown (Fig. 1.2). Three enzymes are involved in sucrose synthesis in plants: sucrose phosphate synthase (SPS, EC 2.4.1.14), sucrose phosphatase (SPP, EC 3.1.3.24) and sucrose synthase (SuSy, EC 2.4.1.13). Sucrose is cleaved in a reversible reaction by SuSy or hydrolysed in an irreversible reaction by invertase (EC 3.2.1.26).

One area of potential significance in the sugarcane sucrose accumulation model is that of a substrate or 'futile' cycle between sucrose and the hexose phosphates. This cycle was described in the early literature by Sacher *et al.* (1963a). The rate of sucrose accumulation is currently thought to be the result of the difference between the rate of sucrose synthesis and sucrose degradation (Wendler *et al.*, 1990; Veith and Komor, 1993; Komor, 1994; Zhu *et al.*, 1997). Evidence for this has come from work on cell suspension cultures (Wendler, 1990) and tissue disc labelling (Komor, 1994). The possible function of such energy wasting cycles has been discussed (Fell, 1997).

The levels of sucrose degrading enzymes such as the invertases and SuSy have been the focus of a number of studies in sugarcane (for review see Moore, 1995). They form an integral part of the potential 'futile' cycle in sugarcane culm tissue (Fig. 1.2). The determination of the levels of invertases in conjunction with the

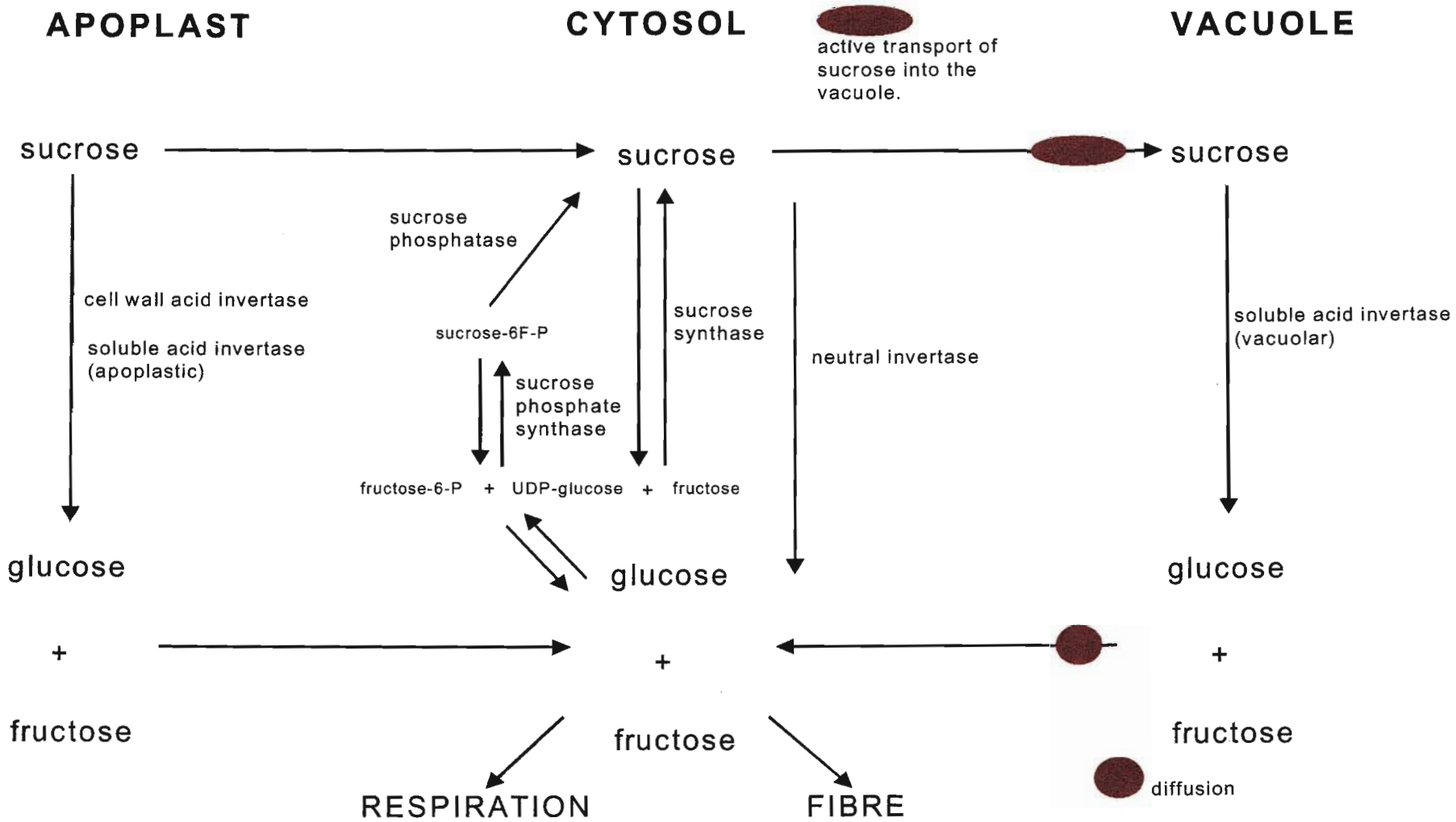

Figure 1.1. Sucrose transport and allocation in sugarcane culm storage parenchyma

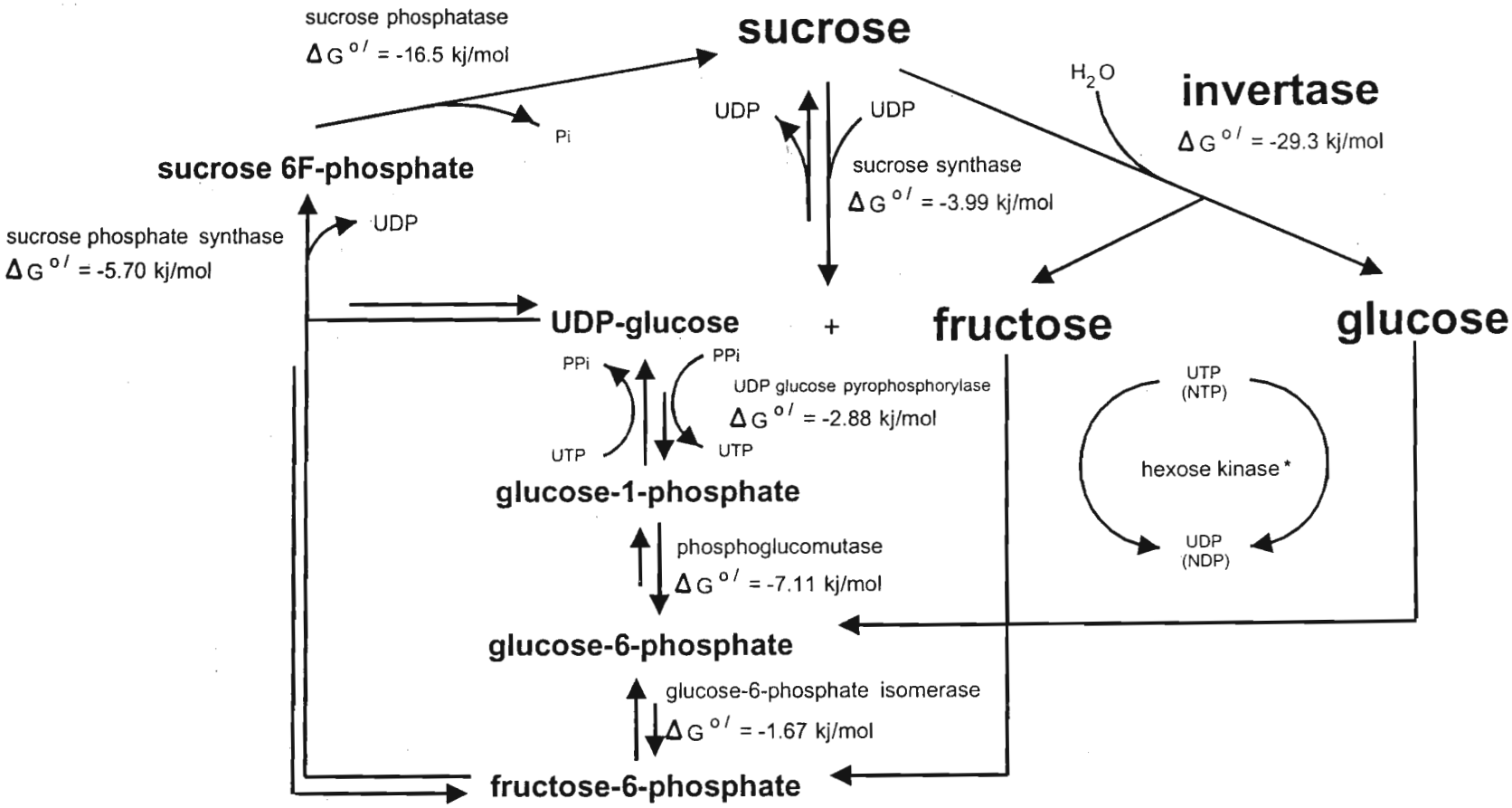

Figure 1.2. Sucrose synthesis and breakdown.

measurement of *in vivo* sucrose hydrolysis will provide information on the cycle and how it changes with invertase levels and maturation of the sugarcane culm.

The acid invertases have been the focus of many studies while NI has been neglected by biochemists (Avigad, 1982; Hawker, 1985). NI has been the focus of a number of recent investigations (Chen and Black, 1992; Van den Ende and Van Laere, 1995; Ross *et al.*, 1996; Lee and Sturm, 1996; Asthir and Singh, 1997). The kinetic properties of sugarcane NI have been investigated (Hatch *et al.*, 1963; del Rosario and Santisopasri, 1977). However, a detailed study of the enzymes kinetic properties, especially with respect to regulation of the enzyme's activity has not been performed. The *in vitro* kinetic properties of enzymes give insight into their *in vivo* roles and behaviour. Sugarcane NI is an enzyme commonly associated with mature sugarcane culm tissue (Moore, 1995). This would place the enzyme in substrate saturating conditions. Is the enzyme regulated by some fine or coarse control? A more comprehensive understanding of the properties of sugarcane NI will further the understanding of sugarcane sucrose metabolism.

Tracer based studies led to much of the early understanding of sugarcane sucrose storage parenchyma metabolism (for review see Gayler, 1972). Subsequent studies have confirmed these findings and led to the re-evaluation of aspects of the sucrose model (for review see Moore, 1995). Investigations of sugar compartmentation and sucrose breakdown have used traditional approaches. The development of a computer based flux model of sugarcane sucrose metabolism may provide insight into metabolic compartmentation and *in vivo* flux.

In order to understand the role of invertases in the sugarcane culm this study has focused on: the distribution of invertases in the culm, the characterisation of NI, sugar compartmentation and the *in vivo* flux of sucrose synthesis and breakdown in sugarcane sucrose metabolism. The change in total enzyme activities with tissue maturation can give insight into the role of the enzymes being investigated. Therefore, the distribution of invertases in the sugarcane culm is investigated in chapter three. Knowledge of the kinetic properties of the enzymes involved in

sucrose synthesis and breakdown in sugarcane is essential to the understanding of the control of this process. The lack of information on the kinetic properties of sugarcane NI led to the investigation presented in chapter four. The maximum extractable activities and *in vitro* properties of the enzymes provide valuable information. However, a complete understanding of the system is not possible with this information alone. Sucrose is the substrate and the hexoses glucose and fructose are the products of the invertases. NI is shown to be subject to product inhibition in chapter four. Knowledge on the distribution of these sugars between the cytosol and vacuole of sugarcane culm cells will provide information for: the interpretation of total enzyme activities; the significance of the kinetic properties of the invertases; and, the calculation of fluxes involving sucrose, glucose and fructose. The compartmentation of sucrose and the hexoses is investigated in chapter five. The estimation of *in vivo* metabolic flux is a vital component in understanding the role of enzymes in the system. Estimation of metabolic flux in sugarcane has been based on conventional approaches (Komor, 1994; Whittaker and Botha, 1997). In chapter five, the sucrose metabolism of sugarcane tissue disc labelling experiments is investigated using conventional approaches. In chapter six, a metabolic flux model is developed for the investigation of flux and compartmentation in the system. The approach adopted is to globally optimize the model to find the feasible flux parameters that best describe the timecourse labelling data. This requires the implementation of constraints to dependant and independent parameters. The optimization results will aid in validation and understanding of current observations and will provide information for the metabolic engineering of sugarcane. The determination of metabolic flux is also important for the validation of kinetic models designed to understand and predict the behaviour of the metabolic system. Particular emphasis is given to sucrose synthesis and breakdown.

Chapter 2

Literature Review

This chapter is divided into three major topics of review. Sucrose metabolism, which focuses on routes of sucrose synthesis and degradation in higher plants and more specifically sugarcane. Current understanding of the role of the invertases in higher plants, especially NI is reviewed. Approaches to the determination of metabolic flux, with emphasis on the application to plant metabolism are reviewed.

2.1 Sucrose Metabolism

2.1.1 Sucrose

Most of the carbon produced in photosynthesis is channelled into sucrose. Sucrose serves as the major form of carbon translocation from source to sink organs and is used in some plants as a means of storing energy, as is the case in sugarcane. Sucrose is a non-reducing disaccharide of (1→2) linked α-D-glucopyranose and β-D-fructofuranose. The significance of the non-reducing nature of sucrose is evident when one considers the role of trehalose in fungi and insects. Trehalose is also a non-reducing disaccharide, which finds a role in fungi and insects similar to the role of sucrose in plants (Hawker, 1985). As a non-reducing molecule it is relatively inert and does not interact with other functional groups encountered in the cell. It is a highly soluble sugar that can reach high concentrations in the cell without significant effects on biochemical reactions. As a neutral molecule it will not interact electrostatically with other charged molecules in the cell and it can be transported across biological membranes. Sucrose can therefore be used to regulate osmotic pressure and the flow of water

between cellular compartments. Sucrose can also be viewed as an unreactive derivative of glucose, protecting it from the action of enzymes that catalyse its metabolism (Hawker, 1985). It is used as a temporary storage carbohydrate in the cytosol and can be moved to the vacuole where it is separated from the metabolic machinery that would facilitate a cycle of degradation and synthesis. The major role of sucrose in most plants is as a temporary storage product in leaves and as a translocation medium of carbon. Starch, as a long term storage carbohydrate in plants is more widespread, the success of plants that store sucrose is largely due to the effects of man. The high sucrose content of sugarcane is an example of how human selective pressures may influence the form of carbohydrate stored by a plant. Due the usefulness of sucrose as a foodstuff and its industrial and technological applications it will remain an important agricultural product.

2.1.2 Sucrose Synthesis and Degradation

Sucrose synthesis and degradation has been comprehensively reviewed (Avigad, 1982; Hawker, 1985; Hawker *et al.*, 1991). Sucrose is synthesised via two pathways, namely: SPS (E.C. 2.4.1.14) coupled with SPP (E.C. 3.1.3.24) and by SuSy (E.C. 2.4.1.13) (Kruger, 1997). The first identification of SPS and SPP was in wheat germ (Leloir and Cardini, 1955). Technical difficulties with stability and assaying SPS resulted in few early detailed studies. Both SPS and SPP have been identified in many different source and sink tissues (for review, see Avigad, 1982). The enzyme shows high specificity for its substrates UDP-Glc and Fru-6-phosphate and is activated by Glc-6-phosphate and inhibited by inorganic monophosphate (Doehlert and Huber, 1983). SPS is considered to be the main sucrose producing enzyme (Akazawa and Okamoto, 1980). The structure and properties of SPS have recently been reviewed (Salvucci *et al.*, 1995). The regulatory properties are also dependent on the phosphorylation status of the enzyme. The reaction catalysed by SPS in which sucrose 6^F-phosphate and UDP are formed from UDP-Glc and Fru 6-phosphate has a standard Gibbs free energy of -5.70 $kJ.mol^{-1}$ (Kruger, 1997). This indicates a reaction that is reversible. However, when coupled with the reaction catalysed by SPP, sucrose synthesis via this pathway becomes irreversible.

SPP catalyses the irreversible conversion of sucrose 6^F-phosphate to sucrose and monophosphate. The reaction has a standard Gibbs free energy of -16.5 $kJ.mol^{-1}$, indicating a largely irreversible reaction (Kruger, 1997). SPP has been shown to occur in a wide variety of plants and tissues (Hawker and Smith, 1984). Detailed information on SPP has mainly come from non-photosynthetic tissues (Hawker, 1966; Hawker and Hatch, 1966; Hawker, 1967; Hawker *et al.*, 1987) and more recently from rice (*Oryza sativa*) leaves (Echeverria and Salerno, 1994). The enzyme has a pH optimum near neutrality and a requirement for Mg^{2+}. It also shows sensitivity to sucrose at concentrations of 100 mM (Hawker, 1966; Hawker and Hatch, 1966).

SuSy is a cytosolic enzyme that synthesises sucrose from UDP-Glc and fructose and also cleaves sucrose to form UDP-Glc and fructose (Kruger, 1997). The standard Gibbs free energy of -3.99 $kJ.mol^{-1}$ indicates a largely reversible reaction in favour of sucrose breakdown. The reversibility of the reaction and the relatively high Km for sucrose indicates that the enzyme will only cleave sucrose in sucrose storing tissues, although it may also synthesise sucrose. Isozymes of SuSy have been investigated and characterised in sugarcane (Buczynski *et al.*, 1993).

Sucrose is hydrolysed by dilute acids but is relatively stable in the presence of alkalis. The acid hydrolysis of sucrose has been shown to be a physiological mechanism for sucrose breakdown (Echeverria and Burns, 1989). Enzymatic hydrolysis of sucrose is catalysed by a number of enzymes in various compartments. Sucrose is hydrolysed by the invertases (β-fructofuranosidase) in plants and fungi or sucrases (α-glucosidase) in insects and mammals to produce glucose and fructose (Hawker, 1985). The invertases are classified by their pH optimum and localisation, occurring in the vacuole, cytoplasm and apoplast of plant tissue. The hydrolysis of sucrose by invertase is an irreversible reaction as indicated by the standard Gibbs free energy of -29.3 $kJ.mol^{-1}$.

2.1.3 Sugarcane Sucrose Metabolism

Conventional plant breeding has not resulted in a significant increase in the net photosynthetic rate per unit leaf area of sugarcane (Gifford. *et al.* 1984). Increases in yield have been achieved by the selection for changes in the carbon allocation towards sucrose (Gifford *et al.*, 1984). Sucrose accumulation for sugarcane has been reviewed by Glasziou and Gayler (1972) and Moore (1995). Particular emphasis will be placed on sucrose accumulation in the metabolic and storage compartments of the sugarcane culm cells and the sugar accumulation cycle where most of the changes in carbon allocation occur.

The earliest work presented on the accumulation and transformation of sugars in the sugarcane culm was by Hartt (1943) and then Glasziou (1960). The work of Glasziou and co-workers in the 1960's led to the development of a general model of sucrose accumulation as described by Sacher and co-workers (1963a) and in the review of Glasziou and Gayler (1972). The initial work of Glasziou (1960) produced a number of observations. A number of criteria were recognised as being necessary for a working hypothesis to be formulated for glucose, fructose and sucrose accumulation in sugarcane: (a), sugar accumulation is an energy requiring process; (b), ^{14}C supplied as CO_2, glucose or sucrose is mainly accumulated as sucrose, furthermore the fructose moiety of sucrose becomes labelled from supplied ^{14}C-Glucose; (c), glucose is taken up at a much higher rate than sucrose; (d), net movement of sugar into the inner space is determined by both influx and efflux; and (e), net rate of loss of sucrose may be independent of the inner space sucrose concentration. Evidence from (b) indicates that sucrose is not synthesised in the inner space. It was postulated that sugars were activated to form sugar-X prior to combination with a carrier for transfer to the inner space. Inversion of sucrose in the inner space was later shown to be due to invertase (Glasziou, 1962).

Three studies focussing on sugarcane sucrose metabolism led to the formulation of a preliminary model of sucrose accumulation in sugarcane (Sacher *et al.*, 1963a). The model described by Sacher and co-workers (1963a) (Fig. 2.1) is an

extension of that proposed by Glasziou (1961). Subsequently Hatch and co-workers (1963) studied the enzymes of the sucrose accumulation cycle. They could not demonstrate the presence of a sucrose phosphorylase, which would lead to the derivative sucrose-X. However they did find that some storage tissue extracts converted UDP-Glc and Fru-6-phosphate to a molecule exhibiting the properties of sucrose phosphate. Hatch and co-workers (1963) isolated and studied the enzymes believed to be involved in the cyclic process of sugar accumulation in sugarcane. Enzymes included were those involved in the synthesis, interconversion, and breakdown of hexose phosphates. Two soluble invertases, one with a pH optimum between 5.0 and 5.5, and the other with a pH optimum of 7.0 were identified. Acid invertase was shown to exhibit seasonal variation with rainfall and temperature.

The study by Hatch and Glasziou (1963) focused on further investigating the observation of seasonal variation of acid invertase in sugarcane and the differences in the levels of invertases between varieties of varying sucrose accumulating capacity. Acid invertase levels were shown to be positively correlated with the rate of elongation of the internode, whether the independent variable was age, temperature or water regime. NI activity positively correlated with sugar levels when the independent variable was tissue maturity or temperature. It was postulated that NI regulated the movement of sucrose from vascular tissue to the storage tissue. Growth and storage sugar were demonstrated to be reciprocally related. It was noted that the hybrid variety used, contained an acid invertase in the immature tissue that diminished in activity with tissue maturation, and a NI that was absent in immature tissue and increased in activity with tissue maturation.

Sacher and co-workers (1963a) proposed a model for the sugar accumulation cycle in sugarcane. It was recognised that three distinct compartments existed, namely the storage compartment (vacuole), metabolic compartment (cytoplasm) and the outer space, which included the cell wall. The outer space was in rapid equilibrium with the bathing solution. The metabolic compartment is the region in which sucrose-X is synthesised.

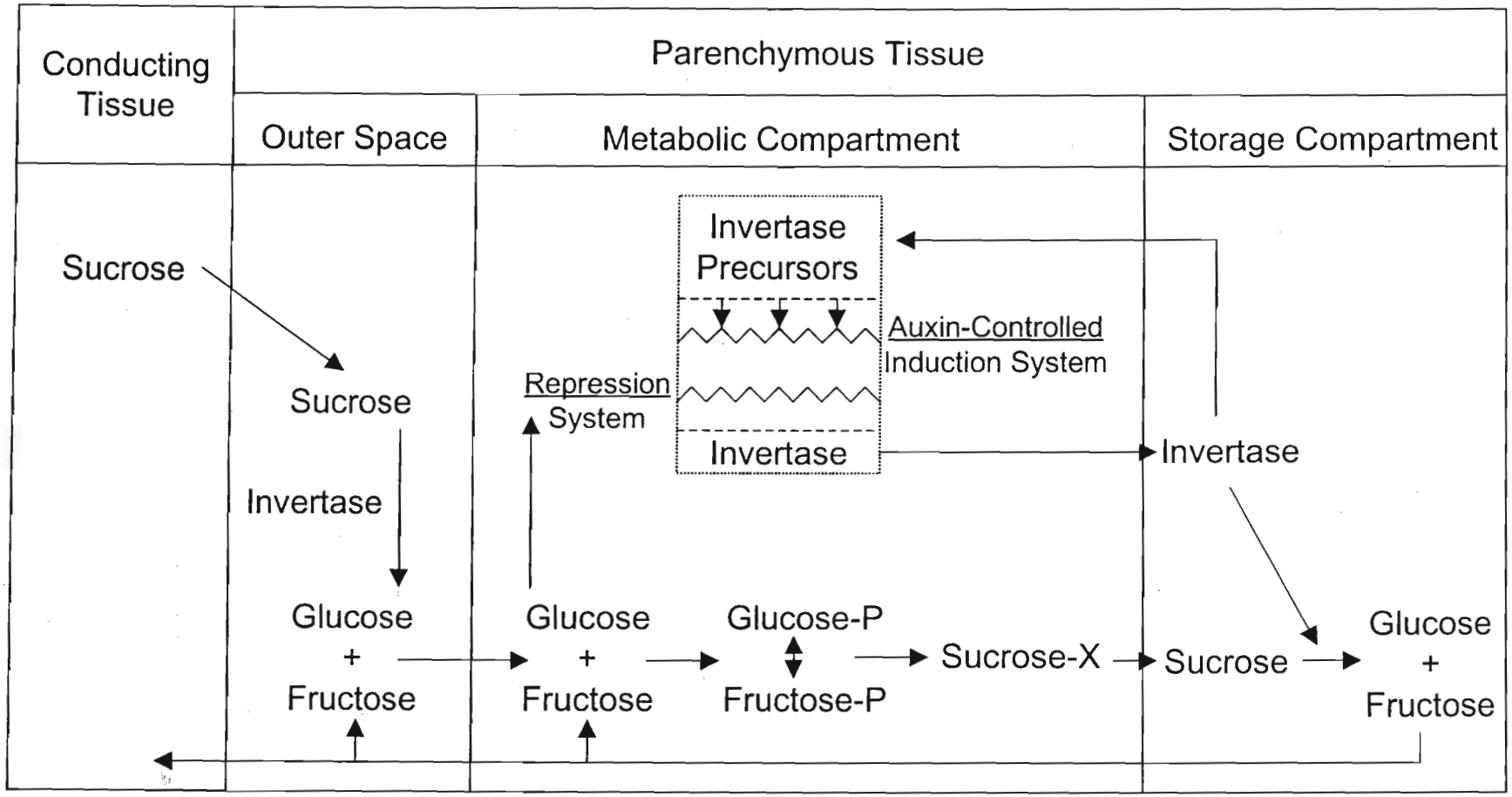

Figure 2.1. Schematic representation of the sugar accumulation cycle in sugar cane storage tissue as illustrated by Sacher et al. (1963a)

The storage compartment is the region in which sucrose, glucose and fructose accumulate. Sucrose is virtually the sole sugar transferred to the storage compartment. All sugars diffuse slowly from the storage compartment with the hexoses diffusing more rapidly than sucrose. Inversion of sucrose prior to uptake was seen as an integral step in the uptake of sugars. Outer space invertase was recognised as a part of the total acid invertase, which also exists in the vacuole. It was recognised that the regulation of invertase levels was controlled by an auxin-carbohydrate mediated system (Sacher and Glasziou, 1962). The storage compartment invertase was proposed to have a role of controlling the rate of return of carbohydrate from the storage compartment. The rapid adjustments observed in invertase levels further supported this hypothesis (Hatch and Glasziou, 1963).

The review of Glasziou and Gayler (1972) summarised the findings reviewed above and information from subsequent studies. This included significant information related to the metabolic and storage compartments. Hatch (1964) described sucrose synthesis in the metabolic compartment in more detail, investigating an irreversible UDP-Glc-Fru-6-phosphate transcosylase (SPS). The hexose phosphates were proposed to be in equilibrium with each other and UDP-Glc. Sucrose-X was also replaced with sucrose phosphate, synthesised from Fru-6-phosphate and UDP-Glc. The importance of SPS in sugarcane sucrose metabolism was first recognised by Hatch (1964). Difficulties in assaying the enzyme at that time precluded further investigation. It was also proposed by Hatch (1964) that a UDP-Glc-Fru transcosylase activity (SuSy) detected by Hatch and co-workers (1963) could mediate sucrose breakdown in sugarcane. A specific SPP was found to be present in sugarcane by Hawker (1966; 1967). SuSy was shown to be mainly associated with immature (Hatch *et al.*, 1963; Slack, 1966) and mature (Hawker and Hatch, 1965) storage tissue vascular strands. This led Glasziou and Gayler (1972) to postulate that SuSy would not play a significant role in sucrose breakdown, especially due to the presence of a specific uridine diphosphatase (Hatch, 1963). Hydrolysis of sucrose phosphate was seen to be associated with transfer of sucrose into the vacuole with cytoplasmic sucrose levels influencing the rate of transfer. Inversion of sucrose in the vacuole was known to be mediated by vacuolar acid invertase (Glasziou,

1962; Sacher *et al.*, 1963a). The enzyme was found to be present in high levels in expanding cells in young internodes and then activity disappeared in the older elongated cells (Slack, 1965).

The physiological functions of AI and NI were investigated by Gayler and Glasziou (1972a). Both vacuolar acid invertase and outer space acid invertase were shown to be positively correlated with cell extension and growth rate. NI was shown to be positively correlated with hexose content while acid invertase was not. These findings in combination with previous evidence led to the development of a hydrodynamic simulation model for the explanation of the relationship between internode extension and invertase levels. A further model was proposed for the regulation of sugar flow during internode extension.

The cyclic accumulation of sucrose in sugarcane was subsequently re-addressed and revised, using a different experimental system, in the from of sugarcane suspension cells (Wendler *et al.*, 1990). Sucrose synthesis was shown to exceed net storage indicating the presence of a cycle of simultaneous rapid synthesis and breakdown of sucrose. Shifts in carbon allocation between net storage and mobilisation of sucrose were interpreted as reflecting changes in the relative rates of sucrose synthesis and degradation. The role of SPS in sucrose synthesis was also confirmed (Wendler *et al.*, 1990). The levels of SPS activity were shown to be much greater than the rate of sucrose synthesis (Wendler *et al.*, 1990; Goldner *et al.*, 1991). The model of sucrose turnover regulating sucrose storage has recently been supported (Komor, 1996). Relative rates of sucrose synthesis and breakdown are shown to vary with sugarcane storage parenchyma maturation. A decrease in the rate of sucrose cycling coincides with an increase in allocation of carbon to sucrose. Similarly, an increased allocation of carbon to sucrose synthesis at the expense of respiration and insoluble matter synthesis has been shown to occur (Botha *et al.*, 1996). The net rate of respiration exceeds that of sucrose storage (Botha *et al.*, 1996; Komor, 1996).

Sugar uptake studies on sugarcane had been conducted as part of some of the first studies (Bielski, 1962). That report demonstrated the uptake of sucrose and both glucose and fructose. Later, it was shown that sucrose was inverted prior to

uptake (Sacher *et al.*, 1963a). Support for that observation was given by Hatch and Glasziou (1964). Later investigations by Bowen (1972) and Bowen and Hunter (1972) on sugarcane culm tissue discs produced more detailed kinetics on sugar uptake for sucrose, glucose and fructose which further supported the observation that sucrose inversion was a prerequisite for sugar uptake. Work on sugarcane suspension cells by Maretzki and Thom (1972a) demonstrated the presence of transport systems for glucose and fructose but not sucrose. Further work indicated that there are two transport systems for glucose. In the review of Glasziou and Gayler (1972) this was however debated as having insufficient evidence to support the hypothesis. Gayler and Glasziou (1972b) conducted a detailed investigation of sugar uptake using the synthetic analogue 3-O-methyl glucose. They concluded that the 3-O-methyl glucose was accumulated by an energy dependent carrier mediated system that could accumulate sugars against a concentration gradient. This appeared to be the rate limiting reaction for glucose uptake and not an enzyme involved in sucrose synthesis (Gayler and Glasziou, 1972b). The prerequisite of sucrose hydrolysis for sugar uptake by sugarcane tissue discs has subsequently been shown to be in error (Lingle, 1989; Thom and Maretzki, 1992). A very low amount of randomisation of asymmetrically labelled sucrose taken up by tissue discs (Lingle, 1989) indicated that inversion prior to uptake did not occur. Furthermore, a synthetic analogue of sucrose that is not cleaved by invertase was taken up in experiments by Thom and Maretzki (1992). The use of an iso-osmotic washing buffer is proposed as the reason for the different behaviour of the tissue discs. Previously tissue discs washed in tap water (Sacher *et al.*, 1963a) could have inactivated the sucrose transporter due to osmotic effects.

Symplastic transport of sucrose via plasmodesmata has been shown to probably increase with tissue maturation as cell walls lignify and suberisation occurs between vascular bundles and the storage parenchyma (Jacobsen *et al.*, 1992). Similarly Welbaum *et al.* (1992) proposed that sucrose enters storage parenchyma cells via plasmodesmata and is extruded to the apoplast. The apoplast contains sugar levels comparable to that of the symplast (Hawker, 1965; Welbaum and Meinzer, 1990). The findings of Walsh *et al.* (1996) indicate that sucrose unloaded from the phloem passes through a fibre sheath into the storage

parenchyma cells, which are connected by plasmodesmata. The direct import of sucrose indicates that both SuSy and NI may play a significant role in sucrose turnover. Significant levels of NI (Lingle and Smith, 1991; Singh and Kanwar, 1991; Venkataramana and Naidu, 1993; Dendsay *et al.*, 1995; Botha *et al.*, 1996) and SuSy (Lingle and Smith, 1991; Buczynski *et al.*, 1993; Lingle and Irvine, 1994; Lingle 1996) are present in the cytosol of sugarcane storage parenchyma. A recent investigation by Lingle (1997) could not find a relationship between different ripening characteristics of sugarcane varieties and SuSy, NI or acid invertase. However Zhu *et al.* (1997) showed that there was a much higher correlation of the difference between acid invertase and SPS activity and sucrose accumulation than acid invertase activity alone. This was true for acid invertase activities below a critical threshold.

An important aspect of plant sucrose metabolism is the transport of sucrose across the tonoplast. The studies on the isolated vacuoles of sugarcane suspension cells (Thom *et al.*, 1982a; Thom *et al.*, 1982b) produced unacceptably low rates of sucrose uptake. The addition of ATP did not enhance uptake either (Thom and Maretzki, 1985). However, high rates of incorporation of UDP-Glc were observed and a UDP-Glc group translocation mechanism for sucrose transfer was proposed (Thom and Maretzki, 1985; Maretzki and Thom, 1986). The UDP-group translocator was later shown to be an artefact due to contamination of the vacuole preparations by plasma membranes (Preisser and Komor, 1988; Maretzki and Thom, 1988). A later investigation on vacuoles isolated by an osmotic and pH dependent lysis method displayed high rates of passive sucrose uptake but no accumulation was observed (Preisser and Komor, 1991). This led to a subsequent investigation of solute distribution between the cytosol and vacuole in which it was found that sucrose did not accumulate in the vacuole of suspension cell cultures (Preisser *et al.*, 1992). Current evidence indicates sucrose transport into the vacuole by facilitated diffusion (Presser and Komor, 1991). However, this may be true only for isolated vacuoles. For intact cells it is expected that an energy-based transport system would be required to accumulate sucrose in vacuoles (Moore, 1995).

The understanding of carbon partitioning in sugarcane culm tissue had been limited to that within the sugar pool, Whittaker and Botha (1997) investigated partitioning in more detail. That study indicated that with tissue maturation carbon is redirected from water-insoluble matter, respiration, amino acids, organic acids, and phosphorylated intermediates to sucrose synthesis. Substrate availability was identified as possibly being one of the prime factors leading to the observed decrease in respiration.

2.2 Invertase

Plant invertases (β-fructofuranosidase, E.C. 3.2.1.26) hydrolyse sucrose by an irreversible reaction into its component monosaccharides glucose and fructose with a standard Gibbs free energy of -29.3 $kJ.mol^{-1}$ (Kruger, 1997). Plant invertases are evolutionarily related to yeast and bacterial invertases (Sturm and Chrispeels, 1990), but have no link with animal cell enzymes. Three isoforms of invertase exist, they are classified by their pH optima and localisation, namely: wall-bound acid invertase, SAI and NI (Tymowska-Lalanne and Kreis, 1998). Plant invertases have been implicated in source/sink relationships, phloem loading/unloading, wound response, growth and developmental processes (Sturm, 1999; Sturm and Tang, 1999). However, the exact physiological roles of the plant invertases have not been elucidated. Invertases are often present as different isoenzymes with variable Km and inhibitor sensitivity. The subject of plant invertases has been reviewed (ap Rees, 1974; Sampietro, 1995; Tymowska-Lalanne and Kreis, 1998; Sturm, 1999). Invertases have ceased to be considered as 'boring enzymes' as both the substrate and product molecules of the primary reaction that they catalyse are nutrients and signal molecules (Weber and Roitsch, 2000).

2.2.1 Neutral Invertase

The least studied of the invertases is NI. Historically neutral and alkaline invertases have been afforded much less attention than the SAI (Avigad 1982,

Hawker 1985). The role of NI has been regarded as that of a maintenance enzyme providing substrate for the TCA cycle in tissues where SuSy and SAI levels are low (ap Rees, 1974). Invertases with a neutral or slightly alkaline pH optimum have been identified (Chen and Black, 1992; Van den Ende and Van Laere, 1995) and are referred to as NI. The cloning and characterisation of NI from *Lolium temulentum* L has lead to the proposal that the neutral/alkaline invertases represent more than one class of enzyme (Gallagher and Pollock, 1998). The cloning of carrot NI showed that the enzyme did not have any sequence similarity with the acid invertases (Sturm *et al.*, 1999). Unlike the *L. temulentum* clone, the carrot sequence did not code for any portion of the NDPNG pentapeptide sequence which is characteristic of acid invertases (Sturm and Chrispeels, 1990; Unger *et al.*, 1994).

The properties of NI have been studied at the enzyme level. NI has been purified to apparent electrophoretic homogeneity and characterised from various sources (Chen and Black, 1992; Van den Ende and Van Laere, 1995; Ross *et al.*, 1996; Lee and Sturm, 1996; Asthir and Singh, 1997). Studies on sugarcane NI utilised dialysed crude extracts (Hatch *et al.*, 1963) or activity eluted after $(NH_4)_2SO_4$ precipitation from sugarcane crusher juice and subsequent size exclusion chromatography (del Rosario and Santisopasri, 1977).

The pH optima of neutral and alkaline invertases purified from other sources vary from pH 6.8 to 8.0 (Chen and Black, 1992; Van den Ende and Van Laere, 1995; Ross *et al.*, 1996; Lee and Sturm, 1996; Asthir and Singh, 1997). Recombinant clones of NI also show maximal activity between pH 6.5 and 7.5 (Gallagher and Pollock, 1998; Sturm *et al.*, 1999). NI displays a monophasic pH profile (Hatch *et al.*, 1963). The near neutral pH optimum is interpreted as partial evidence for a cytosolic localisation of the enzyme (Chen and Black, 1992; Van den Ende and Van Laere, 1995; Ross *et al.*, 1996; Lee and Sturm, 1996).

The Km of sugarcane NI for sucrose has previously been reported to be 25 mM (Hatch *et al.*, 1963) and 0.32 mM (del Rosario and Santisopasri, 1977). Similar estimates to that of Hatch *et al.* have been obtained for other NI, ranging from 10 to 20 mM (Chen and Black, 1992; Van den Ende and Van Laere, 1995; Ross *et*

al., 1996; Lee and Sturm, 1996; Asthir and Singh, 1997). Two recombinant clones have a Km of 18 and 20 mM for sucrose (Gallagher and Pollock, 1998; Sturm *et al.*, 1999) which are similar to those reported for purified and partially purified NI. The temperature optimum found for carrot is 40°C (Lee and Sturm, 1996) and that of chickpea nodules (*Cicer arietinum* L.) is 37°C (Asthir and Singh, 1997).

A cycle of degradation and synthesis of sucrose has been found in sugarcane suspension cells (Wendler *et al.*, 1990) and in the immature sugarcane culm (Sacher *et al.*, 1963a). This may also be true for mature sugarcane culm tissue, which contains high levels of NI activity (Hatch and Glasziou, 1963; Gayler and Glasziou, 1972a; Batta and Singh, 1986; Lingle and Smith, 1991; Dendsay, *et al.*, 1995) and substrate saturating conditions based on sucrose concentrations in the sugarcane culm (Welbaum and Meinzer, 1990).

Product inhibition of NI has been demonstrated in other species (Van den Ende and Van Laere, 1995; Ross *et al.*, 1996; Lee and Sturm, 1996; Gallagher and Pollock, 1998; Sturm *et al.*, 1999) and in a regulatory SAI of the sugarcane leaf sheath (Sampietro *et al.*, 1980). The possible involvement of invertases in the regulation of hexose levels acting on sugar responsive genes has been discussed (Koch *et al.*, 1996). This would be particularly relevant in the case of sugarcane NI due to the repression of SAI expression by glucose (Sacher and Glasziou, 1962; Sacher *et al.*, 1963b; Glasziou and Waldron, 1964a; Glasziou and Waldron, 1964b). It is possible that the NI of sugarcane might be controlled by product inhibition as has been proposed for tuberous roots (Ricardo, 1974) and other plant species (Chen and Black, 1992; Van den Ende and Van Laere, 1995; Lee and Sturm, 1996; Ross et al., 1996).

Inhibition by Tris is a characteristic of invertases and has been demonstrated in sugarcane NI (Hatch *et al.*, 1963) and other NI (Chen and Black, 1992; Van den Ende and Van Laere, 1995; Ross *et al.*, 1996; Lee and Sturm, 1996; Gallagher and Pollock, 1998; Sturm *et al.*, 1999). It was shown that Tris was a more potent inhibitor of sugarcane NI than sugarcane SAI (Hatch *et al.*, 1963). As inhibition of sugarcane SAI increased with increasing pH, it was assumed that a higher pH

resulted in the greater inhibition of sugarcane NI by influencing the Tris-enzyme interaction.

Complete inhibition of NI by Hg^{2+} has been observed in some studies (Chen and Black, 1992; Van den Ende and Van Laere, 1995). In contrast Lee and Sturm (1996) reported that neither neutral nor alkaline *Daucus carota* L. invertase were inhibited by this ion. Ag^{+} is a strong inhibitor of *Chichorium intybus* NI; Zn^{2+} does not inhibit *Chichorium intybus* NI (Van den Ende and Van Laere, 1995). Cu^{2+} is a potent inhibitor of *Daucus carota* L. NI (Lee and Sturm, 1996; Sturm *et al.*, 1999) but not *Chichorium intybus* NI (Van den Ende and Van Laere, 1995). Co^{2+} is a potent inhibitor of the *Chichorium intybus* NI (Van den Ende and Van Laere, 1995). Some NI are uninhibited by Ca^{2+}, Mg^{2+} and Mn^{2+} (Van den Ende and Van Laere, 1995; Lee and Sturm, 1996; Gallagher and Pollock, 1998). Marked differences in the metal ion inhibition profiles of the NI suggest differences in structure related to their catalytic activity. The proposal that the neutral and alkaline invertases are different classes of enzymes which should be characterised by substrate specificity, inhibition and pH optimum has been made (Gallagher and Pollock, 1998). Sulphydryl, imidazole and alpha-amino groups have been implicated in the active site of NI (Asthir and Singh, 1997).

NI characterised from other sources have been found to be homotetramers of native molecular weight from 238 kDa to 260 kDa (Chen and Black, 1992; Van den Ende and Van Laere, 1995; Ross *et al.*, 1996) while that of *Daucus carota* L. was found to be an octamer of 456 kDa (Lee and Sturm, 1996). A previous report of sugarcane NI activity eluting at 160 kDa, 66 kDa, 35 kDa and 15 kDa, suggests a monomer of molecular weight 15 kDa aggregating to form a dimer, tetramer and decamer (del Rosario and Santisopasri, 1977).

Other NI have been shown to probably be non-glycosylated (Chen and Black, 1992; Van den Ende and Van Laere, 1995; Lee and Sturm, 1996). This characteristic, in conjunction with a near neutral pH optimum, suggests that the enzyme has a cytosolic localisation. It has been reported that sugarcane NI is glycosylated (del Rosario and Santisopasri, 1977).

A cDNA clone that shows alkaline/NI activity has been obtained from poison rye grass (*Lolium temulentum* L.) (Gallagher and Pollock, 1998). The cDNA for NI has also been obtained from carrot plants (*Daucus carota* L. cv. Nantaise) (Sturm *et al.*, 1999). The sequences of these cDNA clones will enable the isolation of a sugarcane NI sequence. Molecular studies may then reveal the role of NI in sugarcane sucrose metabolism. The role of NI in sugarcane may be different from the majority of other plants as it uncharacteristically uses sucrose as a primary storage carbohydrate.

2.2.2 Acid Invertases

The SAI is the most studied of the invertases, it is glycosylated, has a pH optimum of 4.5 to 5 and is thought to be localised in the vacuole (Tymowska-Lalanne and Kreis, 1998). SAI has been purified from a number of sources and its kinetic and physical properties have been investigated (for review, see Tymowska-Lalanne and Kreis, 1998).

Studies indicated that SAI activity decreases, and NI activity increases (Hatch and Glasziou, 1963; Gayler and Glasziou, 1972a; Batta and Singh, 1986) or decreases (Dendsay *et al.*, 1995) in sugarcane with tissue maturation and sucrose accumulation. Previously it was reported that SAI was present in immature but not mature tissue of high sucrose accumulating varieties and that NI showed no particular distribution pattern related to species (Hatch and Glasziou, 1963). Other work has indicated that there is no specific tissue maturity associated distribution of the invertases, and that the expression of invertase can show significant seasonal variation (Lingle and Smith, 1991; Dendsay *et al.*, 1995).

Levels of SAI have been shown to vary seasonally (Hatch *et al.*, 1963; Gayler and Glasziou, 1972a). Hatch and Glasziou (1963) used controlled environment facilities to show that invertase levels are dependent upon environmental conditions such as temperature and water stress. The rapid decrease and increase of SAI and NI respectively, with sugarcane tissue maturation was

observed in a number of high sucrose accumulating varieties (Hatch and Glasziou, 1963). Gayler and Glasziou (1972a) showed that NI activity correlated positively with hexose levels in the sugarcane culm while SAI did not. More recently it has been shown that SAI shows a strong positive correlation with hexose levels in the sugarcane culm, while NI shows a weak negative correlation (Singh and Kanwar, 1991). Sucrose content of the juice of young cane has been shown to be negatively correlated with soluble acid and NI (Venkataramana and Naidu, 1993). Sugarcane SAI has been the subject of investigation in a number of studies (Hatch *et al.*, 1963; del Rosario and Santisopasri, 1977; Sampietro *et al.*, 1980; Batta *et al.*, 1991).

Regulation of invertase activity has been found to be mediated by high molecular weight inhibitors in other plants (Pressey, 1968; Jaynes and Nelson, 1971; Bracho and Whitaker, 1990; Pressey, 1994). However in sugarcane there is no evidence for the presence of low or high molecular weight inhibitors (Glasziou and Waldron, 1964a). Sugarcane SAI is not inhibited (competitive or allosteric inhibition) by glucose (Glasziou and Waldron, 1964a).

The potential for the regulation of SAI levels by cytosolic glucose levels which could be regulated by NI is at present based on work showing the repression of acid invertase expression by glucose (Sacher and Glasziou, 1962; Sacher et al., 1963b; Glasziou and Waldron, 1964a; Glasziou and Waldron, 1964b).

Cell-wall bound acid invertase has been purified from a number of sources and its kinetic and physical properties have been investigated (for review, see Tymowska-Lalanne and Kreis, 1998). The wall-bound acid invertase is glycosylated, generally has a pH optimum of 4.5 to 5 and is found ionically associated with wall extracts. Barley (*Hordeum vulgare*) CWA was found to have a native molecular weight of approximately 60 kDa and a pH optimum of 4.5 (Karuppiah *et al.*, 1989). CWA has been associated with assimilate import into apoplasmically supplied sink tissues (Morris, 1982; Eschrich, 1989; Miller and Chourney, 1992).

2.3 Metabolic Flux Analysis

2.3.1 An Overview of Metabolic Flux Analysis

The majority of information concerning the regulation of metabolic pathways comes from *in vitro* measurements of enzyme activities and kinetic properties. Although it is possible to investigate mechanisms of control using *in vitro* enzymatic data, it is recognised that estimation of *in vivo* fluxes from this data is difficult (Salon and Raymond, 1988). This is due to the lack of information on the *in vivo* environment and the details of modulators, effectors, allosteric effects and the effective concentrations of these metabolites and enzymes. Therefore a direct approach to determining *in vivo* flux must be adopted. In most cases labelled substrates are used. This can yield qualitative data, which enables the elucidation of metabolic pathways. However, quantitative data is required for the investigation of *in vivo* flux. Due to the complexity of metabolic pathways, the use of theoretical models will aid in the interpretation of the experimental results.

An important aspect of metabolic flux analysis is the choice of tracer to be used. Historically, radioactive isotopes such as ^{14}C, ^{3}H and ^{32}P have been used due to the sensitivity and ease of detection techniques. Drawbacks include lengthy and delicate purification procedures. The assumption is made that there is no isotopic discrimination (Northrop, 1981). Stable isotopes have been detected by mass spectrometry. Since the 1980's the use of NMR (nuclear magnetic resonance) to detect heavy isotopes like, ^{13}C and ^{15}N provided similar information to radioactive isotopes without the need for extensive purification (Gadian and Radda, 1981). NMR has the additional advantage of the possibility of non-destructive continuous sampling depending on the application. However, the drawback of low sensitivity can limit its application.

Experimental systems can be classified by metabolic and isotopic steady state. At metabolic steady state the concentration of reaction intermediates and the system

fluxes are constant. At isotopic steady state the reaction intermediates are at constant specific activity. The occurrence and establishment of metabolic and isotopic steady states has been examined by Borowitz *et al.* (1977). The time to reach isotopic steady state is dependent on the ratios of the metabolic fluxes through intermediates to the pool sizes of the intermediates.

Three types of investigations can be performed: (a), pulse labelling with a very short period; (b), during the establishment of isotopic steady state or; (c), at isotopic steady state. Short time studies (a), lasting a few seconds or minutes can be used to investigate precursor-product or precursor-intermediate relations. However, it does require rapid application of the label and that the label is not recycled. Following the establishment of steady state (b) presents a more complex problem. In real systems one may be dealing with not only specific activity variation but also metabolite pool size variation with time. Compartmentation and the associated difficulties of measurement add to the complexity. Studies at steady state (c) have been afforded far more attention due to the systems being more amenable to analysis (Blum and Stein, 1982).

The theoretical treatment of modelling metabolic fluxes was investigated as early as the 1960's. A mathematical treatment for the determination of pool sizes and turnover factors was given by Bergner (1964). The use of isotopes in the study of glucose metabolism is reviewed by Katz (1979). The widespread use of computers has influenced the techniques used to solve these problems. General mathematical computer program environments for the implementation of flux models such as SAAM (Weiss, 1974), MLAB (Knott, 1975) and DSS (Zellner, 1970) have been available since the 1970's. Sherwood *et al.* (1979) developed a less expensive, specific computer program (TFLUX) for the interpretation of radioactive tracer experiments. TFLUX has been applied in the investigation of compartmentation and flux in *Dictyostelium discoideum* and *Rhizopus oryzae* metabolism (Kelly *et al.*, 1979; Wright and Reimers, 1988; Wright *et al.*, 1996; Longacre *et al.*, 1997). More recently efforts have been made to advance the theoretical treatment of metabolic flux analysis. Most of the research has been performed on microbial systems. This is due to the need for this information in bioengineering and the relative simplicity of microorganisms, especially with

respect to compartmentation. Metabolic flux balancing has been applied to microbial systems, for review see Varma and Palsson (1994). The mathematical formalism for the network analysis of intermediary metabolism has been developed by Savinell and Palsson (1992a) and applied to hybridoma cell metabolism (Savinell and Palsson, 1992b). The problem of the selection of the optimal fluxes for measurement has also been addressed (Savinell and Palsson, 1992c) and applied to *Escherichia coli* and hybridoma cell metabolism (Savinell and Palsson, 1992d). The theoretical treatment of determining fluxes using carbon isotopes under metabolic steady-state conditions has been dealt with by Wiechert and de Graaf (1997) and Wiechert *et al.* (1997). General texts dealing with modelling biological systems such as Haefner (1996) and Cullen (1985) introduce general modelling principles and more specifically Carson *et al.* (1983) deals with the application to metabolic problems.

2.3.2 Metabolic Flux Analysis in Plants

Fluxes through metabolites have been calculated in previous studies. Fluxes of carbohydrate metabolism in ripening bananas have been investigated by Hill and ap Rees (1994). However the application of flux analysis to plant metabolism using complex computer simulation models is limited. Carbon fluxes through the tricarboxylic acid cycle of early germinating lettuce embryos have been investigated by Salon *et al.* (1988) where the theoretical model was implemented as a computer simulation model in the BASIC language. More recently compartmented metabolic fluxes in maize root tips have been quantified using isotope distribution from ^{13}C- or ^{14}C-labelled glucose (Dieuaide-Noubhani *et al.*, 1995).

Previous work on the cycle of sucrose synthesis and degradation (Glasziou, 1961; Sacher *et al.*, 1963a) has estimated a maximum turnover time for the sucrose pool in internodes 4 to 5 as 46 hours (Glasziou, 1961). The percentage distribution of label between sucrose and hexoses over time due to turnover of sucrose in intact and crushed immature tissue discs was described by Sacher *et al.* (1963a). A simple two compartment model was used to describe the turnover

of sucrose, simplifying assumptions for the crushed discs allowed the integration and solution of the differential equation describing sucrose turnover. The model was used to demonstrate the presence of a cycle of sucrose synthesis in the metabolic compartment and degradation in the vacuole. Sugarcane cell suspension cultures have been used as a model system where the cycle has been investigated (Wendler *et al.*, 1990). A number of fluxes were calculated including, sucrose synthesis, net sucrose accumulation and sucrose degradation. Simplifying assumptions were made in order to make the calculations. In the case of sucrose synthesis (unidirectional) the hexose specific activity was assumed to be that of the bathing medium. This would mean that no isotopic dilution occurred with an internal pool and that recycling of hexose from sucrose did not significantly affect the calculation (Wendler *et al.*, 1990). The net rate of sucrose storage was estimated from the rate of sucrose accumulation in the cells. This allowed the calculation of the rate of sucrose degradation (unidirectional) as the difference between the rate of sucrose synthesis and the rate of accumulation. Similar assumptions were made for flux calculations in potato tuber discs (Viola, 1996).

The quantitative calculation of metabolic flux in sugarcane tissue discs has been made using similar non-model based approaches (Komor *et al.*, 1996; Whittaker and Botha, 1997). The relative rates of the fluxes in discs from immature, maturing and mature sugarcane culm tissue were determined (Komor *et al.*, 1996). Generally, a decrease in all fluxes was observed, except for the exchange of sucrose with the bathing medium. Vacuolar acid invertase, NI and SuSy were all implicated in sucrose degradation. SPS synthesised sucrose in all tissue types while SuSy synthesis activity was only observed in immature tissue. A general observation was that the flux through the sucrose cycle was always greater than the net flow of sugar into storage, growth and energy metabolism. The rate of sucrose degradation was calculated based on the decay of label in the sucrose pool during a chase after a 30 min. pulse with labelled glucose. Similarly other fluxes were calculated using simplifying assumptions. Estimates of the flux into metabolism from sucrose due to invertase or invertase and SuSy were made for sugarcane culm tissue discs derived from internodes two and seven (Whittaker and Botha, 1997). This was achieved by feeding either labelled fructose or

glucose. As previously mentioned (Wendler *et al.*, 1990) labelled glucose can only be derived from labelled fructose due to the hydrolysis of sucrose. Fluxes into metabolism from the hexose pools were calculated using the sum of the release of radioactivity as CO_2 and other forms other than the applied hexose. In that research on sugarcane metabolic flux no attempt was made to develop a more comprehensive computer based model to investigate flux.

Model based interpretation of labelling experiments can also be used to investigate compartmentation. More specifically the distribution of metabolites between the cytoplasm and vacuole in sugarcane remains an open area for investigation. Total metabolite concentrations for sugarcane culm tissue have been measured for the symplast (Welbaum and Meinzer, 1990). However, solute distribution between the cytosol and vacuole has only been investigated in sugarcane suspension cells (Preisser *et al.*, 1992). The estimation of *in vivo* fluxes from labelling experiments of potato (*Solanum tuberosum* L.) tubers was conducted by Viola (1996). The equilibration of incoming labelled glucose with a large measured internal glucose pool could not be reconciled with maximum catalytic activities of glucokinase (Viola, 1996). The size of the equilibrating internal glucose pool was therefore estimated using a model implemented in SB-ModelMaker (Zeton Ltd, Nottingham UK) (Viola, 1996).

Chapter 3

Distribution of Invertases in the Culm

3.1 Introduction

A gradient of sucrose concentration, ranging from low levels in young internodes to more than 200 $g.kg^{-1}$ fresh weight in older internodes, occurs in most commercial sugarcane varieties (Glasziou and Gayler, 1972; Hawker, 1985). Evidence suggests that the sucrose is not confined to the vacuole but that it is present in similar concentration in the apoplastic space and symplast (Hawker, 1985; Welbaum and Meinzer, 1990). During the maturation of the internodal tissue the purity (ratio between sucrose and total sugar) increases from less than 5% to more than 9% (Welbaum and Meinzer, 1990; Moore, 1995). Despite numerous studies, the biochemical basis for the accumulation of sucrose in sugarcane is still poorly understood (for review see Moore, 1995). A recent study has shown the significance of the combined effects of SAI (β-D-fructofuranosidase, E.C. 3.2.1.26) and SPS (UDP-Glc:D-Fru-6-P 2-α-D-glucosyltransferase, E.C. 2.4.1.14) on sucrose accumulation in the sugarcane culm (Zhu *et al.*, 1997).

Invertase occurs in plants in isoforms with differing pH optima and cellular localisation. The best characterised isoforms are the acid invertases, which occur in the apoplastic space in free form, and bound to the cell wall (Avigad, 1982; Hawker, 1985), and soluble isoforms presumably present in the vacuole (Avigad, 1982; Hawker, 1985). The neutral or alkaline invertases occur in the cytosol and have not been well characterised (Avigad, 1982; Hawker, 1985).

Although the assumption is often made that sucrose accumulation in sugarcane is associated with decreasing invertase activity, conflicting evidence has

accumulated. Earlier studies indicated that SAI activity decreases (Hatch and Glasziou, 1963; Gayler and Glasziou, 1972; Batta and Singh, 1986), and NI activity increases (Hatch and Glasziou, 1963; Gayler and Glasziou, 1972; Batta and Singh, 1986) or decreases (Dendsay *et al.*, 1995) with tissue maturation and sucrose accumulation. If sucrose accumulation occurred largely in the vacuole, these results could offer a possible explanation for the increase in purity and sucrose content during maturation. Other work has indicated that there is no specific tissue maturity associated distribution of the invertases, and that the expression of invertase can show significant seasonal variation (Lingle and Smith, 1991; Dendsay *et al.*, 1995).

Levels of SAI have been shown to vary seasonally (Hatch *et al.*, 1963; Gayler and Glasziou, 1972). Hatch and Glasziou (1963) used controlled environment facilities to show that invertase levels are dependent upon environmental conditions such as temperature and water stress. The rapid decrease of SAI and increase of NI activities with sugarcane tissue maturation was observed in a number of high sucrose accumulating varieties (Hatch and Glasziou, 1963). Gayler and Glasziou (1972) showed that NI activity positively correlated with hexose levels in the sugarcane culm while SAI did not. More recently, it has been shown that SAI displays a strong positive correlation with hexose levels in the sugarcane culm while NI shows a weak negative correlation (Singh and Kanwar, 1991). Sucrose content of the juice of young cane has been shown to be negatively correlated with SAI and NI (Venkataramana and Naidu, 1993).

The fragmented nature of the current information on the levels of invertase in sugarcane internodes and correlations with sugar levels makes it difficult to draw definite conclusions. The apparent variation in invertase activity could imply that sucrose accumulation is not directly related to expression of the enzyme or that extractable activity does not represent *in vivo* activity.

This chapter reports the activity and distribution of NI, SAI and CWA in the culm of a single high sucrose accumulating sugarcane cultivar. Extracted activity is compared with the total amount of invertase protein present. Radiolabelled fructose is used to verify endogenous invertase activity.

3.2 Materials and Methods

3.2.1 Plant Materials

Tissue of sugarcane cultivar NCo376 was obtained from the field at the SASA Experiment Station, Mt Edgecombe, South Africa, in midsummer. Tissue samples were obtained from a bulk of 12 culms that were cut in the early morning. Internodes three to 10 were sampled for enzyme activity. Internode one is defined as the internode above the node from which the leaf with the first exposed dewlap originates. Internodes three and four are considered to be immature tissue and internodes nine and 10 mature tissue based on sucrose levels. A sample from the mid-region of each internode was excised, sliced, weighed and powdered in liquid nitrogen. Equal masses of sample were combined for each internode and aliquots were stored at -80 °C.

3.2.2 Sucrose Determination

Approximately 2 g of sample was boiled in 10 mL of ethanol (800 $mL.L^{-1}$) for 10 min. and centrifuged at 4000 xg for 15 min. (modified from Ball and ap Rees, 1988), the supernatant was then dried in a rotary evaporator at 50 °C and resuspended in 500 µL deionised H_20. Sucrose was measured using the enzymatic assay as in Bergmeyer and Bernt (1974).

3.2.3 Enzyme Extraction

The enzymes were extracted in an ice-cold, degassed stabilising buffer consisting of 10 $mmol.L^{-1}$ sodium phosphate, 10 $mmol.L^{-1}$ DTT, 0.2 $mmol.L^{-1}$ PMSF, 1 $mmol.L^{-1}$ EDTA and glycerol (100 $mL.L^{-1}$) at pH 7.0 in a 2:1 v/w ratio. The suspended material was centrifuged at 14000 xg for 10 min., 1 mL of the supernatant containing the soluble protein was removed and desalted on a 5 mL Presto™ Desalting Column (Pierce) equilibrated with the extraction buffer according to the manufacturers instructions. The fibre obtained from the soluble

protein extraction was washed three times in extraction buffer to remove residual soluble protein and reducing sugars. CWA was then extracted by a 20 min. incubation in the same extraction buffer containing 500 mmol.L^{-1} NaCl and 100 mmol.L^{-1} $CaCl_2$ in a 2:1 v/w ratio (Masuda *et al.*, 1988). All extractions were performed in triplicate.

3.2.4 Invertase Assays

Invertases were assayed at pH optima as determined by Hatch *et al.* (1963) and temperature optimum as determined in preliminary studies. NI specific activity was determined by incubating the sample at 30 °C in 50 mmol.L^{-1} HEPES pH 7.0 and 125 mmol.L^{-1} sucrose in a final volume of 1 mL for 3 h. The assay system was the same for the acid invertases except that a 50 mmol.L^{-1} citrate/phosphate buffer at pH 5.5 was used. Substrate was assumed to be saturating for NI and the acid invertases based on K_m determinations by Hatch *et al.* (1963). Reactions were stopped by a 2 min. incubation at 90 °C, which removed all invertase activity, and were then stored at -80 °C. Reducing sugars were measured using an enzyme system coupled to NAD (Huber and Akazawa, 1986) with a Beckman DU® 7500 spectrophotometer. Specific activities were linear with time and proportional to the amount of protein being assayed. One unit of invertase activity (U) is defined as the hydrolysis of one μmol of sucrose per min.

3.2.5 SDS Page and Protein Blotting

Proteins were resolved on discontinuous 120 g.L^{-1} polyacrylamide gels with a 50 g.L^{-1} (m/v) stacking gel (acrylamide : *N,N'*-methylene-bisacrylamide was 100 : 1) according to Laemmli (1970). Molecular weight standards used were: BSA (66 kDa), egg albumin (45 kDa), glyceraldehyde-3-P-dehydrogenase (36 kDa), bovine carbonic anhydrase (29 kDa), bovine pancreas trypsinogen (24 kDa), soybean (*Glycine max*) trypsin inhibitor (20 kDa) and bovine milk α-lactalbumin (14.2 kDa).

The separated polypeptides were transferred to nitrocellulose membranes using the SEMI-PHOR™ system (Hoefer Scientific Instruments, San Francisco) at 0.8

$mA.cm^{-2}$ for 1 h according to manufacturer's instructions. The transfer buffer contained 25 $mmol.L^{-1}$ Tris, 192 $mmol.L^{-1}$ glycine and 200 $mL.L^{-1}$ methanol.

Nitrocellulose membranes (Amersham) were blocked in 30 $g.L^{-1}$ fat free milk powder in TBST (20 $mmol.L^{-1}$ Tris-HCl pH 7.6, 150 $mmol.L^{-1}$ NaCl and 1 $mL.L^{-1}$ Tween 20) overnight at 4 °C, all subsequent steps were performed at room temperature. Blots were rinsed three times in TBST, then incubated in the primary antibody (sugarbeet (*Beta vulgaris*) NI or potato (*Solanum tuberosum*) SAI rabbit polyclonal antibody) at 1:1000 dilution in TBST containing 30 $g.L^{-1}$ BSA for 1 h. Blots were washed five times for five min. in TBST before incubation in the secondary antibody (alkaline phosphatase conjugated goat anti-rabbit IgG) diluted 1:1000 in TBST containing 30 $g.L^{-1}$ fat free milk powder. The blots were then washed for five min. in TBST, rinsed in TBST containing 1 $g.L^{-1}$ SDS and then washed for five min. in TBST. Cross reacting polypeptides were detected by the enzymatic cleavage of the phosphate group of 5-bromo-4-chloro-3-indolyl-phosphate using nitroblue tetrazolium as a stain enhancer (Blake *et al.*, 1984).

3.2.6 Labelling with Fructose

Transverse sections (1.0 to 2.0 g) of internodal tissue, spanning the core, mid-internodal and peripheral internodal regions were excised, sliced (approximately 0.5 mm diameter) and washed according to Lingle (1989). [U-^{14}C]Fructose (2.0 $GBq.mmol^{-1}$) was supplied to tissues in 2 mL 25 $mmol.L^{-1}$ K-MES (pH 5.7) containing 250 $mmol.L^{-1}$ mannitol. Prior to incubation, the labelled substrates were vacuum-infiltrated into the tissues for 1 min. Tissues slices were then incubated at 28 °C in airtight containers (500 mL) on a rotary shaking incubator at 175 rpm for 5.5 h. The tissue slices were then washed for 30 min. in 15 mL 25 $mmol.L^{-1}$ K-MES (pH 5.7) containing 250 $mmol.L^{-1}$ mannitol and 1 $mmol.L^{-1}$ $CaCl_2$ to remove apoplastic label as described by Lingle (1989). Liquid nitrogen frozen material was ground to a fine powder and cellular components extracted in 15 mL methanol:chloroform:water (12:5:3 by vol) (Dickson, 1979). The water-soluble pool was dried down in a rotary evaporator at 40 to 50 °C, the residue dissolved in HPLC grade H_2O and passed through prewashed Sep-Pak Alumina A cartridges (Waters Chromatography). Samples were filtered (0.22 µm Millex-GV4

filters, Millipore) prior to fractionation of the sugars by HPLC on a Sugar-Pak I column (Waters Chromatography). Sugars were separated over 15 min. with HPLC grade H_2O containing 1.33 mmol.L^{-1} EDTA (disodium calcium salt) at a flow rate of 0.5 mL.min^{-1}. Fractions (0.5 mL) were collected and the ^{14}C in sucrose, glucose and fructose determined. Extraction efficiencies for sucrose, glucose and fructose were 92 ± 7 %. ^{14}Carbon in the fractions was determined by liquid scintillation spectroscopy using a Packard Tricarb 1900 TR using Ultima Gold XR quench resistant scintillation cocktail from Packard.

3.2.7 Protein Determination

Protein concentration was determined by the method of Bradford (1976) using the BioRad (Richmond, CA) micro assay with gamma globulin as a standard.

3.2.8 Calculation of Sucrose Utilisation

The time required for the utilisation of the sucrose pool is taken as the time required to utilise one equivalent of the total sucrose pool by the combined invertase activities. In the case of the invertase:SPS mediated 'futile cycle', it is assumed that it costs three ATP equivalents for each sucrose molecule resynthesised after hydrolysis. Each sucrose molecule is assumed to yield approximately 72 ATP equivalents when metabolised.

3.3 Results

The sucrose concentration (µmol.mg^{-1} protein) increases between internodes two and nine (Table 3.1). The progressive increase in sucrose content of the younger internodes coincides with an increase in the glucose and fructose content. This is also evident from the ratio of sucrose to total reducing sugars, which shows a relatively small change between internodes two to five. In the older internodes (five to 10) the sucrose content rapidly increases and the amounts of both the reducing sugars decrease (Table 3.1).

Table 3.1. The glucose, fructose and sucrose content and purity of sugarcane (NCo376) internodal tissue.

Internode Number [a]	Glucose	Fructose	Sucrose	Purity [b]
	(μmol.mg^{-1} protein)			(%)
2	3.81 ± 1.0	2.81 ± 0.7	4.53 ± 0.5	41
3	5.68 ± 0.9	5.15 ± 0.9	8.18 ± 1.1	43
4	9.79 ± 1.2	9.47 ± 0.7	15.79 ± 2.9	45
5	9.69 ± 1.4	10.42 ± 0.8	25.9 ± 4.5	56
6	8.61 ± 1.9	8.03 ± 2.6	51.77 ± 2.6	76
7	5.81 ± 0.8	7.77 ± 1.3	73.09 ± 10.4	84
8	3.97 ± 1.0	2.69 ± 0.8	83.95 ± 0.8	93
9	2.22 ± 1.1	4.89 ± 1.1	102.75 ± 4.0	94
10	2.08 ± 1.2	3.16 ± 1.8	106.49 ± 6.2	96

a. Internode one is defined as the internode above the node from which the leaf with the first exposed dewlap originates

b. (sucrose/total sugars) x 100

± = standard deviation

After feeding labelled fructose, most of the radiolabel in the sugar pool was recovered in sucrose (Table 3.2). It is evident that the net flux of label into sucrose increases from the younger to older internodes. However, a significant portion of the label was present in glucose. This strongly suggests invertase-mediated hydrolysis of labelled sucrose.

Table 3.2. The distribution of ^{14}C in sucrose, glucose and fructose after labelling of internodal discs of NCo376 with [U-^{14}C]Fructose for 5.5 h at 28 °C.

Internode Number [a]	Radioactivity present in:		
	Sucrose	Fructose	Glucose
	(kBq.mg^{-1} protein)		
2	7.6 ± 3.3	1.1 ± 0.3	0.7 ± 0.1
7	12.0 ± 3.5	2.4 ± 0.5	1.1 ± 0.3
10	14.3 ± 3.1	2.6 ± 0.8	0.9 ± 0.4

a. Internode one is defined as the internode above the node from which the leaf with the first exposed dewlap originates

± = standard deviation

A detailed study of the invertase activity distribution was performed using internodes three to 10 (Fig. 3.1). A very similar pattern of activity was observed when the enzyme activity was expressed on a protein (specific activity) or fresh mass (volume) basis. The specific activities (mU.mg^{-1} protein) of all three invertases showed a low level of activity in internode three with a sharp rise to internode four (Fig. 3.1B). However, when expressed on a fresh mass basis (Fig. 3.1A) a lower activity was not observed in internode three. Invertase activities therefore remained constant on a volume basis as shown by the activity expressed on a fresh mass basis from internodes three to four but formed a smaller portion of total protein in internode three.

All of the invertases showed an overall decrease in activity with tissue maturation (Fig. 3.1A and 3.1B). CWA was also present in significant quantities in both immature and mature internodal tissue (Fig. 3.1A and 3.1B).

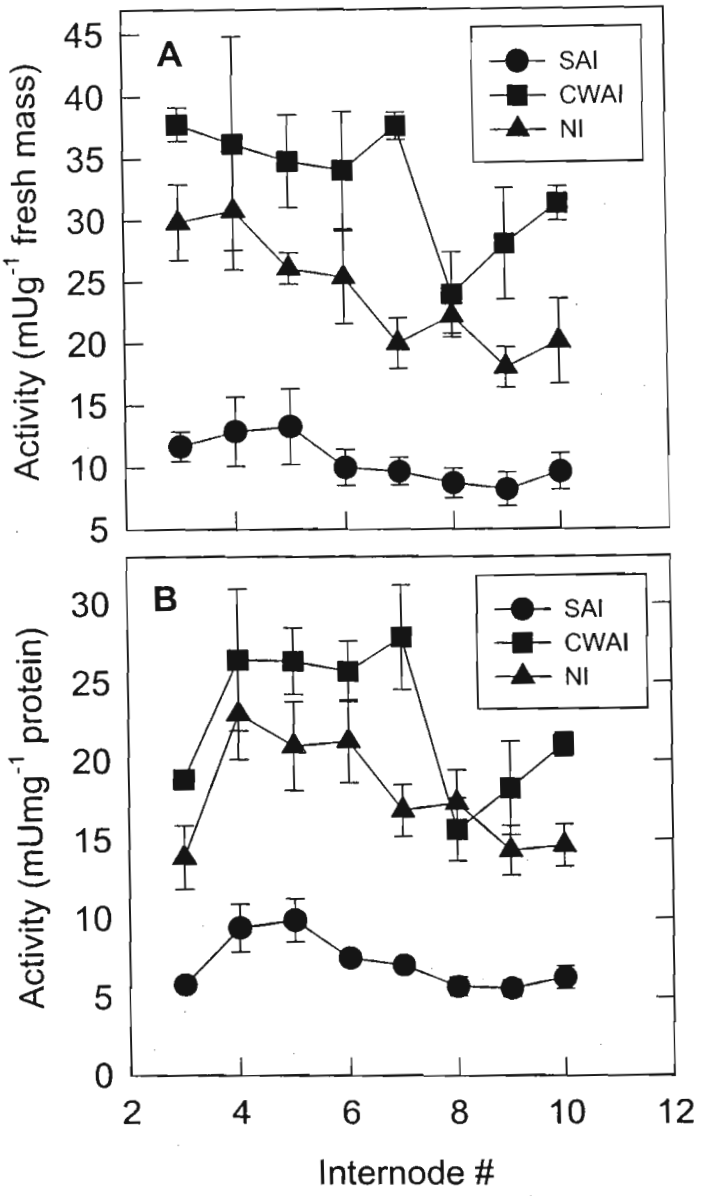

Figure 3.1. Activity distribution of CWA, NI and SAI (vacuolar and apoplastic) down the culm of sugarcane variety NCo376, expressed on a fresh mass (A) and protein (B) basis. All values represent the mean and standard deviation of three replicates. Internode one is defined as the internode above the node from which the leaf with the first exposed dewlap originates.

In order to verify whether the measured activity is a true reflection of the endogenous invertase concentration, three approaches were followed. Firstly, the presence of possible high molecular weight activators or inhibitors was determined by preparing a series of extracts, each containing internodal tissue from at least two different stages of development. Recombination experiments yielded percentage activities of 93.5 ± 4.7 % (NI), 108 ± 6.6 % (SAI) and 97.4 ± 8.6 % (cell-wall bound acid invertase). Secondly, to test for a heat stable invertase inhibitor as is present in tomato fruit (Pressey, 1994), assays were spiked with boiled crude extracts from different internodal tissue. No inhibition was observed in these experiments, indicating that no such activators or inhibitors were present in sugarcane culm tissue. Thirdly, acid and NI specific antibodies were used on protein blots of total crude protein extracts (Fig. 3.2). With the polyclonal NI antibody a single cross reacting polypeptide of 58 kDa was detected (Fig. 3.2A). The signal intensity reached a maximum between internodes four to eight which is in close agreement with the measured activity (Fig. 3.1). With the acid invertase antibodies two cross-reacting polypeptides of 62 kDa and 56 kDa were detected (Fig. 3.2B). Whether this reflects different forms of acid invertase is unclear. Although precautions were taken to prevent breakdown of the 62 kDa polypeptide by using protease inhibitors and extracting at 4 °C the 56 kDa polypeptide could be a breakdown product. The 62 kDa polypeptide content appears to be constant in the different internodes. The 56 kDa polypeptide displayed a slight increase with tissue maturation.

Based on the sucrose present in the sugarcane culm (Table 3.1) and the activities of neutral and SAI (Fig. 3.1), the time required for the hydrolysis of the sucrose pool by combined sucrolytic activities of NI and SAI was calculated (Table 3.3). Similarly the time required for the utilisation of the sucrose pool for only the maintenance of an invertase-mediated cycle of sucrose degradation and synthesis is shown in Table 3.3.

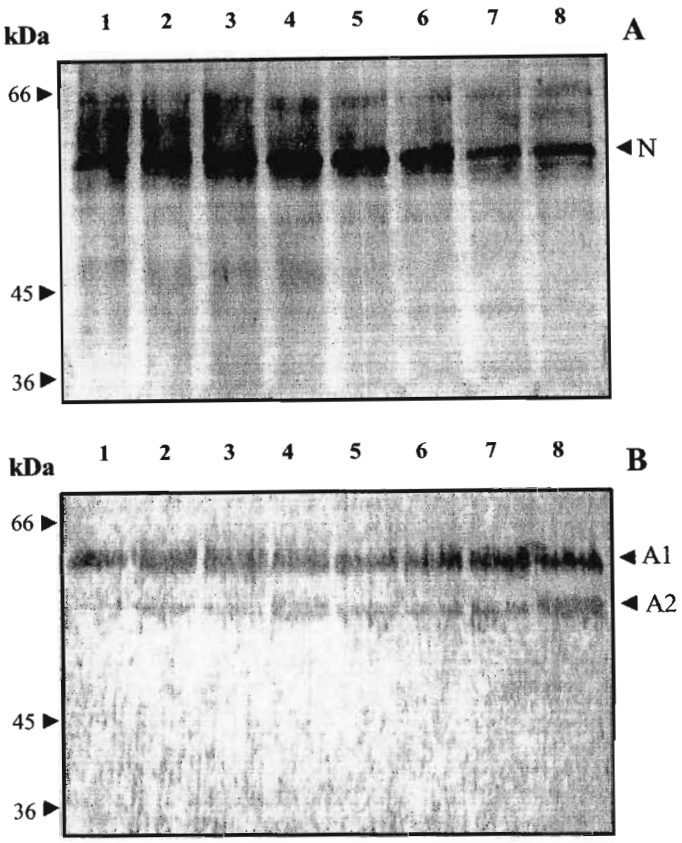

Figure 3.2. Immunoblots of NI (A) and SAI (B) from sugarcane variety NCo376. After electrophoretic separation, proteins were transferred to nitrocellulose membranes and were detected with a 1 : 1000 dilution of a polyclonal NI (A) and polyclonal SAI (B) antibody. NI (N) is approximately 58 kDa, SAI (A1 and A2) are approximately 62 kDa and 56 kDa respectively. Lanes one to eight represent internodes three to 10 respectively. Protein loading was 20 µg/lane. Internode one is defined as the internode above the node from which the leaf with the first exposed dewlap originates.

Table 3.3. Calculated time required for combined invertase activity mediated utilisation of the sucrose pool equivalent by hydrolysis only, or maintenance of an invertase:SPS mediated 'futile cycle'. Data from Table 3.1 and Fig. 3.1 and assuming a cost of three ATP equivalents/resynthesised sucrose molecule.

Internode Number	Hydrolysis	'Futile cycle'
	(days)	
3	0.15	3.54
4	0.19	4.47
5	0.31	7.54
6	0.66	15.83
7	0.98	23.50
8	1.51	36.15
9	1.87	44.86
10	1.76	42.35

3.4 Discussion

Despite numerous studies on the translocation, metabolic fate and storage of sucrose in the sugarcane culm, the process is still poorly understood (for review see Moore, 1995). Evidence suggests that sucrose in the storage parenchyma cells is equally distributed between the symplast and apoplast (Hawker, 1985; Welbaum and Meinzer, 1990) and therefore all hydrolytic and cleavage activities could be important in sucrose storage. It has been shown that hexose levels positively correlate with NI and not SAI levels in mature sugarcane culm tissue (Gayler and Glasziou, 1972). It has, however, also been shown that invertase activities are not significantly correlated with hexose levels but positively correlated with sucrose concentration in the sugarcane culm (Singh and Kanwar, 1991).

As previously reported (for review see Moore, 1995) three forms of invertase, bound and soluble acid activities, and a neutral activity are present in the internodal tissue of sugarcane. Previously it was reported that SAI was present in immature but not mature tissue of high sucrose accumulating varieties and that NI showed no particular distribution pattern related to species (Hatch and Glasziou, 1963). The data presented here clearly shows that all of the invertases are present in significant amounts down the sugarcane culm, from low to high sucrose containing tissue (Table 3.1 and Fig. 3.1).

It is evident from the protein blot data that the measurements of SAI and NI activities are a true reflection of the invertase protein content. The molecular weight of 58 kDa of the sugarcane NI is similar to that of the enzyme from other sources (Chen and Black, 1992; Van den Ende and Van Laere, 1995; Lee and Sturm, 1996; Ross *et al.*, 1996). In contrast to the report by del Rosario and Santisopasri (1977), no evidence of smaller forms (35 kDa and 15 kDa) of NI were evident. This is investigated further in chapter four. Similarly, the molecular weights of 62 kDa and 56 kDa obtained for SAI are in agreement with other sources (Karuppiah *et al.*, 1989; Walker and Pollock, 1993; Milling *et al.*, 1993). The two molecular forms of SAI could represent two isoforms (apoplastic and vacuolar). At present the possibility that they represent hydrolysis products of the native form cannot be excluded. This aspect is under further investigation.

Despite the high levels of invertase activity in the sugarcane culm, sucrose accumulation does occur. This can only happen if the endogenous invertase activity is inhibited, or if the synthesis capacity exceeds the hydrolytic activity. Regulation of invertase activity has been found to be mediated by high molecular weight inhibitors in other plants (Pressey, 1968; Jaynes and Nelson, 1971; Bracho and Whitaker, 1990; Pressey, 1994). However, similar to a previous report (Glasziou and Waldron, 1964a) we could find no evidence for the presence of low or high molecular weight inhibitors in sugarcane. Sugarcane SAI is not inhibited (competitive or allosteric inhibition) by glucose (Glasziou and Waldron, 1964a). It is possible that the NI is controlled by product inhibition as has been proposed for tuberous roots (Ricardo, 1974) and is a characteristic of other plant

NI (Chen and Black, 1992; Van den Ende and Van Laere, 1995; Ross *et al.*, 1996; Lee and Sturm, 1996), an aspect investigated in chapter four.

The appearance of label in the glucose pool after the tissue was fed with labelled fructose in both young and mature tissue (Table 3.2) clearly shows that significant invertase mediated sucrose hydrolysis occurs *in vivo*. Based on these results it is proposed that invertase mediated sucrose turnover will occur at all stages of maturation of the sugarcane culm. Extractable activities (Fig. 3.1) indicate that NI has the capacity to make a significant contribution to this turnover.

A cycle of synthesis and degradation of sucrose has been observed in sugarcane cell suspension cultures (Wendler *et al.*, 1990) and in the sugarcane culm (Glasziou, 1961; Sacher *et al.*, 1963a). In the study of Sacher *et al.* (1963a) it was concluded that the cycling would be characteristic of only those tissues with high acid invertase activity. It has been shown that in maize root tips a 'futile cycle' of sucrose turnover consumes 69% of the ATP produced by mitochondrial respiration (Dieuaide-Noubhani *et al.*, 1995), this is lower than that found in banana tissue (Hill and ap Rees, 1994). Both studies emphasise the magnitude of the investment that plants have to make to maintain sucrose turnover in some tissues.

The sucrolytic potential of NI and SAI is evident in Table 3.3. The turnover-time for the utilisation of the sucrose pool by the combined unregulated invertase activities ranges from 0.14 days in internode three to 1.77 days in internode 10. Previous work has estimated a maximum turnover-time for the sucrose pool in internodes four to five as 46 hours (Glasziou, 1961). This rate is comparable to that presented in Table 3.3 assuming that there is some form of regulation of invertase activities. Assuming that a 'futile cycle' of sucrose turnover occurs *in vivo*, the time required for the utilisation of the sucrose pool to maintain the cycle mediated by the combined unregulated invertase activities would range from three days in internode three, to 42 days in internode 10 (Table 3.3). Taking into account that sugarcane is harvested on a 12 to 18 month growth cycle, the potential rate of energy utilisation to maintain the 'futile cycle' is therefore highly significant, even in mature internodal tissue.

The potential for the regulation of SAI levels by cytosolic glucose levels which could be influenced by NI is at present based on work showing the repression of acid invertase expression by glucose (Sacher and Glasziou, 1962; Sacher *et al.*, 1963b; Glasziou and Waldron, 1964a; Glasziou and Waldron, 1964b).

Cycling of sucrose is energetically wasteful. Targeting invertase for genetic manipulation through antisense technology in sugarcane could be a viable option for potential increases in sucrose load.

Chapter 4

Characterisation of Sugarcane Neutral Invertase

4.1 Introduction

NI (β-fructofuranosidase, E.C. 3.2.1.26) catalyses the hydrolysis of terminal non-reducing β-fructofuranoside residues in β-D-fructofuranosides like sucrose. In the past NI have been neglected by biochemists in comparison to the acid invertases (Avigad, 1982; Hawker, 1985). However, the enzyme has recently been purified and characterised from at least four sources (Chen and Black, 1992; Van den Ende and Van Laere, 1995; Lee and Sturm, 1996; Ross *et al*, 1996).

Sugarcane invertases are found in a number of isoforms, namely: NI; vacuolar SAI; CWA and an apoplastic SAI (for review see Moore, 1995; Glasziou and Gayler, 1972). Sugarcane NI has been shown to be associated with mature culm tissue and sugarcane SAI with immature, actively growing tissue (Hatch and Glasziou, 1963; Gayler and Glasziou, 1972; Batta and Singh, 1986). A similar tissue distribution has been reported for other species (for review see Avigad, 1982; Hawker, 1985).

A cycle of synthesis and degradation of sucrose has been reported in sugarcane cell suspension cultures (Wendler *et al*, 1990) and in the sugarcane culm (Glasziou, 1961; Sacher *et al*, 1963a; Komor *et al*, 1996). Based on previously reported activities of sugarcane NI (Hatch and Glasziou, 1963; Gayler and Glasziou, 1972; Batta and Singh, 1986; Lingle and Smith, 1991; Dendsay *et al*, 1995), it is possible that the enzyme is involved in sucrose turnover in sugarcane culm tissue.

There has been no study to comprehensively characterise sugarcane NI or investigate possible mechanisms for fine control. Previous studies on sugarcane NI utilised dialysed crude extracts (Hatch *et al*, 1963) or activity eluted after $(NH_4)_2SO_4$ precipitation from sugarcane crusher juice and subsequent size exclusion chromatography (del Rosario and Santisopasri, 1977). This chapter reports the characterisation of sugarcane NI and, based on the findings, the possible *in vivo* control of the enzyme activity is discussed.

4.2 Materials and Methods

4.2.1 Plant Material

NI was extracted from field grown mature sugarcane culms of sugarcane variety NCo376. Culms were cut in the early morning and used immediately.

4.2.2 Enzyme Purification

Mature rindless culm tissue was homogenised in ice cold, degassed extraction buffer (10 mM HEPES pH 7.2, 10 mM DTT, 1.5% (wt/v) prehydrated PVPP, 0.2 mM PMSF, 2 mM Benzamidine-HCL) at a ratio of 2:1 (v/wt), and filtered through two layers of nylon mesh. Insoluble material was removed by centrifugation at 10 000 xg for 5 min. at 4°C. Protein was precipitated with gentle stirring by the addition of ground, solid $(NH_4)_2SO_4$ at 4°C to 20% saturation and centrifugation at 10 000 xg for 20 min. at 4°C. The supernatant was further saturated with solid $(NH_4)_2SO_4$ to 60% and the precipitated protein collected by centrifugation at 10 000 xg. The 20-60% $(NH_4)_2SO_4$ precipitate containing the majority of the NI activity was resuspended in a minimal volume of buffer A (25 mM HEPES, 0.02% $Na(N)_3$, pH 7.2) and desalted on a Sephadex G-25 column equilibrated with buffer A. The sample was applied to a DEAE-Sephacell anion exchange column pre-equilibrated with buffer A. The column was washed with buffer A until the $A_{280\ nm}$ had decreased to a zero level. Activity was eluted with a linear gradient of 0-500 mM NaCl in buffer A and 5 mL fractions were collected. Protein elution was monitored by $A_{280\ nm}$; fractions containing NI activity were pooled. Pooled fractions

were desalted and concentrated by ultrafiltration at 4°C in buffer A.

4.2.3 Enzyme Assays and Protein Determination

NI was assayed at 30°C in 50 mM HEPES (pH 7.2), and 125 mM sucrose in a final volume of 1 mL. The assay system was the same for the acid invertases except that a 50 mM citrate/phosphate buffer at pH 5.5 was used. Reactions were stopped by a two min. incubation at 90°C and were then stored at -80°C. Reducing sugars were measured using the method of Bergmeyer and Bernt (1974). All reactions were shown to be linear with time. For NI kinetic constant determination, an appropriate amount of partially purified enzyme was used. Sucrose concentration was varied from 0-100 mM; K_m and V_{max} were determined by non-linear curve fitting. Inhibition by various metabolites and Tris was assessed by including them at various concentrations; metal ions were at a final concentration of 1 mM in the same assay system. In the case of glucose inhibition, excess glucose was removed with glucose oxidase and catalase prior to fructose determination (Bergmeyer and Bernt, 1974). The combined inhibitory effect of glucose and fructose was determined by including ^{14}C-Sucrose in the standard assay and subsequently quantifying the ^{14}C-reducing sugars by HPLC and inline isotope detection. The pH optimum was determined using the same assay conditions with a 25 mM citrate/phosphate buffer (pH 4-9). The energy of activation was determined by measuring the rate of the enzyme catalysed reaction at various temperatures between 20°C and 40°C in substrate saturating conditions at pH 7.2. Hydrolysis of cellobiose (Glc-β-1,4-Glc) or trehalose (Glc-α-1,1-α-Glc) by sugarcane NI was assayed under standard conditions with the sugars at a concentration of 100 mM. Protein concentration was determined by the method of Bradford (1976), using gamma globulin as a standard.

4.2.4 Native M_r Determination

Native M_r was determined using a calibrated Biorad Econo Column (1.5 cm x 50 cm) packed with Sephacryl S300 (Pharmacia) to a bed height of 30 cm and equilibrated with elution buffer (HEPES pH 7.2, 200 mM NaCl, 0.02% $Na(N)_3$). An aliquot (1 mL) of the NI sample concentrated after the anion exchange purification

step was applied to the size exclusion column and eluted at a flow rate of 0.5 $mL.min^{-1}$. Fractions (0.6 mL) were collected and assayed for NI activity. Native M_r was estimated from a standard curve of K_{av} (partition coefficient) *vs* log M_r. Standard proteins were prepared from the Combithek (Boehringer Mannheim) M_r standards kit and protein elution was monitored at 280 nm.

4.2.5 Glycosylation State Determination

An aliquot (100 µl) of Concanavalin A (Type III ASCL, Sigma) was incubated with 2 mg of the desalted 20-60% $(NH_4)_2SO_4$ fraction for 5 min. at 25°C and then spun down at 10 000 xg at 4°C for 5 min. An aliquot of the supernatant was removed. Protein and NI activity were determined as described previously (4.2.3).

4.3 Results

4.3.1 Purification of Neutral Invertase

Sugarcane NI was purified to a point of no competing β-fructofuranosidase activity (verified by assay at pH 5.5 and 7.2) by sequential $(NH_4)_2SO_4$ precipitation and anion exchange chromatography. A typical purification produced a 25 fold purification and an 81% yield (Table 4.1). The majority of NI activity was precipitated at 20-60% $(NH_4)_2SO_4$ saturation while obtaining a reasonable degree of purification (Table 4.1). The precipitate was resuspended and desalted which resulted in a dilution of the activity with no significant loss. NI activity eluted from the anion exchange column at *ca* 300 mM NaCl in the linear gradient. Desalting and concentration by ultrafiltration resulted in no significant loss of activity.

Table 4.1. Purification table of a typical purification of NI from mature culm tissue.

Step	Total Protein (mg)	Total Activity (nkat)	Specific Activity (nkat.mg^{-1} protein)	Purification (fold)	Yield (%)
Crude extract	329.1	89.9	0.273	1	100
$(NH_4)_2SO_4$ ppt.	49.0	86.1	1.76	6	96
Anion exchange chromatography	10.5	73.2	6.97	25	81

4.3.2 Kinetic Properties

The purified sugarcane NI displayed a monophasic pH profile (Fig. 4.1) with a pH optimum of 7.2 and half maximal activity at pH 6.4 and 8.2. Sugarcane NI displayed typical hyperbolic saturation kinetics (h = 1) with sucrose as substrate (Fig. 4.2). The K_m and V_{max} of sugarcane NI for sucrose are 9.8 ± 0.37 mM and 7.32 ± 0.092 nkat.mg^{-1} protein, respectively. An Arrhenius plot for the enzyme (Fig. 4.3) showed that it has an energy of activation for sucrose of 62.5 kJ.mol^{-1} below 30°C. A transition occurred, resulting in an energy of activation of –11.6 kJ.mol^{-1} above 30°C. Sugarcane NI showed no significant hydrolysis of cellobiose (Glc-β-1,4-Glc) or trehalose (Glc-α-1,1-α-Glc) at 100 mM.

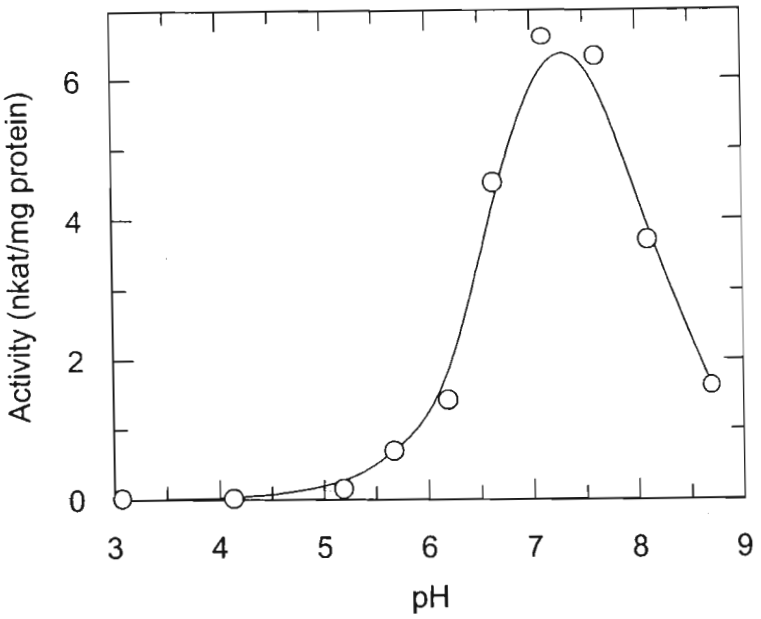

Figure 4.1. The effect of pH on the maximum catalytic activity of sugarcane NI from culm tissue.

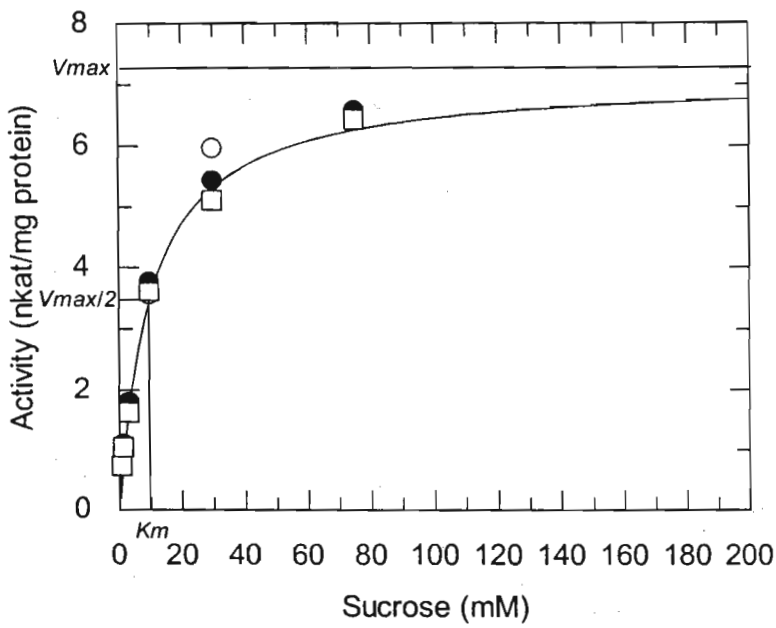

Figure 4.2. Substrate saturation curve for sugarcane NI at pH 7.2. The curve fit was made to the average of three independent determinations of K_m and V_{max}.

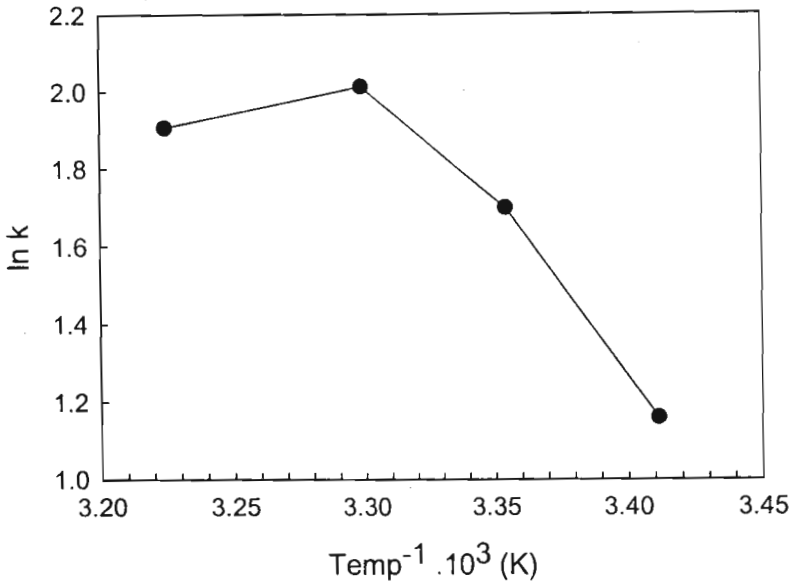

Figure 4.3. The effect of temperature on sugarcane NI activity.

4.3.3 Inhibition

Sugarcane NI is significantly inhibited by Tris at 10 mM (Table 4.2). Sugarcane NI was inhibited by its products fructose and glucose at 10 mM, with fructose being the more effective inhibitor (Table 4.2). In contrast, PEP, citrate, MgATP, MgADP or MgAMP did not significantly inhibit the enzyme at near physiological concentrations (Table 4.2).

Inhibition of the enzyme by a number of metal ions at 1 mM was observed (Table 4.3). Almost complete inhibition was found with $HgCl_2$, $ZnCl_2$, $AgNO_3$ and $CuSO_4$, while only partial inhibition was observed in the presence of $CoCl_2$, $CaCl_2$, $MgCl_2$ and $MnCl_2$ had no effect on enzyme activity.

Table 4.2. Inhibition of sugarcane NI by Tris and various metabolites.

Compound	Inhibition (%)
[a]Tris	85 ± 5.3
[a]Fructose	37 ± 4.1
[a]Glucose	27 ± 7.4
[b]Glucose + Fructose	14 ± 5.3
[c]PEP	1 ± 1.3
[c]Citrate	2 ± 1.5
[c]MgATP	0 ± 0.68
[c]MgADP	2.1 ± 3.5
[c]MgAMP	0.84 ± 1.7

± = s.d. of n = 3

a. 10 mM

b. 5 mM of each hexose

c. 1 mM

Table 4.3. Inhibition of sugarcane NI by metal ions.

Compound (1 mM)	Inhibition (%)
$HgCl_2$	100 ± 7.3
$ZnCl_2$	99 ± 2.4
$AgNO_3$	98 ± 2.1
$CuSO_4$	97 ± 2.6
$CoCl_2$	32 ± 1.8
$CaCl_2$	0 ± 7.0
$MgCl_2$	0 ± 1.7
$MnCl_2$	0 ± 2.5

± = s.d. of n = 3

4.3.4 Molecular Properties and Glycosylation State

Size exclusion chromatography resulted in peaks of NI activity at *ca* 60 kDa, 120 kDa and 240 kDa, suggesting monomeric, dimeric and tetrameric forms of the enzyme. The majority of the activity eluted as the 60 kDa form. The enzyme is probably non-glycosylated, as it was not bound by Concanavalin A.

4.4 Discussion

Sugarcane NI was catalytically active in 240 kDa, 120 kDa and 60 kDa forms. Different forms of sugarcane NI have been reported previously (del Rosario and Santisopasri, 1977). The enzyme was found to elute from a gel filtration column at 160 kDa, 66 kDa, 35 kDa and 15 kDa, suggesting a monomer of M_r 15 kDa aggregating to form a dimer, tetramer and decamer. However, most of the activity eluted as the 66 kDa form. Lower M_r forms of sugarcane NI found previously (del Rosario and Santisopasri, 1977) could be hydrolysis products of a *ca* 66 kDa monomer. Evidence from other sources supports this hypothesis, as the monomeric form of other NI are *ca* 57-65 kDa. Which is a homotetramer of native M_r *ca* 238-260 kDa (Chen and Black, 1992; Van den Ende and Van Laere, 1995; Ross *et al*, 1996) or an octamer of 456 kDa (Lee and Sturm, 1996).

Sugarcane NI displayed a monophasic pH profile, showing that there was no significant competing SAI activity. The pH optimum of sugarcane NI was pH 7.2, which is consistent with that reported previously (Hatch *et al*, 1963). The pH optima of neutral and alkaline invertases purified from other sources vary from pH 6.8-8.0 (Chen and Black, 1992; Van den Ende and Van Laere, 1995; Lee and Sturm, 1996; Ross *et al*, 1996). Sugarcane NI was not bound by Concanavalin A, suggesting that it is not glycosylated, in contrast to a previous report (del Rosario and Santisopasri, 1977). Other NI have been shown to probably be non-glycosylated (Chen and Black, 1992; Van den Ende and Van Laere, 1995; Lee and Sturm, 1996) which, in conjunction with an observed near neutral pH optimum, suggests that the enzyme has a cytosolic localisation.

The K_m of sugarcane NI for sucrose was 9.8 ± 0.37 mM. The K_m of sugarcane NI for sucrose has previously been reported to be 25 mM (Hatch *et al*, 1963) and 0.32 mM (del Rosario and Santisopasri, 1977). The K_m for sucrose of other NI is *ca* 10-20 mM (Chen and Black, 1992; Van den Ende and Van Laere, 1995; Lee and Sturm, 1996; Ross *et al*, 1996). Mature sugarcane culm tissue contains high levels of NI activity (Hatch and Glasziou, 1963; Gayler and Glasziou, 1972; Batta and Singh, 1986; Lingle and Smith, 1991; Dendsay *et al*, 1995). The variation in calculated K_m values for sucrose will not significantly affect the fact that the enzyme will be in substrate saturating conditions, based on the symplastic sucrose concentrations in the sugarcane culm of 110-616 mM (Welbaum and Meinzer, 1990). NI is therefore likely to be partially responsible for the cycle of degradation and synthesis of sucrose that has been found in sugarcane suspension cells (Wendler *et al*, 1990), the immature culm (Sacher *et al*, 1963a) and tissue discs (Glasziou, 1961; Komor *et al*, 1996).

Tris is a potent inhibitor of sugarcane NI as has been found previously (Hatch *et al*, 1963). Inhibition by Tris is also a characteristic of other NI (Chen and Black, 1992; Van den Ende and Van Laere, 1995; Lee and Sturm, 1996; Ross *et al*, 1996).

Sucrose hydrolysis by sugarcane NI obeys hyperbolic saturation kinetics as would be expected from a single substrate enzyme catalysed reaction obeying simple Michaelis-Menten kinetics. Sugarcane NI did not significantly hydrolyse cellobiose (Glc-β-1,4-Glc) or trehalose (Glc-α-1,1-α-Glc), indicating that it is a true β-fructofuranosidase. The energy of activation of sugarcane NI for sucrose below 30°C is the energy of activation for the enzyme catalysed reaction in which temperature dependent effects on the enzyme are negligible. The negative energy of activation observed above 30°C reflects the significant contribution of temp. dependent effects on the enzyme, which result in a decreased rate of the reaction (Cornish-Bowden, 1979). A sugarcane leaf-sheath SAI is reported to undergo a similar transition at 30°C (Sampietro *et al*, 1980). This was postulated

to be a mechanism for the control of *in vivo* enzyme activity when the temp. in the field exceeds 30°C, in mid-summer.

Sugarcane NI was almost completely inhibited by Hg^{2+}, Zn^{2+}, Ag^{+} and Cu^{2+} at 1 mM. Such complete inhibition by Hg^{2+} is consistent with some reports on NI (Chen and Black, 1992; Van den Ende and Van Laere, 1995) but not with others (Lee and Sturm, 1996). This suggests a distinct difference between these enzymes due to the probable requirement of a reduced sulphydryl group in the NI inhibited by Hg^{2+}. Marked differences in the metal ion inhibition profiles of the NI suggests differences in structure related to their catalytic activity.

Sugarcane NI was inhibited by its products, fructose and glucose. At 10 mM fructose was 1.4 times more effective than glucose at inhibiting the enzyme. Fructose is a competitive inhibitor (Van den Ende and Van Laere, 1995; Ross *et al.*, 1996; Lee and Sturm, 1996) and glucose is a noncompetitive inhibitor of NI in other species (Lee and Sturm, 1996). The combined inhibitory effects of glucose and fructose were not additive. This suggests that the inhibitors act at different sites. Similar determinations for NI in other species could not be found. Product inhibition of sugarcane NI may provide a mechanism for the fine control of hexose production and sucrose cycling mediated by sugarcane NI in the cytosol. Product inhibition of sugarcane NI could be significant at the symplastic sugar concentrations of internode two (fructose (55 mM), glucose (62 mM), sucrose (110 mM)) and internode 10 (fructose (11 mM), glucose (7 mM), sucrose (539 mM)), but not at the symplastic sugar concentrations of internode 20 (fructose (2 mM), glucose (0 mM), sucrose (652 mM)) and greater (Welbaum and Meinzer, 1990). High sucrose concentrations would diminish the inhibitory effect of fructose. It must be noted that the symplast data represents possible contributions from both the cytoplasm and vacuole. Knowledge of cytosolic hexose and sucrose concentrations in the sugarcane culm, and further investigation to determine if the same type of inhibition is observed with sugarcane NI will enable a more accurate prediction of the effect of product inhibition on *in vivo* sugarcane NI activity.

In this study, phosphorylated adenine nucleosides (MgATP, ADP and AMP) did not effect any significant inhibition of sugarcane NI unlike the inhibitory effect of MgATP reported for *Daucus carota* L. NI (Lee and Sturm, 1996).

Sugarcane NI has been shown to be positively correlated with hexose levels in the sugarcane culm (Gayler and Glasziou, 1972). Invertase may be relatively more important in comparison to SuSy (E.C. 2.4.1.13) as an enhancer of signals to sugar responsive genes, due to the production of two hexoses (Koch *et al*, 1996). This is particularly relevant in the case of sugarcane NI due to the repression of SAI expression by glucose (Sacher and Glasziou, 1962; Sacher *et al*, 1963b; Glasziou and Waldron, 1964a; Glasziou and Waldron, 1964b), which is a product of invertase and not SuSy.

Sugarcane NI displays many of the characteristics common to other characterised NI. The significance of these characteristics, especially the possible mechanisms of fine control are yet to be determined. Differences in metal ion inhibition profiles between NI indicate differences at the structural level. The involvement of sugarcane NI in sucrose turnover will require the quantification of flux in sugarcane culm tissue; an area investigated in chapters five and six. Sugarcane NI may also play a key role in the control of hexose concentrations in the cytosol of sugarcane culm cells, thus effecting control over the expression of sugar responsive genes. The exact role of sugarcane NI remains unknown.

Chapter 5

Sucrose Turnover and Sugar Compartmentation

5.1 Introduction

Cyclic pathways are common structures in metabolism. A special case of a cyclic pathway has been recognised and classed as a substrate or 'futile cycle' (for discussion, see Fell, 1997). In sugarcane, a substrate or 'futile cycle' of particular interest and potential commercial value is that of sucrose synthesis and degradation, mediated by SPS, SuSy and the invertases. The cycle of sucrose synthesis and degradation has been observed in sugarcane cell suspension cultures (Wendler *et al.*, 1990) and in the sugarcane culm (Glasziou, 1961; Sacher *et al.*, 1963a). In the study of Sacher *et al.* (1963a) it was concluded that the cycling would be characteristic of only those tissues with high acid invertase activity.

The study of Glasziou (1961) was conducted on immature storage tissue in which it was calculated that the maximum turnover time of the sucrose pool would be 46 hours in internodes four to five, which represents a significant rate of sucrose degradation. It has also been shown that in maize root tips a 'futile cycle' of sucrose turnover consumes 69% of the ATP produced by mitochondrial respiration (Dieuaide-Noubhani *et al.*, 1995) which is lower than that found in banana tissue (Hill and ap Rees, 1994). Both studies emphasise the magnitude of the investment that plants have to make to maintain sucrose turnover in some tissues. Evidence of invertase mediated sucrose turnover in sugarcane culm tissue has been presented in chapter three. Levels of invertase activity to support this turnover are present in high sucrose containing tissue (chapter three; Botha *et al.*, 1996; Vorster and Botha, 1999).

The lack of information on metabolic flux and compartmentation of metabolites in higher plants has been recognised as a major factor limiting the understanding of metabolic control (ap Rees and Hill, 1994). Sugarcane is no exception, the highly compartmented nature of both the culm and cell add to the complexity when interpreting experimental results. This and the intractable nature of the culm have been identified as reasons why this system, once regarded as simple, is difficult to investigate (Moore, 1995).

In this chapter, the sucrose turnover in sugarcane storage parenchyma tissue of the sugarcane cultivar NCo376 is investigated. Carbon allocation is also investigated using ^{14}C pulse labelling experiments. The rate of label increase and relative distribution of label between metabolite pools provides information on the rate of metabolic turnover and the distribution of the metabolites between compartments.

5.2 Materials and Methods

5.2.1 Plant Materials

Tissue of sugarcane cultivar NCo376 was obtained from the field at the SASA Experiment Station, Mt Edgecombe, South Africa, in midsummer (Jan-Mar). Tissue samples were obtained from culms that were cut in the early morning. Internode one is defined as the internode above the node from which the leaf with the first exposed dewlap originates. Internodes three and four are considered to be immature tissue, and internodes nine and 10 mature tissue, based on sucrose levels.

5.2.2 Invertase and Sugar Determinations

Enzyme extractions, invertase assays, and sugar determinations were performed as described in 3.2.

5.2.3 Labelling with Glucose or Fructose

Longitudinal cores of culm tissue were excised using a cork borer (5 mm I.D.) from multiple sugarcane culms. Transverse discs, 0.5 mm in diameter, were sliced using a hand microtome fitted with a custom insert with 0.5 mm diameter holes for tissue support during slicing. Sliced tissue was washed according to Lingle (1989). Randomised tissue discs were then incubated in 1.5 mL 25 $mmol.L^{-1}$ K-MES (pH 5.7) containing mannitol (250 $mmol.L^{-1}$), glucose and fructose (5 $mmol.L^{-1}$). [U-^{14}C]Glucose or [U-^{14}C]Fructose (2.0 $GBq.mmol^{-1}$) was added to the incubation buffer. The labelled hexose and the non-labelled hexose in the external medium are referred to as the source and non-source hexoses respectively. The labelled substrates were vacuum-infiltrated into the tissues for 1 min. Tissues slices were then incubated at 28 °C in airtight flasks (250 mL) on a rotary shaking incubator at 175 rpm. CO_2 was collected in 500 µL 12 % (w/v) KOH. Discs were removed at intervals and washed for 3x5 min in 15 mL 25 $mmol.L^{-1}$ K-MES (pH 5.7) containing 250 $mmol.L^{-1}$ mannitol and 1 $mmol.L^{-1}$ $CaCl_2$ to remove apoplastic label similar to that of Lingle (1989) prior to metabolite extraction.

5.2.4 Metabolite Extraction and Fractionation

Liquid nitrogen frozen tissue slice material was ground to a fine powder and cellular components extracted in 15 mL methanol:chloroform:water (12:5:3 by vol) (Dickson, 1979). The water-soluble pool was passed through tandem cation (Dowex AG 50W, 200-400 mesh, H form) and anion (Dowex AG 1-X8, 100-200 mesh, Cl) exchangers. Metabolites were eluted according to Dickson (1979) to yield the neutral sugar, amino acid, organic acid and sugar phosphate components. The neutral sugar containing fraction was dried down in a rotary evaporator at 40 to 50 °C, the residue was dissolved in HPLC grade H_2O. Sugar samples were then passed through prewashed Sep-Pak Alumina A cartridges (Millipore Corporation, Waters Chromatography Division, Milford, MA) and filtered through 0.22 µm Millex-GV4 filters (Millipore Corporation, Bedford, MA).

5.2.5 Metabolite Analysis

Sugars were resolved by HPLC on a Supelcosil LC-NH_2 column (Supelco Inc, Bellefonte, PA, USA) over 20 min by isocratic elution (acetonitrile:water, 80:20) at a flow rate of 1.5 $mL.min^{-1}$. ^{14}C in sucrose, glucose and fructose was quantified with a Packard Flo-one Beta in-line isotope detector. Ultima Flo scintillant was used at a ratio of 2:1. Extraction efficiencies for sucrose, glucose and fructose were 92 ± 7 %. ^{14}Carbon in the fractions was determined by liquid scintillation spectroscopy using a Packard Tricarb 1900 TR using Ultima Gold XR quench resistant scintillation cocktail. Isotope detection equipment and scintillants were from Packard Instrument Company, Meriden, CT.

5.2.6 Protein Determination

Protein was determined by the method of Bradford (1976) using the BioRad (Richmond, CA) micro assay with gamma globulin as a standard.

5.3 Results

5.3.1 Sucrose Synthesis and Breakdown

Internode seven sugarcane tissue discs containing almost maximum sucrose load were fed ^{14}C-Fructose for five hours and then chased for six hours with unlabelled hexose. The increase in sucrose and glucose specific activities over time were used to calculate sucrose synthesis and invertase mediated sucrose hydrolysis (Fig. 5.1). Rate calculations were based on the assumption that the cytosolic volume was 10% of the total cellular volume and the hexoses were of uniform concentration and specific activity between compartments unless stated otherwise. The sucrose synthesis rate was calculated using the sucrose total activity change from T_0 of the chase to 3 hr and a fructose specific activity of that at T_0 of the chase. The sucrose hydrolysis rate was calculated using the glucose total activity change from T_0 of the chase to 3 hr and a sucrose specific activity of that at T_0 of the chase. Rates of 42 $nmol.min^{-1}.g^{-1}$ fw synthesis of sucrose and 15

$nmol.min^{-1}.g^{-1}$ fw hydrolysis of sucrose were calculated. Hydrolysis would be due to invertase as return of label to glucose could only be via invertase and not SuSy.

Internode three and six sugarcane culm tissue discs from a ripe sugarcane culm were fed either ^{14}C-Glucose or ^{14}C-Fructose. Specific activities of sugars were measured over time (Table 5.1). The change in specific activities of the sucrose and the respective hexoses were used to calculate the rates of sucrose synthesis and breakdown (Table 5.2). All rate calculations used the difference in activity between the 60 and 120 min. time points. Three methods were used to calculate the sucrose synthesis rate. Method one assumes that the hexose label is uniformly distributed within the cell and the sugar phosphate pool is the specific activity of the external medium. Method two assumes that the hexose label is uniformly distributed within the cell and the sugar phosphate pool is the average specific activity of the hexoses between 60 and 120 min. Method three assumes that the hexose label is exclusively in the cytosol and the sugar phosphate pool is the average specific activity of the hexoses between 60 and 120 min. The rate of sucrose synthesis was greater in internode three than internode six (Table 5.2). The rate of sucrose synthesis for the ^{14}C-Glucose feeding experiment is greater than the ^{14}C-Fructose feeding experiment (Table 5.2).

Two methods were used to calculate the rates of sucrose breakdown (Table 5.2). Method one assumes that the label is uniformly distributed within the cell and the specific activity of the sucrose pool is the average of 60 and 120 min. Method two assumes that the label is exclusively in the cytosol and the specific activity of the sucrose pool is the average of 60 and 120 min. The rate of sucrose breakdown was greater in internode three than in internode six. The rate of sucrose hydrolysis from the ^{14}C-Fructose feeding experiments exceeded that of the ^{14}C-Glucose feeding experiments (Table 5.2). The sucrose synthesis rate was greater than the breakdown rate when comparing rates with the same assumptions i.e. synthesis (rate 2) vs breakdown (rate 1) or synthesis (rate 3) vs breakdown (rate 2) (Table 5.2).

Table 5.1. Specific activities of metabolite pools from tissue disc labelling experiments using ^{14}C-Glucose or ^{14}C-Fructose in the presence of 5 mM of each hexose.

			Specific Activity (Bq.µmol^{-1})		
Internode	Labelled (source) Hexose	Time (min.)	Glucose	Fructose	Sucrose
3	Glucose	0	0	0	0
		60	32.27	20.06	119.1
		120	39.67	25.25	282.6
	Fructose	0	0	0	0
		60	7.577	25.54	81.80
		120	14.53	56.42	150.3
6	Glucose	0	0	0	0
		60	219.1	0	6.598
		120	312.7	0	11.56
	Fructose	0	0	0	0
		60	0	87.19	3.377
		120	0	107.4	4.348

Table 5.2. Sucrose synthesis and breakdown for internodes three and six of sugarcane culm.

Internode	Labelled sugar	Synthesis rate ($nmol.min^{-1}.g^{-1}$ fw)			Breakdown rate ($nmol.min^{-1}.g^{-1}$ fw)	
		Rate 1[a]	Rate 2[b]	Rate 3[c]	Rate 1[d]	Rate 2[e]
3	Glucose	3.039	5112	511.2	17.89	1.789
	Fructose	1.273	2412	241.2	20.12	2.012
6	Glucose	0.4299	159.4	15.94	0	0
	Fructose	0.08399	85.10	8.510	0	0

a. Sugar phosphate pool is the specific activity of the external medium.

b. The hexose label is uniformly distributed within the cell. The sugar phosphate pool is the average specific activity of the hexoses between 60 and 120 min.

c. The hexose label is exclusively in the cytosol. The sugar phosphate pool is the average specific activity of the hexoses between 60 and 120 min.

d. The label is uniformly distributed within the cell. The specific activity of the sucrose pool is the average of 60 and 120 min.

e. The label is exclusively in the cytosol. The specific activity of the sucrose pool is the average of 60 and 120 min.

5.3.2 Compartmentation of Sugars

The release of $^{14}CO_2$ was measured during a pulse of ^{14}C-Fructose and a chase with both hexoses of internode seven sugarcane culm tissue discs. The decrease in the specific activity of the hexose pool (Fig. 5.1) was not consistent with the rapid decrease in $^{14}CO_2$ release after the pulse (Fig. 5.2). Sucrose specific activity was greater than that of the hexoses (Fig. 5.1). The release of $^{14}CO_2$ was measured during a pulse-chase labelling of sugarcane culm tissue discs from internodes three and six (Fig. 5.3). An initial pulse of 180 min. with ^{14}C-Fructose was followed by a chase of 360 min. with 5 mM of each cold hexose. Internode three showed a higher rate of $^{14}CO_2$ release than internode six. The ratio of the $^{14}CO_2$ release for internodes three and six to the time zero of the chase was calculated. Internode six showed a more rapid relative decrease in $^{14}CO_2$ release than internode three (Fig. 5.4).

Internode three and six sugarcane culm tissue discs from a ripe sugarcane culm were fed either ^{14}C-Glucose or ^{14}C-Fructose. Specific activities of sugars were measured over time (Table 5.1). The specific activity of both hexoses is lower than that of sucrose in internode three while the specific activity of the source hexose is greater than sucrose in internode six (Table 5.1). The specific activity of the source hexose is consistently greater than the specific activity of the non-source hexose (Table 5.1).

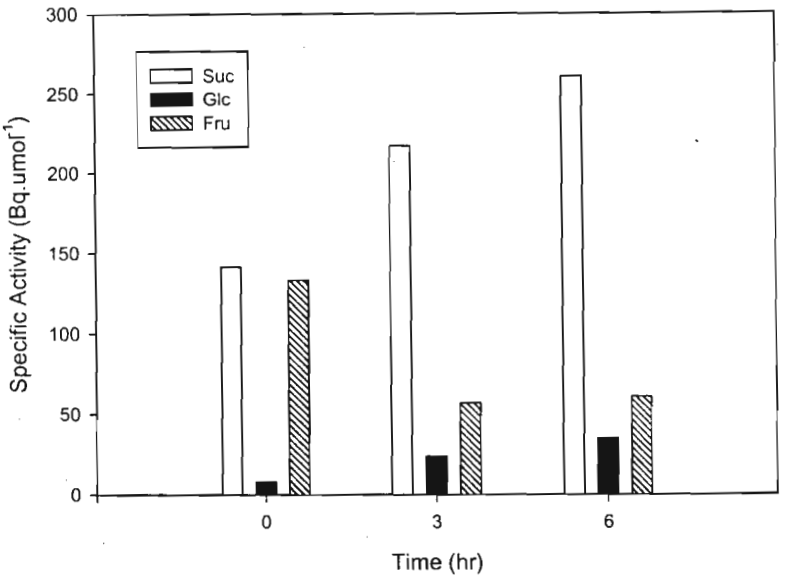

Figure 5.1. Specific activities of sucrose, glucose and fructose. Tissue discs (internode seven) were pulsed for five h with 370 kBq [U]^{14}C-Fructose and chased with 50 mM each of glucose and fructose.

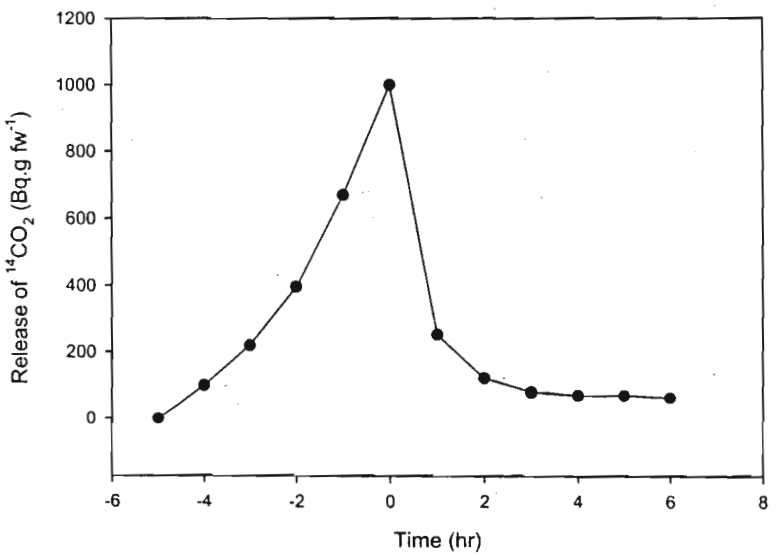

Figure 5.2. Release of $^{14}CO_2$ from sugarcane tissue discs. Tissue discs (internode seven) were pulsed for five h with 370 kBq [U]^{14}C-Fructose and chased with 50 mM each of glucose and fructose. Cold chase initiated at time zero.

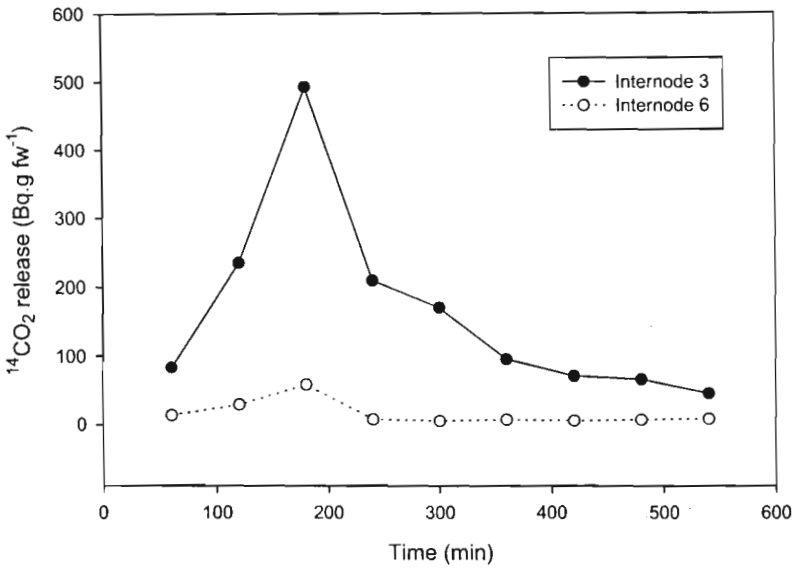

Figure 5.3. Release of $^{14}CO_2$ during a pulse-chase labelling of sugarcane tissue discs with [U]^{14}C-Fructose (T_{180} = T_0 of cold chase).

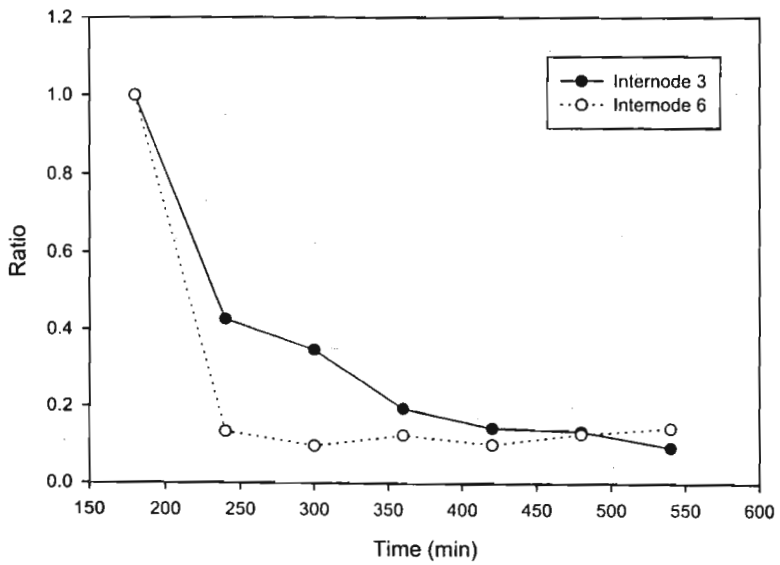

Figure 5.4. Ratio of $^{14}CO_2$ release to T_0 of cold chase after a pulse with [U]^{14}C-Fructose. Tissue slice material from internodes three and six.

5.3.3 Percentage Distribution of Carbon

Total label distribution in sugarcane culm tissue fed ^{14}C-Glucose was determined over time. The use of randomised tissue discs from multiple sugarcane culms resulted in the average behaviour being measured. Smaller immature internodes contained less sample material and were a factor in the decision to use randomised discs from multiple culms. It was also decided to obtain more time points rather than replicate samples per time point.

Tissue was removed at regular time intervals over a 180 min. pulse labelling. For comparative purposes, data was normalised and expressed as a percentage distribution. Label was fractionated into water/alcohol, lipid, insoluble matter and $^{14}CO_2$ with the majority of the label appearing in the water/alcohol and insoluble matter fractions (Fig. 5.5). Internode three had a far lower proportion of label in the water alcohol fraction than that of internodes six and 12 (Fig. 5.5A). All three tissue maturities showed a gradual decrease in the percentage label in the lipid fraction (Fig. 5.5B). The percentage label appearing in the insoluble matter fraction shows internode three having a far greater proportion than that of internodes six and 12 (Fig. 5.5C). The percentage of total label released as $^{14}CO_2$ varied considerably with no significant differences between the internodes or observable trends (Fig. 5.5C). Developmentally, the difference in the percentage distribution in the two major fractions is greatest between internodes three and six with internodes six and 12 showing a far less significant change in distribution (Fig. 5.5A and Fig. 5.5C).

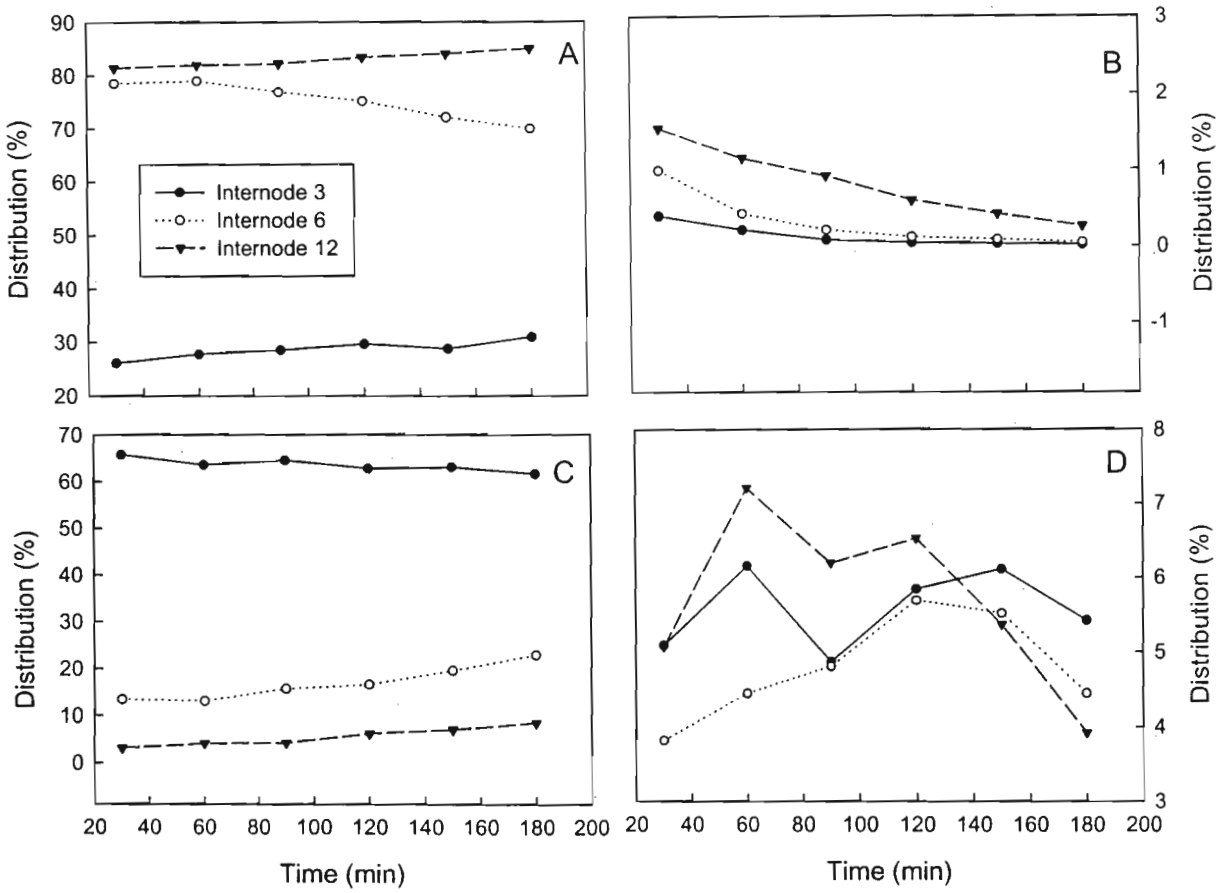

Figure 5.5. Total label distribution in sugarcane culm tissue discs. Tissue was fed [U]^{14}C-Glucose. Water/alcohol fraction (A), lipid (B), insoluble matter (C), $^{14}CO_2$ (D).

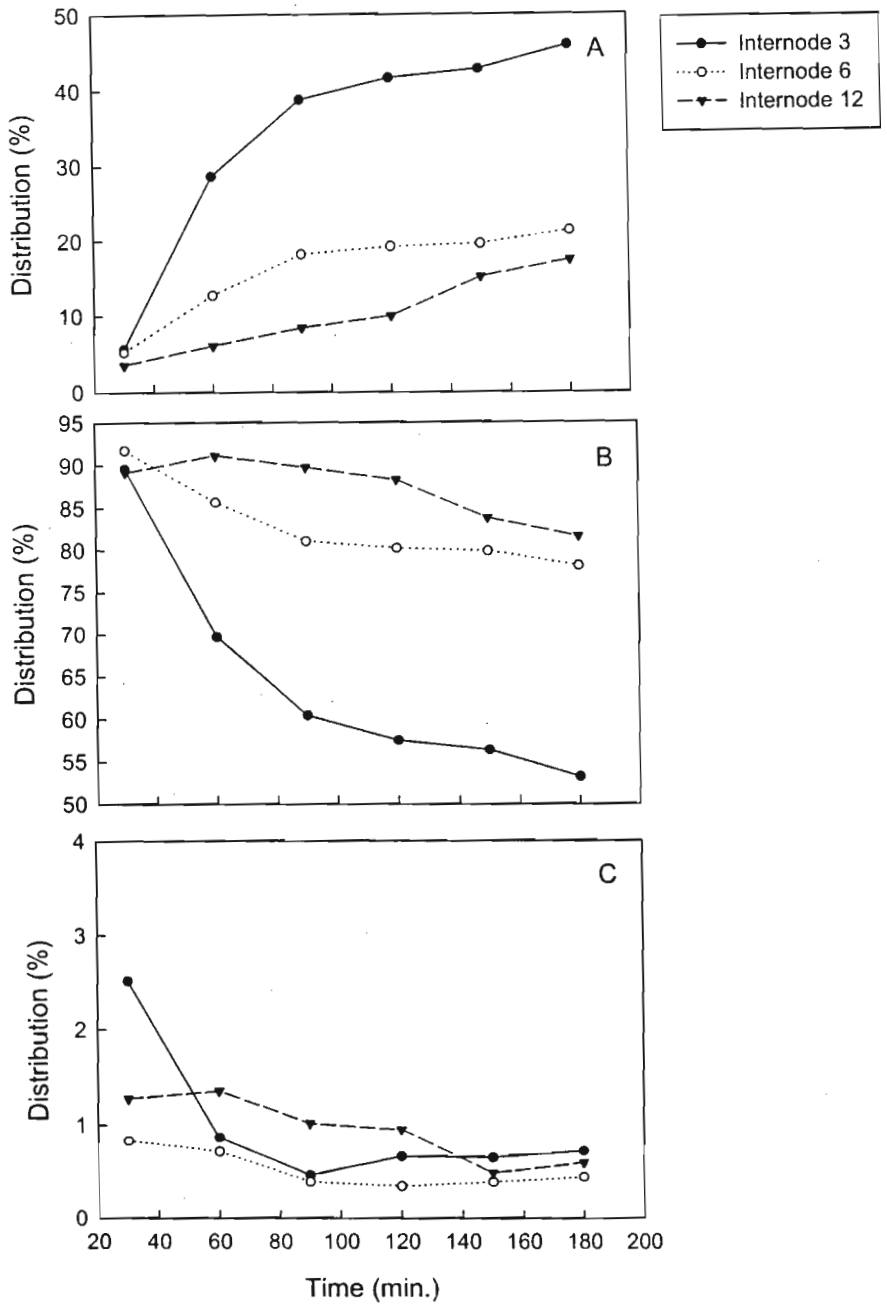

Figure 5.6. Label distribution in the water/alcohol fraction. Tissue was fed [U]^{14}C-Glucose. Anionic (A), neutral (B), cationic (C).

The water/alcohol fraction was further fractionated into anionic, neutral and cationic fractions (Fig. 5.6). At time zero, very little label appears in the anionic fraction (Fig. 5.6A), with the majority of the label in the neutral fraction (Fig. 5.6B). During the pulse the percentage of label increases in the anionic (Fig. 5.6A) fraction with a concomitant decrease in the neutral fraction (Fig. 5.6B). The rate of increase in the percentage distribution of label in the anionic fraction of internode three is far greater than that of internodes six and 12 (Fig. 5.6A). Developmentally, the difference in the percentage distribution is far greater between internodes three and six than between internodes six and 12. A steady state distribution of label between the fractions was not attained during this time period. The hyperbolic shape (Fig. 5.6A) indicates a movement toward a steady state distribution as a percentage of total label. The cationic fraction (Fig. 5.6C) showed an initial decrease and then a relatively stable distribution with no significant differences between internodes.

5.4 Discussion

5.4.1 Sucrose Synthesis and Breakdown

Results obtained from the ^{14}C-Fructose pulse-chase experiments (Fig. 5.1) enabled the estimation of invertase-mediated carbon flux from sucrose. The appearance of label in glucose in these experiments was ascribed to the action of both neutral and acid invertases (Wendler *et al.*, 1990). Label transported to the vacuole as ^{14}C-Sucrose, would equilibrate with cytosolic sucrose and hexoses after inversion via acid invertase. Consequently, the increase in the specific activity of glucose was used to calculate an invertase mediated flux from sucrose. The rates of 42 nmol.min^{-1}.g^{-1} fw synthesis of sucrose and 15 nmol.min^{-1}.g^{-1} fw hydrolysis of sucrose were significant for sugarcane culm tissue containing almost maximum sucrose load. These fluxes were consistent with a regulated invertase activity for internode seven (chapter three) and well within the capacity of SPS (Botha *et al.*, 1996), which is the primary contributor to sucrose synthesis in internode seven (Whittaker and Botha, 1997). The rate of sucrose synthesis

exceeded that of sucrose hydrolysis as would be expected for a sucrose accumulating tissue. However, in a region of the sugarcane culm that is almost at the sucrose plateau (Whittaker and Botha, 1997), a significant cycle of sucrose synthesis and degradation was observed. This is in agreement with the cycle observed in sugarcane suspension cells (Wendler *et al.*, 1990; Goldner *et al.*, 1991) and that shown previously for culm tissue (Komor *et al.*, 1996).

In order to investigate sucrose synthesis and the relative contributions of invertases and SuSy to sucrose breakdown, internode three and six culm tissue discs were fed either ^{14}C-Glucose or ^{14}C-Fructose (Table 5.1). In this experiment, both internodes displayed sucrose synthesis but only the internode three tissue showed evidence of sucrose breakdown (Table 5.2). Sucrose synthesis rates were calculated using different assumptions about the distribution of label. These calculated rates represent the lower and upper extremes of the rates of sucrose synthesis (Table 5.2). The assumption that the sugar phosphate pool had the same specific activity as the external input metabolite was supported by the work of Viola (1996). In this investigation, the same assumption was made to determine its influence on the rate calculation. It resulted in the calculated synthesis rate one being low due to the high estimated specific activity of the internal hexose pool.

A more accurate estimation of the sugar phosphate pool specific activity was that of the average of the two hexose specific activities. The broad range of rates (Table 5.2) demonstrates the uncertainty in flux calculation without knowledge of the distribution of label between the intracellular compartments. The rates of sucrose breakdown were calculated (Table 5.2), with the same assumptions about the distribution of label. When comparing synthesis and breakdown rates with common assumptions, the synthesis rate always exceeded the rate of sucrose breakdown. This was expected for a sucrose accumulating tissue such as sugarcane culm tissue. It must be noted that sucrose breakdown may have been occurring in the internode six tissue. The level of label in the non-source hexose was below the detection limit. The relatively short duration of the experiment in comparison to that conducted on internode seven internodal tissue (Fig. 5.1), would have contributed significantly. The low specific activity of the

sucrose pool (Table 5.1) in comparison to that of Fig. 5.1 supports this hypothesis. Simulation of the system using a computer based flux model presented in chapter six provides additional insight into this observation.

5.4.2 Compartmentation of Sugars

The rapid decrease in $^{14}CO_2$ (Fig. 5.2) relative to the decrease in specific activities of the sugars (Fig. 5.1) indicated the existence of two sugar pools, probably the cytoplasm and vacuole. Previous work on sugarcane using pulse-chase experiments showed that two compartments of sucrose exist (Glasziou, 1961). Later investigations on compartmentation and the cyclical nature of sucrose accumulation supported these findings (Sacher *et al.*, 1963a).

To further investigate compartmentation and metabolite turnover in internode three and six sugarcane storage parenchyma tissue, the release of $^{14}CO_2$ was measured during a pulse-chase experiment (Fig. 5.3). The higher rate of label release of internode three tissue (Fig. 5.3) is a reflection of the higher sugar uptake rate of younger internodal tissue and/or a higher rate of respiration (Komor *et al.*, 1996). The higher uptake rate of internode three would have resulted in a higher specific activity of the glycol tic and TCA cycle metabolites. This would have increased the specific activity of the $^{14}CO_2$ released through respiration. A higher rate of respiration in internode three would have also increased the amount of radioactivity released.

The ratio of $^{14}CO_2$ to the T_0 of the chase (Fig. 5.4) indicates that the internode six cytosolic label was removed more rapidly than that of internode three. This could have been a reflection of a larger cytosolic sugar and organic acid pool in internode three and/or a longer turnover time of these pools. This would have caused the rate of release of $^{14}CO_2$ to decrease more slowly in internode three than internode six. Interestingly, both internodes reached an apparent plateau ratio of approximately 0.1 (Fig. 5.4). Label in $^{14}CO_2$ toward the end of the chase would have been derived from the vacuolar pool of label, which had a lower turnover rate. This common basal ratio could therefore reflect a common ratio of label that is being returned from the vacuole. This could be due to the combined

effects of the specific activities of the vacuolar sugars and the rates of transfer from the vacuole to the cytosol. Return of hexose from the vacuole to the cytosol is thought to be by diffusion across the tonoplast (Moore, 1995). Any difference in hexose concentration between the cytosol and the vacuole would therefore directly influence the rate of labelled hexose return. Once in the cytosol the sugars are accessible to respiration. Due to the lack of information on the specific activity and rates of transfer of compartmented sugars, it is not possible to determine which of these is the major contributing factor.

The specific activities of sugars during the timecourse labelling of internodes three and six tissue discs with either ^{14}C-Glucose or ^{14}C-Fructose provided interesting information on sugar compartmentation. The specific activity of the source hexose is greater than that of the non-source hexose (Table 5.1). In a single compartment system, the specific activity of the source hexose would be greater than the specific activity of the non-source hexose. Assuming the same distribution between the cytosol and vacuole for the hexoses, this would also be true for a two compartment system. The cytosolic pool of the source hexose receives label from the high specific activity external medium and sucrose breakdown, whereas the non-source hexose only receives label from sucrose breakdown. This is the case for both internode three and internode six (Table 5.1). The non-source hexose specific activity is less than the sucrose specific activity in internodes three and six (Table 5.1). This is what would be expected as the non-source hexose label is derived from sucrose. If all sugars were in a single compartment, the specific activity of the non-source hexose would approach the specific activity of sucrose. That is assuming complete randomization of label within the sucrose molecule; otherwise the specific activity of the hexose moiety of sucrose in question would be approached. The distribution of label within the sucrose molecule will influence the rate of label increase in the non-source label hexose. The difference between source and non-source hexose specific activities in internode six is much greater than internode three (Table 5.1). This indicates that a significant change has occurred in the distribution of label from internodes three to six.

An assumption for rate calculations has been that the cytosol contains 10% and the vacuole 90% of the cellular volume. Assuming equal concentrations of sugars in the cytosol and the vacuole the percentage cellular volume would reflect the molar percentage distribution of the sugars. Using the assumptions stated, the sucrose specific activity could not exceed ten times that of the source hexose specific activity. The sucrose specific activities of internode three and six are below this limit (Table 5.1). The low sucrose specific activity in internode six is caused by reduced uptake rates and the higher sucrose load of the tissue (Table 5.1). This would also contribute to the non-source hexose label being below the detection limit.

A significant observation is that the source hexose specific activity is lower than the sucrose specific activity for internode three (Table 5.1). Sucrose label is derived from the hexose phosphates, which are synthesized from both hexoses. In a single compartment system, the sucrose specific activity would therefore be greater than the non-source hexose specific activity and less than the source hexose specific activity. The sucrose specific activity for internode three is greater than the source and non-source hexose specific activity (Table 5.1). This is possible in a two compartment system due to the reduction of the average specific activity of the hexoses by the vacuolar hexose pool. This effect would be enhanced by increasing the vacuolar:cytosolic hexose molar ratio. The effect of the manipulation of the sugar vacuolar:cytosolic molar ratio on the labelling profiles is investigated using a computer based flux model in chapter six.

5.4.3 Carbon Allocation

The distribution of label from tissue fed ^{14}C-Glucose was followed during a continuous feeding experiment of internodes three, six and 12 (Fig. 5.5 and Fig. 5.6). Internode three had a far lower percentage of label in the water/alcohol fraction than internodes six and 12 (Fig. 5.5A) and a far greater percentage in the insoluble fraction (Fig. 5.5C). This is in agreement with the observation that the young internodes are actively growing and directing carbon toward the biosynthesis of structural polysaccharides (Whittaker and Botha, 1997). There is a greater difference in percentage distribution between internodes three and six

than between internodes six and 12 even though the age difference is double between internodes six and 12 than that between internodes three and six. This indicates that significant changes influencing the control of the distribution of carbon between the major fractions occur between internodes three and six. The lipid (Fig. 5.5B) and the $^{14}CO_2$ (Fig. 5.5D) did not form a significant portion of the label.

The percentage of label in $^{14}CO_2$ is similar to that found previously (Whittaker and Botha, 1997). The percentage label released over time as $^{14}CO_2$ does not show any apparent trend based on the maturity of the internode; as values are relatively close and change rank over time (Fig. 5.5D). The consistency of the percentage distribution does indicate that the $^{14}CO_2$ forms a constant percentage of the total label. This could be due to the $^{14}CO_2$ being derived from the anionic fraction, which increases as a percentage of the water/alcohol fraction over time (Fig. 5.6A). This would result in the rate of $^{14}CO_2$ release increasing with the increase in the anionic percentage. The lack of appreciable change in proportional contribution of the water/alcohol fraction to the total label distribution (Fig. 5.5A) would suggest that the proportional contribution of $^{14}CO_2$ to the total label distribution (Fig. 5.5D) would reflect the increase observed in the anionic fraction (Fig. 5.6A). The lack of this observation cannot be explained given the current data set, although the release of $^{14}CO_2$ under experimental conditions using a higher amount of labelled metabolite and tissue showed very a definite trend (Fig. 5.2). Further investigation of this area under experimental conditions similar to those used for the internode seven experiment may produce results with observable trends.

Gradual trends can be observed over time. Internode three exhibited an increase in percentage label while internode six showed a decrease and internode 12 a very slight increase in the water/alcohol fraction (Fig. 5.5A). A similar trend, which mirrors that of the water/alcohol fraction, is observable in the insoluble fraction (Fig. 5.5C). This could be a reflection of the relative rates of these pools competing for label and the effects of approaching a steady state percentage of label. The initial decrease in the lipid fraction may indicate that the pool received

label early but decreased as a percentage with time due to the other larger pools accumulating label.

The water/alcohol fraction was further fractionated (Fig. 5.6). In all tissues the anionic fraction (Fig. 5.6A) began with a very low percentage of label and the neutral fraction (Fig. 5.6B) with a high percentage. The neutral fraction is known to primarily consist of sucrose, glucose and fructose in sugarcane (Whittaker and Botha, 1997). The majority of the label was initially in the neutral fraction as would be expected due to the tissue being fed ^{14}C-Glucose. Label as a percentage of the water/alcohol fraction increased with time in the anionic fraction (Fig. 5.6A) and decreased in the neutral fraction (Fig. 5.6B).

Internode three shows a far more noticeable change in distribution than internodes six and 12. (Fig. 5.6A and 5.6B). The distinct hyperbolic shapes of the curves for internode three indicate that it is approaching a steady state percentage distribution of label within the time frame of this experiment. This may also be true for internode six, although the shape is less obvious. Knowledge of the final steady state distributions would enable a comparison of the different internodes progress toward that steady state.

The cationic fraction showed an initial decrease (Fig. 5.6C), and rapidly became an insignificant proportion of the label. The difference in the trend between the anionic and cationic fractions could be due to the cationic fraction being smaller than the anionic fraction (Whittaker and Botha, 1997). The cationic fraction would therefore approach isotopic equilibrium more rapidly due to the shorter turnover time. It would become a lower percentage of the total label as the larger pools accumulated more label.

5.4.4 General Conclusion

Sucrose is synthesised at a rate that is greater than the rate of breakdown at all stages of maturity in sugarcane culm tissue. Sucrose is hydrolysed by invertase in sugarcane culm tissue that has reached the sucrose plateau. The rates of sucrose cycling are potentially energetically wasteful. Roles have been proposed

for the cycle of sucrose synthesis and degradation; conclusive proof remains to be presented (Fell, 1997).

Two intracellular compartments of sugars exist, namely the cytosol and the vacuole (Moore, 1995). A more rapid turnover of the internode six cytosolic label pools occurs than internode three. This indicates that internode three has a larger cytosolic pool and/or a longer turnover time than internode six.

Carbon allocation is in agreement with previous work (Whittaker and Botha, 1997). The main competing pools are the insoluble and neutral fractions. As the tissue matures, less carbon is allocated to the insolubles and more enters the neutral fraction. The neutral fraction consists mainly of the sugars sucrose, glucose and fructose. Developmentally, the greatest change in carbon allocation occurs from internodes three to six.

Chapter 6

Metabolic Flux Model

6.1 Introduction

The determination of metabolic flux within a system that is a target for metabolic engineering is invaluable. Metabolic control theory provides a theoretical framework within which metabolic control analysis can be performed (Kacser and Burns, 1973). Core information is the determination of the fluxes within the metabolic system. The determination of metabolic flux enables the assessment of the impact of the manipulation of enzyme activities.

Estimation of metabolic flux by labelling experiments and modelling has been performed in animals, plants and protozoa (for review, see Salon and Raymond, 1988). A number of experimental and modelling approaches have been followed, depending on the nature of the metabolic network, and the amount and type of information available. Sugarcane storage parenchyma tissue presents more challenges than the model systems used in many metabolic flux determinations. This is due to the large metabolic pool sizes, long turnover times, and the intractable nature of the sugarcane stem tissue. These factors limit the experimental methods and conditions that can be utilised. Furthermore, the experimental data obtained for metabolites are often the average of multiple compartments. This leads to an underdetermined system, that is not amenable to the linear algebraic methods used to determine fluxes in determined or over determined systems.

Experimental systems are distinguished as being in metabolic steady state or non-steady state and in isotopic steady state or non-steady state. Systems in metabolic and isotopic steady state are the most convenient to solve. In

sugarcane it may be assumed that metabolic quasi-steady state exists in the time frame of a labelling experiment. In tissue that contains large pools of metabolites, such as the sugarcane internode, it is not possible to attain isotopic steady state within a realistic experimental time period. Isotopic non-steady state must therefore be assumed. Isotopes commonly employed in labelling experiments are ^{13}C or ^{14}C. Not all systems are suitable for the application of ^{13}C due to the need for a substantial increase in the specific activity of metabolites above the natural 1.1% abundance. Systems with large pools of a metabolite of interest are therefore inaccessible, as is the case with sugarcane.

Due to practical considerations and time constraints, flux estimation in sugarcane was investigated using specifically and uniformly labelled ^{14}C metabolites. Additional considerations that affected experimental design were compartmentation and bidirectional fluxes. For a discussion of the analysis of metabolic networks see, Blum and Stein (1982). Estimations of the relative *in vivo* contributions of NI, SAI and SuSy to sucrose turnover in sugarcane have been made through feeding of ^{14}C labelled glucose or fructose (Komor *et al.*, 1996). Here a computer flux model based on an approach similar to that of Sherwood *et al.* (1979) for the simulation of tracer experiments has been developed. The change in specific activity of metabolic pools was followed over time and used to investigate *in vivo* flux and compartmentation of sugars. A significant advancement used here is the application of a global optimization algorithm which employs a box bounded strategy, with limits, linear and non-linear constraints.

Sugarcane maturation coincides with the accumulation of sucrose in the sugarcane culm (Gayler, 1972; for review see Moore, 1995). Carbon partitioning changes down the sugarcane culm reflecting changes in the metabolism with a redirection of carbon from water insoluble matter to sucrose (Whittaker and Botha, 1997). The profiles of percentage distribution of label in internodes three, six and 12 indicate that the greatest developmental changes occur between internodes three and six (chapter five). This is supported by the distinctly different labelling profiles within the neutral fractions of internodes three and six (chapter five). An observation of particular interest is the difference in specific activity of the source and non-source hexoses. The development of a mathematical

metabolic flux model of the system will provide insight into the mechanisms responsible for the observed differences. A clearer understanding of the *in vivo* fluxes and metabolite compartmentation will aid in the interpretation of the changes in sugarcane metabolism that occur with maturation. This will also aid in the estimation of the significance of sucrose turnover in sugarcane culm tissue. The model provides the foundation for further investigation.

6.2 Modelling Framework

6.2.1 Experimental Data

Experimental data for the model was derived from chapter five.

6.2.2 Model Implementation Platform

The model is a form of compartment model. The metabolic network is described by a series of differential equations. The implementation follows a similar methodology to that of Sherwood *et al.* (1979) and Blum and Stein (1982). The flux model is implemented in MATLAB version 5 (The Math Works Inc., NJ, USA) using the ODE45 solver of differential equations. The use of the technical computing environment provided in MatLab vastly improves the productivity and the reliability of the model development process.

6.2.3 *Euclidean n-space* Reduction

Conservation of mass relations and stoichiometries are used to solve for flux parameters using the symbolic math toolbox of MatLab version 5. The number of independent flux parameters was reduced from 17 to seven.

6.2.4 Model Optimization

Optimization of the model is achieved using the algorithm 'DIRECT' (Jones, 1999). The algorithm is based on a box bounded strategy. This is one of the only global optimization algorithms that ensures the entire parameter space is

explored. It is more efficient than a combinatorial search of parameter space, which becomes impractical due to the exponential increase in the number of simulations required with each additional independent parameter. A limitation of a standard box bounded approach is the inability to apply linear and non-linear constraints. The implementation of the algorithm DIRECT, as a standalone version in the file gclsolve.m in the MatLab toolbox, TomLab (Applied Optimization and Modelling (TOM), Center for Mathematical Modelling (CMM), Dept of Mathematics and Physics (IMa), Malardalen University, Vasteras, Sweden) incorporates the capacity to implement linear and non-linear constraints. This vastly improves the practical value of the optimization algorithm. In the current form, the mass balance criteria are met as a result of the parameter space reduction, which included the mass balance equations as part of the system of equations used to solve for the flux parameters. This will not necessarily be true for all systems in which case the linear constraints will force the model to solve for parameter sets that satisfy the mass balance criteria.

A particular problem was that of the model finding solutions that contained negative fluxes. The independent flux parameters are guaranteed to be in positive parameter space due to the box bounded limits placed on them. This does not ensure that the dependent flux parameters will always be positive. The dependent flux parameters can be expressed in terms of the independent flux parameters. The equations describing the dependent flux parameters in terms of the independent flux parameters were derived manually. They were then implemented as linear constraints in the optimization algorithm. This ensured that the model would be optimized for parameter sets that were physiologically meaningful.

Experimental data sets had either glucose or fructose as the source ^{14}C labelled hexose. The heavier isotope is thought to have no discernable effect on the metabolism of metabolites (Northrop, 1981). Data for each hexose was generated in the same experiment under identical conditions other than the labelled hexose. The rates within the system for each data set for a particular internode should therefore be comparable. This experimental design provided two data sets for each internode that could be used simultaneously for optimization of the model.

A simple non-weighted error statistic was employed, which was the sum of the square of the deviation of the model output from the experimental data. The error was calculated for each of the interpolated glucose source and fructose source data sets. The objective function that was minimised, was the sum of the two error statistics generated for the two interpolated experimental data sets. This resulted in the minimisation of the deviation of the model output from the interpolated experimental data for both the glucose and fructose source data. The best performing model parameter sets were used in the graphical visualisation.

The optimization algorithm does not have stopping criteria other than the total number of iterations or function evaluations. This is partly due to the fact that it is a global optimization algorithm. The density of the search should be determined by the resources available and what is acceptable to the operator. The optimization algorithm was run for $1x10^5$ function evaluations. Further optimization was performed by restricting the optimization to the local parameter space of the best parameter set of the primary global optimization.

6.2.5 Data Visualisation

As a result of the need to visualise the results graphically for interpretation, an automated chart generation tool was developed. Charts were plotted for the combined metabolite pool activities vs the interpolated experimental data activities. Model simulation points were generated at 15 min. intervals. The change in activity of individual pools was plotted to aid in the interpretation of the combined pool activities.

6.2.6 Model Notation

The model is described using a modified notation of Sherwood *et al.* (1979), where external pools are represented using the standard notation below.

m = total moles (labelled and unlabelled)
m^* = moles of labelled material
A_{ij} = flux from pool j to pool i
n = no. of non-external pools
nt = total no. of pools, some of which are external

In total moles, flux of label into pool j is:

$$\frac{dm_j^*}{dt} = \sum_{i=1}^{nt} A_{ji}(m_i^* / m_i) - \sum_{i=1}^{n} A_{ij}(m_j^* / m_j) \qquad (6.1)$$

Using specific activity, $y = m^* / m$ equation 6.1 becomes under steady state pool size:

$$\frac{dy_j}{dt} = \frac{1}{m_j}\left(\sum_{i=1}^{nt} A_{ji}y_i - \sum_{i=1}^{n} A_{ij}y_j\right) \qquad (6.2)$$

6.2.7 Model Assumptions

1. SuSy was assumed to both cleave and synthesize sucrose.

2. The sugar phosphates: UDP-Glc, Glc-1-phosphate, Glc-6-phosphate and Fru-6-phosphate were treated as a single metabolic pool (Viola, 1996). The metabolites were regarded as being in rapid equilibrium relative to the sugars: glucose, fructose and sucrose. Fru-1,6-bisphosphate was treated as being in equilibrium with the triose phosphates. For the purpose of pool size estimation it was assumed that Fru-1,6-bisphosphate does not form a part of pool m_3 (Table

6.3). This does not affect the interpretation of the results as the model was optimized against the combined pools m_3 and m_{10} (Table 6.3).

3. If ^{14}C-Fructose were fed to sugarcane tissue, ^{14}C-Glucose would result from the cleavage of sucrose by invertase. If ^{14}C-Glucose were fed to sugarcane tissue ^{14}C-Fructose would have resulted from the cleavage of sucrose by invertase and SuSy.

4. Total label moving out of the system with no significant return of label within the experimental period was assumed to be: $^{14}CO_2$, fibre, lipids and organic acids.

5. Metabolic steady state was assumed for all of the metabolic pools except sucrose. Sucrose was recognized as being in metabolic non-steady state as this is a characteristic of sugarcane tissue. However, due to the large pool size it was treated as being in a quasi-steady state within the time frame of the experiment for the purpose of specific activity calculations.

6. It was recognized that it was not possible to reach isotopic steady state within a realistic experimental time period due to the sizes of the metabolic pools.

7. Hexose uptake is assumed to be at a constant rate as determined by linear regression of the total label uptake over the 120 min. labelling period.

8. A relatively short experimental time period was adopted to minimize any time dependent effects on sliced internodal tissue.

6.2.8 Conceptual Structure

All of the metabolic fluxes from the graphical representation (Fig. 6.1) of the metabolic network have been described in the flux label key (Table 6.1). All stoichiometric relationships between metabolic pools in the metabolic scheme are 1:1 (Fig 6.1). The change in the specific activity of state variables is described according to equation 6.2 in equations 6.3 - 6.12.

Table 6.1. Model flux label key.

Symbol Key [a]	Matrix Key [b]	Description
a	$A_{3,1}$ [c]	Glc_{cyt} to SugP (Glucokinase)
b	$A_{8,1}$ [c]	Glc_{cyt} to Glc_{vac} (Diffusion)
c	$A_{3,2}$ [c]	Fru_{cyt} to SugP (Fructokinase)
d	$A_{4,2}$ [c]	Fru_{cyt} to Suc-Fru_{cyt} (SuSy Synthesis)
e	$A_{9,2}$	Fru_{cyt} to Fru_{vac} (Diffusion)
f	$A_{4,3}$	SugP to Suc-Fru_{cyt} (SPS)
g	$A_{6,3}$ [c]	SugP to Suc-Glc_{cyt} (SPS + SuSy Synthesis)
h	$A_{10,3}$	SugP to $Total_{out}$ (Output to TCA and external pools)
I	$A_{2,4}$ [c]	Suc-Fru_{cyt} to Fru_{cyt} (NI + SuSy Degradation)
j	$A_{5,4}$	Suc-Fru_{cyt} to Suc-Fru_{vac} (Suc Active Transport)
k	$A_{9,5}$	Suc-Fru_{vac} to Fru_{vac} (Acid Invertase)
l	$A_{1,6}$	Suc-Glc_{cyt} to Glc_{cyt} (NI)
m	$A_{3,6}$	Suc-Glc_{cyt} to SugP (SuSy Degradation)
n	$A_{7,6}$	Suc-Glc_{cyt} to Suc-Glc_{vac} (Sucrose Active Transport)
o	$A_{8,7}$	Suc-Glc_{vac} to Glc_{vac} (Acid Invertase)
p	$A_{1,8}$	Glc_{vac} to Glc_{cyt} (Diffusion)
q	$A_{2,9}$ [c]	Fru_{vac} to Fru_{cyt} (Diffusion)
r	f_1	Glc_{ext} to Glc_{cyt} (Glucose Uptake)
s	f_2	Fru_{ext} to Fru_{cyt} (Fructose Uptake)

[a] identifier for the symbolic math

[b] flux matrix location or flux vector location

[c] independent flux parameters

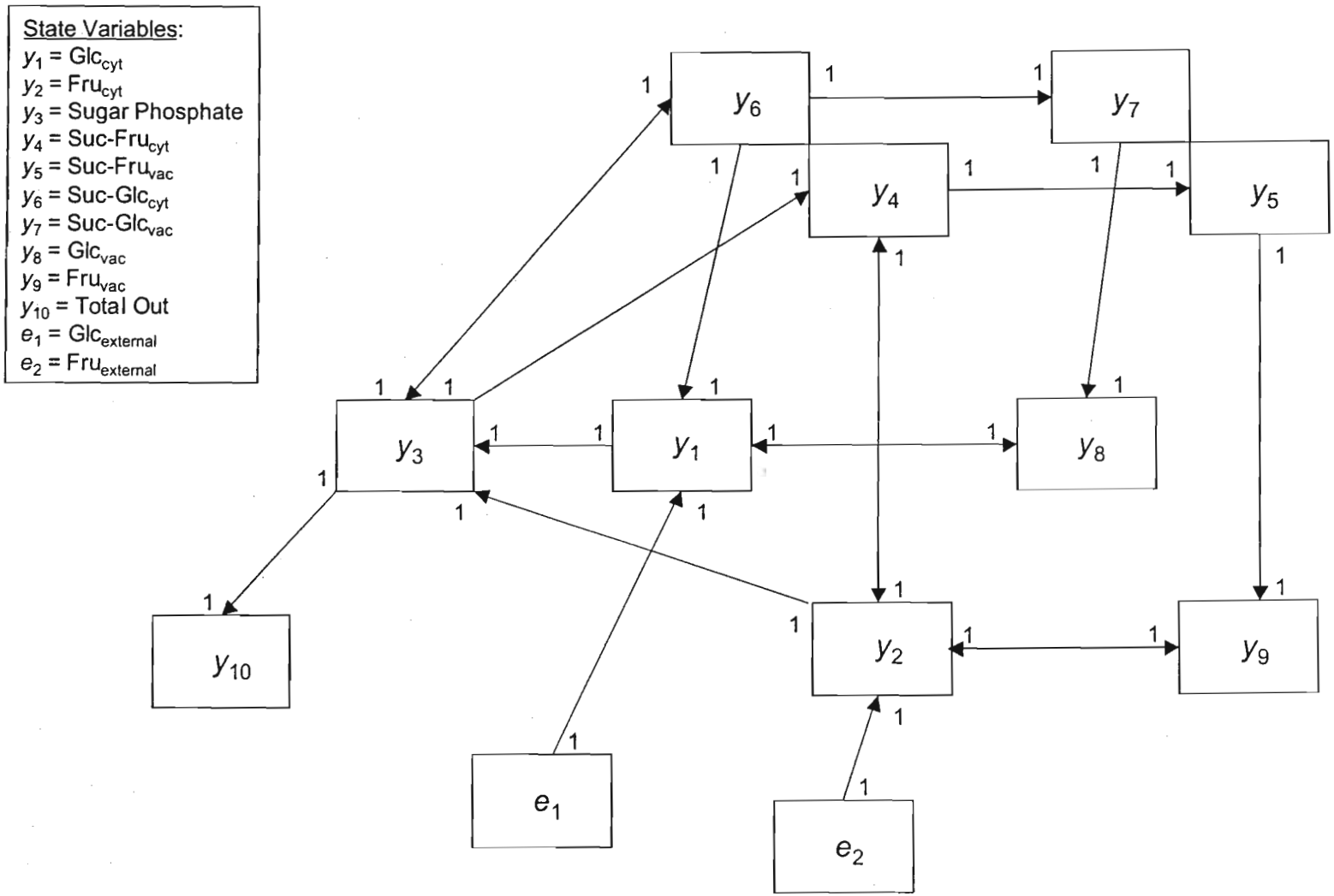

Figure 6.1. Sugarcane sucrose Metabolism Metabolic Model Network.

6.2.9 Differential Equations

$$\frac{dy_1}{dt} = \frac{1}{m_1}((A_{1,6}y_6 + A_{1,8}y_8 + f_1e_1) - y_1(A_{3,1} + A_{8,1})) \quad (6.3)$$

$$\frac{dy_2}{dt} = \frac{1}{m_2}((A_{2,4}y_4 + A_{2,9}y_9 + f_2e_2) - y_2(A_{3,2} + A_{4,2} + A_{9,2})) \quad (6.4)$$

$$\frac{dy_3}{dt} = \frac{1}{m_3}((A_{3,1}y_1 + A_{3,2}y_2 + A_{3,6}y_6) - y_3(A_{4,3} + A_{6,3} + A_{10,3})) \quad (6.5)$$

$$\frac{dy_4}{dt} = \frac{1}{m_4}((A_{4,2}y_2 + A_{4,3}y_3) - y_4(A_{2,4} + A_{5,4})) \quad (6.6)$$

$$\frac{dy_5}{dt} = \frac{1}{m_5}((A_{5,4}y_4) - y_5(A_{9,5})) \quad (6.7)$$

$$\frac{dy_6}{dt} = \frac{1}{m_6}((A_{6,3}y_3) - y_6(A_{1,6} + A_{3,6} + A_{7,6})) \quad (6.8)$$

$$\frac{dy_7}{dt} = \frac{1}{m_7}((A_{7,6}y_6) - y_7(A_{8,7})) \quad (6.9)$$

$$\frac{dy_8}{dt} = \frac{1}{m_8}((A_{8,1}y_1 + A_{8,7}y_7) - y_8(A_{1,8})) \quad (6.10)$$

$$\frac{dy_9}{dt} = \frac{1}{m_9}((A_{9,2}y_2 + A_{9,5}y_5) - y_9(A_{2,9})) \quad (6.11)$$

$$\frac{dy_{10}}{dt} = \frac{1}{m_{10}}(A_{10,3}y_3) \quad (6.12)$$

The parameters e_1 and e_2 represent the external hexose specific activities in each experiment; f_1 and f_2 are the input flux rates for the external source hexoses.

6.2.10 Conservation of Mass Relations

The conservation of mass relations are described by equations 6.13 to 6.22. Metabolic steady state is assumed for metabolite pools m_1, m_2, m_3, m_8 and m_9. Metabolite pools m_4, m_5, m_6, m_7 and m_{10} are in non-steady state. $\ddot{A}(m_4 + m_5 + m_6 + m_7)$ is assumed to be negligible relative to the sucrose pool size for the purpose of

specific activity calculations within the experimental time frame. It is therefore in a metabolic quasi-steady state. Stoichiometric relationships are included.

$$\frac{dm_1}{dt} = (A_{1,6} + A_{1,8} + f_1) - (A_{3,1} + A_{8,1}) = 0 \quad (6.13)$$

$$\frac{dm_2}{dt} = (A_{2,4} + A_{2,9} + f_2) - (A_{3,2} + A_{4,2} + A_{9,2}) = 0 \quad (6.14)$$

$$\frac{dm_3}{dt} = (A_{3,1} + A_{3,2} + A_{3,6}) - (A_{4,3} + A_{6,3} + A_{10,3}) = 0 \quad (6.15)$$

$$\frac{dm_4}{dt} = (A_{4,2} + A_{4,3}) - (A_{2,4} + A_{5,4}) \geq 0 \quad (6.16)$$

$$\frac{dm_5}{dt} = (A_{5,4}) - (A_{9,5}) \geq 0 \quad (6.17)$$

$$\frac{dm_6}{dt} = (A_{6,3}) - (A_{1,6} + A_{3,6} + A_{7,6}) = \frac{dm_4}{dt} \quad (6.18)$$

$$\frac{dm_7}{dt} = (A_{7,6}) - (A_{8,7}) = \frac{dm_5}{dt} \quad (6.19)$$

$$\frac{dm_8}{dt} = (A_{8,1} + A_{8,7}) - (A_{1,8}) = 0 \quad (6.20)$$

$$\frac{dm_9}{dt} = (A_{9,2} + A_{9,5}) - (A_{2,9}) = 0 \quad (6.21)$$

$$\frac{dm_9}{dt} = A_{10,3} > 0 \quad (6.22)$$

6.2.11 Constraints

6.2.11.1 Internode Three

Dependent flux parameters were expressed in terms of the independent flux parameters $A_{3,1}$, $A_{8,1}$, $A_{3,2}$, $A_{4,2}$, $A_{6,3}$, $A_{2,4}$ and $A_{2,9}$. The vector *xl* represents the lower bound for each of the independent parameters listed above in the order listed (Eq. 6.26). Similarly, the vector *xu* represents the upper bounds of the independent parameters (Eq. 6.27). These vectors were used as the input to the optimization

algorithm as the box bounded limits. Upper bounds for the independent flux parameters were set to physiologically feasible values and the optimization results were compared to limits obtained by experimental measurement (Table 6.2).

The matrix *Al* represents the linear constraint equations used to ensure that positive parameter space is searched and physiologically meaningful relationships are maintained between flux parameters (Eq. 6.23). The matrix contains the coefficients of the independent parameters, listed above in the same order, by column. The matrix rows are the constraints for the properties: $A_{9,2}$; $A_{4,3}$; $f_1 + f_2 \geq \frac{dm_{10}}{dt} \geq 0$; $A_{9,5}$; $A_{1,6}$; $A_{3,6}$; $A_{1,8}$; $\frac{dm_4}{dt} \geq 0$; $\frac{dm_5}{dt} \geq 0$; $\frac{dm_5}{dt} \geq \frac{dm_4}{dt}$ and $SPS_{synth} \geq SuSy_{synth}$. The vector *bl* is the lower bounds on the linear constraints (Eq. 6.28), as the vector *bu* is the upper bound on the linear constraints (Eq. 6.29). The lower bounds were determined by the limit on the constraint that would always be greater than or equal to zero. Optional non-linear constraints were derived for the vacuolar:cytosolic sucrose accumulation ratio and SPS:SuSy sucrose synthesis ratio (Eq. 6.24 - 6.25).

$$Al = \begin{bmatrix} 0 & 0 & -1 & -1 & 0 & 1 & 1 \\ 0 & 0 & 0 & -1 & 1 & 0 & 0 \\ 0 & 0 & 2 & 2 & -2 & 0 & 0 \\ 0 & 0 & 1 & 1 & 0 & -1 & 0 \\ 1 & 0 & -1 & -1 & 0 & 1 & 0 \\ -1 & 0 & 1 & 1 & 0 & 0 & 0 \\ 0 & 1 & 1 & 1 & 0 & -1 & 0 \\ 0 & 0 & 0 & 0 & 1 & -2 & 0 \\ 0 & 0 & -1 & -1 & 0 & 2 & 0 \\ 0 & 0 & -1 & -1 & -1 & 4 & 0 \\ 0 & 0 & 0 & -2 & 1 & 0 & 0 \end{bmatrix} \qquad (6.23)$$

$$\frac{SucAcc_{vac}}{SucAcc_{cyt}} = \frac{-A_{3,2} - A_{4,2} + 2A_{2,4} + f_2}{A_{6,3} - 2A_{2,4}} \quad (6.24)$$

$$\frac{SPS_{synth}}{SuSy_{synth}} = \frac{A_{4,3}}{A_{4,2}} \quad (6.25)$$

$$xl = \begin{bmatrix} 0 \\ 0 \\ 0 \\ 0 \\ 0 \\ 0 \\ 0 \end{bmatrix} \quad (6.26) \qquad xu = \begin{bmatrix} 0.05 \\ 0.05 \\ 0.05 \\ 0.05 \\ 0.05 \\ 0.05 \\ 0.05 \end{bmatrix} \quad (6.27)$$

$$bl = \begin{bmatrix} -0.009884 \\ 0 \\ -0.009135 \\ 0.009884 \\ 0.009135 \\ -0.009135 \\ 0.009884 \\ 0 \\ -0.009884 \\ -0.009884 \\ 0 \end{bmatrix} \quad (6.28) \qquad bu = \begin{bmatrix} 0.05 \\ 0.05 \\ 0.05 \\ 0.05 \\ 0.05 \\ 0.05 \\ 0.05 \\ 0.05 \\ 0.05 \\ 0.05 \\ 0.05 \end{bmatrix} \quad (6.29)$$

6.2.11.2 Internode Six

The internode six model parameter optimization was simplified due to the lack of significant sucrose breakdown and sucrose synthesis by SuSy. This enabled the model to be optimized for the vacuolar:cytosolic ratio of glucose, fructose and sucrose. The vectors *xl* and *xu* (Eq. 6.30 - 6.31) represent the lower and upper

bounds of the flux parameter $A_{4,3}$, and the vacuolar:cytosolic ratios of glucose, fructose and sucrose in descending order.

$$xl = \begin{bmatrix} \mathbf{0} \\ \mathbf{10} \\ \mathbf{10} \\ \mathbf{10} \end{bmatrix} \qquad (6.30) \qquad xu = \begin{bmatrix} \mathbf{0.01} \\ \mathbf{1000} \\ \mathbf{1000} \\ \mathbf{1000} \end{bmatrix} \qquad (6.31)$$

6.2.12 Experimental Data

Rate limits of enzymes (Table 6.2) were obtained from various sources. NI and SAI activities are derived from chapter three, while other activities are from Whittaker PhD thesis, 1997 and Botha *et al.*, 1996. As an initial assumption the model compartments are 90% vacuolar and 10% cytosolic by volume. Sugars are assumed to be at equal concentration in the two compartments. Total molar amounts of sugars in each compartment are shown (Table 6.3), data obtained from Whittaker PhD thesis, 1997.

The average specific activity of two mixed pools (glucose and fructose) was calculated using equation 6.32. The average specific activity of four mixed pools (sucrose) was calculated using equation 6.33.

$$\bar{y}_{(a+b)} = \frac{m_a{}^* + m_b{}^*}{m_a + m_b} \qquad (6.32)$$

$$\bar{y}_{(a+b+c+d)} = \frac{m_a{}^* + m_b{}^* + m_c{}^* + m_d{}^*}{m_a + m_b + m_c + m_d} \qquad (6.33)$$

Experimental specific activities were obtained during a 120 min. pulse labelling of internode three and six culm tissue with either ^{14}C-Glucose or ^{14}C-Fructose (Table 6.4). Both hexoses were present in the external medium at a concentration of 5 mM. The constant specific activity of the two external pools e_1 and e_2 was 4.93 x 10^4

$Bq.\mu mol^{-1}$. An additional initial condition is that all internal pools have a specific activity of zero at time zero. The total of the output pool m_{10} (Table 6.3) is set at an arbitrary value for the convenience of simulation.

Table 6.2. Experimentally determined limits and constraints on fluxes for internodes three and six.

Flux Label		Internode 3 Rate ($nmol.min^{-1}.g^{-1}$ fw)	Internode 6 Rate ($nmol.min^{-1}.g^{-1}$ fw)	Description
$A_{3,1}$	≤	19.2	13.8	Glucokinase
$A_{8,1}$	≤	50	50	Cyt to Vac diffusion (Glc)
$A_{3,2}$	≤	30.6	15	Fructokinase
$A_{4,2}$	≤	44.4	51.8	SuSy (Suc Synth Fru)
$A_{4,3}$	≤	22.2	25.9	SPS
$A_{6,3}$	=	$A_{4,3} + A_{4,2}$	$A_{4,3} + A_{4,2}$	SPS + SuSy Synth
$A_{2,4}$	=	$A_{3,6} + A_{1,6}$	$A_{3,6} + A_{1,6}$	SuSy Cleavage + NI (Cyt Fru)
$A_{1,6}$	≤	29.9	25.4	NI
$A_{3,6}$	≤	47.1	44.2	SuSy (Cleavage)
$A_{2,9}$	≤	50	50	Vac to Cyt diffusion (Fru)
f_1	=	19.019	4.952	Glc Uptake
f_2	=	9.884	2.551	Fru Uptake

Table 6.3. Metabolite pool concentrations. Note. $m_4 = m_6$ and $m_5 = m_7$

Pool Label	Internode 3 ($\mu mol.g^{-1}$ fw)	Internode 6 ($\mu mol.g^{-1}$ fw)	Description
m_1	3.1	0.6	Glc_{cyt}[a]
m_2	2.7	1.5	Fru_{cyt}[a]
m_3	0.08	0.05	Sugar Phosphate[b]
m_4	2.75	12.8	Suc-Fru_{cyt}[a]
m_5	24.75	115.2	Suc-Fru_{vac}[a]
m_6	2.75	12.8	Suc-Glc_{cyt}[a]
m_7	24.75	115.2	Suc-Glc_{vac}[a]
m_8	27.9	5.4	Glc_{vac}[a]
m_9	24.3	13.5	Fru_{vac}[a]
m_{10}	100	100	Total Output

a. Assuming a vacuolar:cytosolic molar ratio of 9:1.

b. Excluding Fru-1,6-bisphosphate.

Table 6.4. Total radioactivity in specific metabolite pools from tissue disc labelling experiments, using ^{14}C-Glucose or ^{14}C-Fructose in the presence of 5 mM of each hexose.

			Activity (Bq.g^{-1} fw)			
Internode	Labelled Sugar	Time (min.)	Glucose[a]	Fructose[b]	Sucrose[c]	Total output[d]
3	Glucose	0	0	0	0	0
		60	1000.521	541.6667	6551.563	39552.28
		120	1229.688	681.7708	15542.19	99465.67
	Fructose	0	0	0	0	0
		60	234.8958	689.5833	4498.958	23786.66
		120	450.5208	1523.438	8265.104	48298.94
6	Glucose	0	0	0	0	0
		60	1314.583	0	1689.063	15152.95
		120	1876.042	0	2960.417	22726.86
	Fructose	0	0	0	0	0
		60	0	1307.813	864.5833	8566.776
		120	0	1611.458	1113.021	10782.6

a. Glucose: $m_1^{\cdot}+m_8^{\cdot}$

b. Fructose: $m_2^{\cdot}+m_9^{\cdot}$

c. Sucrose: $m_4^{\cdot}+m_5^{\cdot}+m_6^{\cdot}+m_7^{\cdot}$

d. Total out: $m_3^{\cdot}+m_{10}^{\cdot}$

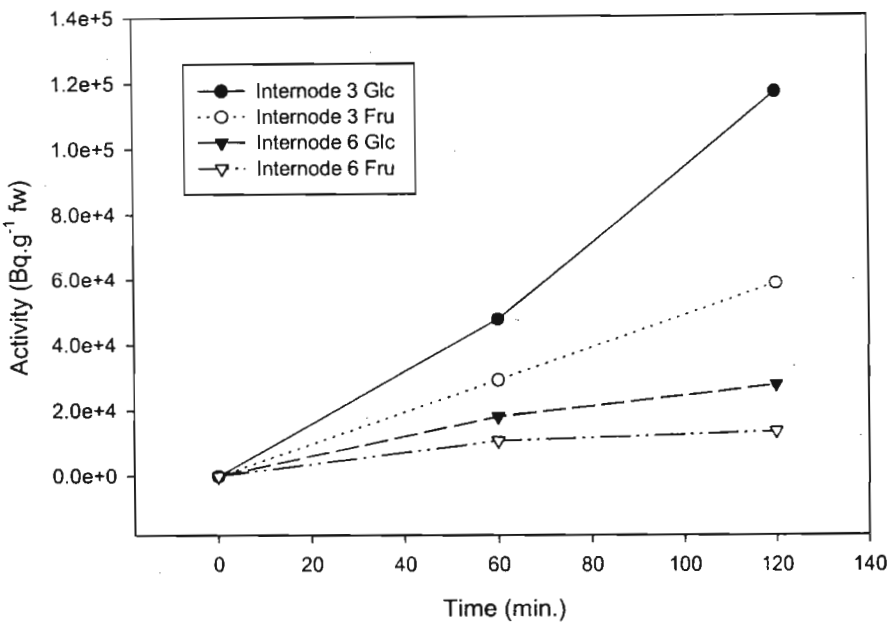

Figure 6.2. Total label uptake for internodes three and six with glucose and fructose external labelled hexose.

6.3 Results and Discussion

The metabolic flux model was developed as a tool to investigate *in vivo* flux and compartmentation in sugarcane culm tissue discs. A primary objective was to determine if the model design could describe the difference in labelling profiles observed between internodes three and six in chapter five. The model network is based on the underlying metabolic pathways of plant carbohydrate metabolism. The design takes the specific attributes of sugarcane carbohydrate metabolism into consideration. Intuitively, the change in the labelling profiles observed in chapter five agree with the transition of the internodal tissue from that of active growth to a primarily sucrose storing tissue, with tissue maturation. What are the changes in metabolic flux that result in the transition?

Previous work has used conventional approaches and has not followed labelling of metabolites over time (Gayler and Glasziou, 1972; Komor *et al.*, 1996; Whittaker and Botha, 1997). Sugars in the sugarcane storage parenchyma cell are compartmented (Moore, 1995). The inability to experimentally determine the distribution of sugars and label between compartments leads to an underdetermined model. This is recognised as a fundamental problem of complex metabolic networks, especially when using data from conventional approaches (Bonarius *et al.*, 1997). Here, a flux model is used to investigate the behaviour of the system. This includes, the fluxes between pools, compartmentation, and the change of the total and specific activities of the constituent and combined metabolite pools.

Table 6.5. Model optimization parameter sets used for simulation for internodes three and six.

Flux Parameter	Rate ($nmol.min^{-1}.g^{-1}$ fw)	
	Internode 3 [b]	Internode 6 [c]
$A_{3,1}$ [a]	31.855211	4.952
$A_{8,1}$ [a]	0.0102884	0
$A_{3,2}$ [a]	18.724139	2.551
$A_{4,2}$ [a]	4.032781	0
$A_{9,2}$	1.89284	0
$A_{4,3}$	8.930323	0.469
$A_{6,3}$ [a]	12.963104	0.469
$A_{10,3}$	28.722631	6.566
$A_{2,4}$ [a]	6.462006	1×10^{-7}
$A_{5,4}$	6.462006	0.469
$A_{9,5}$	6.410913	1×10^{-7}
$A_{1,6}$	6.425297	1×10^{-7}
$A_{3,6}$	0.0367087	0
$A_{7,6}$	6.462006	0.469
$A_{8,7}$	6.410913	1×10^{-7}
$A_{1,8}$	6.421202	0
$A_{2,9}$ [a]	8.303753	0
f_1	19.019	4.952
f_2	9.884	2.551

[a] independent flux parameters

[b] Glc, Fru and Suc vacuolar:cytosolic ratio = 499:1

[c] Vacuolar:cytosolic ratio (Glc = 350:1, Fru = 962:1, Suc =987:1)

6.3.1 Optimization

The total label uptake was approximately linear over the time frame of the experiment for internodes three and six (Fig. 6.2). This is an important observation for the purpose of steady state flux determination. A non-linear uptake rate would imply that the internal fluxes were not constant and would complicate the flux determination considerably. The rate of hexose uptake is known to decrease with sugarcane storage parenchyma maturation (Moore, 1996). This is supported by the experimental data used for the flux model, where the internode six uptake rate is less than that of internode three (Fig. 6.2).

Optimization of the model for the experimental data (Table 6.4) resulted in the best performing data sets being selected for each internode (Table 6.5). The model was optimized by minimising the deviation of the model output from the experimental total activities of both source hexose labelling experiments. Interpolation was used to increase the number of data points available for the optimization. Minimisation of the deviation from the total activity ($Bq.g^{-1}$ fw) was used rather than the specific activity ($Bq.\mu mol^{-1}$) as it is independent of metabolite pool size.

Initial optimizations of the model did not fit the source hexose in internode three, even when relaxing boundary conditions of the model. This indicated that an assumption of the model may be restricting the models capacity to simulate the source hexose labelling. Intuitively, the first assumption to manipulate would be the distribution of the sugars between the compartments. The significance of the distribution of the sugars between the vacuolar and cytosolic compartments has been indicated in chapter five. By increasing the vacuolar:cytosolic sugar molar ratio from the initial 9:1 to 499:1, the model performance was improved for internode three (Fig. 6.3 and 6.5). Altered molar ratios are assumed to be the result of altered metabolite pool concentrations and not altered intracellular compartment volume ratios.

The model did not optimize well for internode six using the same strategy as that employed for internode three. The significant difference in the labelling profiles between internodes three and six provides some insight into the possible differences in the metabolic fluxes (Fig. 6.3, 6.5, 6.7, 6.9). Intuitively, one would expect a relatively low rate of sucrose turnover in internode six. Additionally, the relative contribution of SPS would increase, and that of SuSy would decrease with tissue maturation (Whittaker PhD thesis, 1997). The solution would be difficult to find using the same strategy as that employed for internode three due to the solution values for some fluxes being found near the parameter bounds. The optimization was therefore simplified by excluding flux parameters which could be assumed to be near zero. This also afforded the luxury of being able to optimize the vacuolar:cytosolic ratio of sucrose, glucose and fructose.

The model optimization found a reasonable fit for the internode six data (Fig. 6.7, 6.9). The model may appear to be performing poorly for the internode six non-source hexose data (Fig. 6.7B, 6.9A), this is however an acceptable fit to the experimental data. This can be explained by the activity for the non-source hexose in the internode six tissue being set to an arbitrarily low level for optimization purposes. The levels were effectively below instrumentation detection limits. The activity simulated by the model is well below the detection limit and is therefore considered to be comparable to the experimental data.

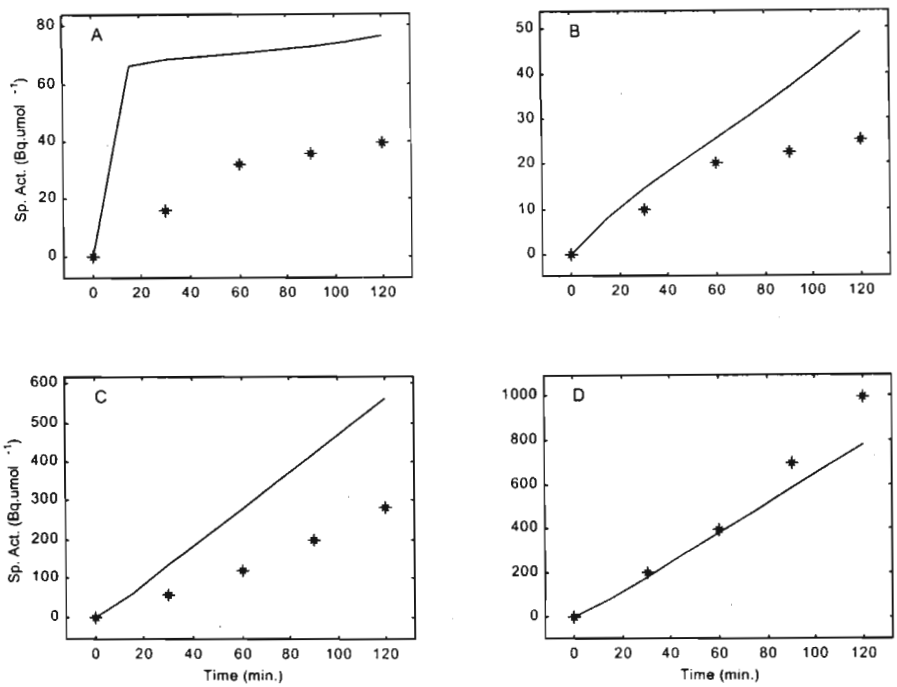

Figure 6.3. Changes in the specific activity of glucose (A), fructose (B), sucrose (C) and other components (D) in internode three tissue after feeding labelled glucose. Symbols represent experimental data and the solid line the model simulation.

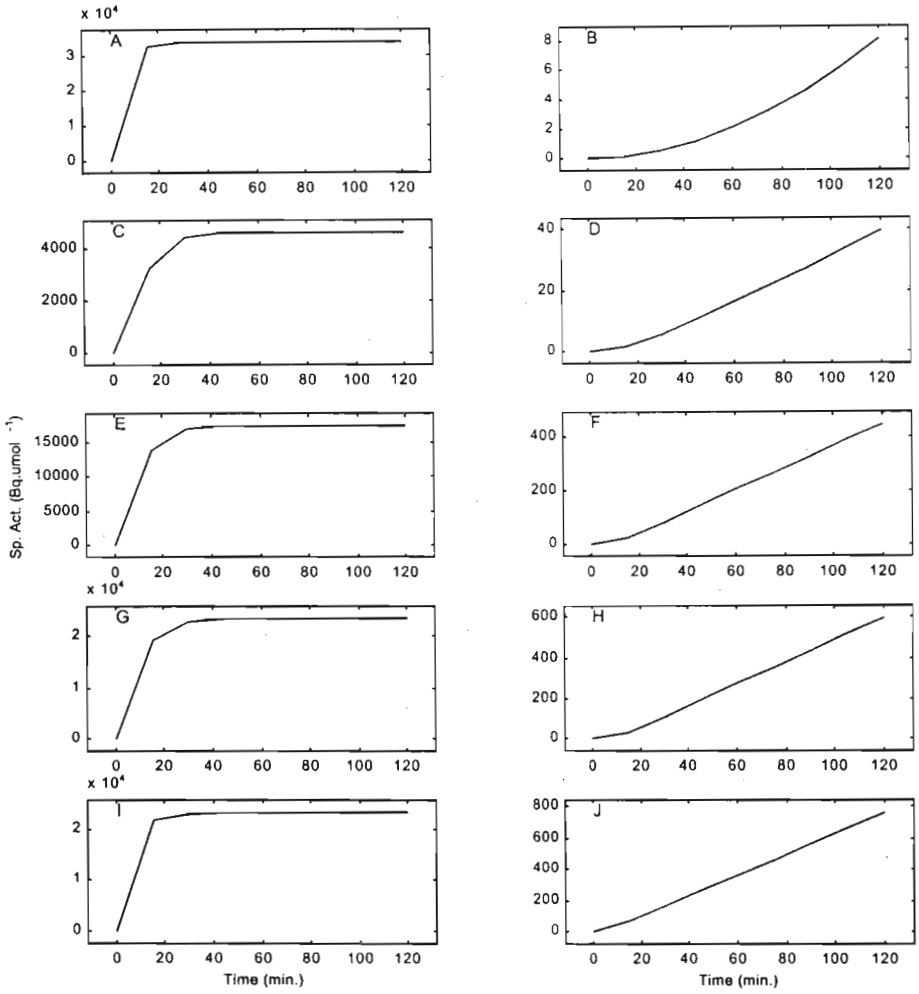

Figure 6.4. Flux model simulation of the changes in the specific activity of individual pools in internode three tissue after feeding labelled glucose. Glc_{cyt} [y_1] (A), Glc_{vac} [y_8] (B), Fru_{cyt} [y_2] (C), Fru_{vac} [y_9] (D), Suc-Fru_{cyt} [y_4] (E), Suc-Fru_{vac} [y_5] (F), Suc-Glc_{cyt} [y_6] (G), Suc-Glc_{vac} [y_7] (H), sugar phosphates [y_3] (I) and total output [y_{10}] (J).

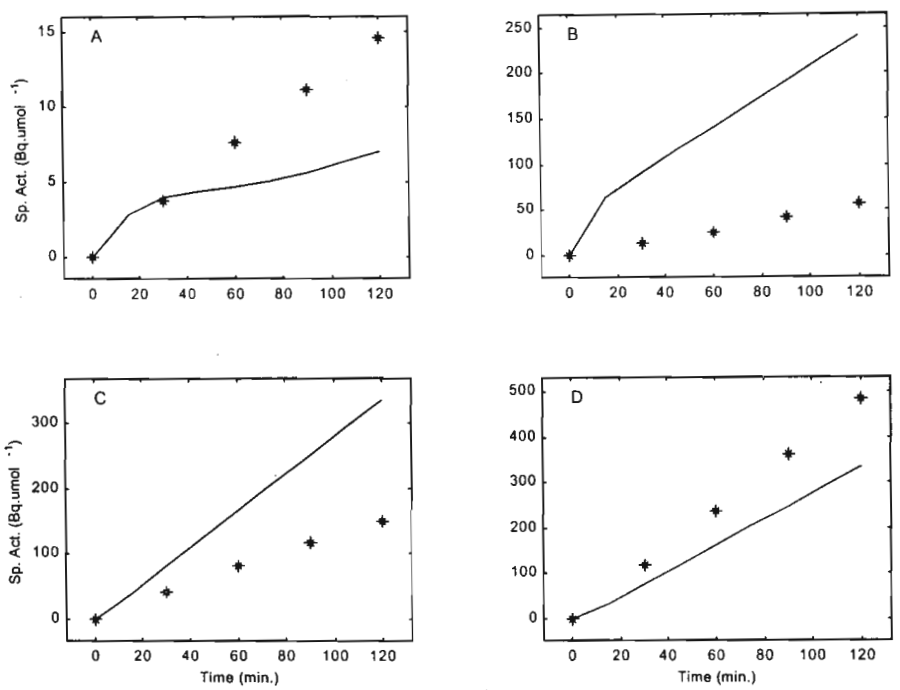

Figure 6.5. Changes in the specific activity of glucose (A), fructose (B), sucrose (C) and other components (D) in internode three tissue after feeding labelled fructose. Symbols represent experimental data and the solid line the model simulation.

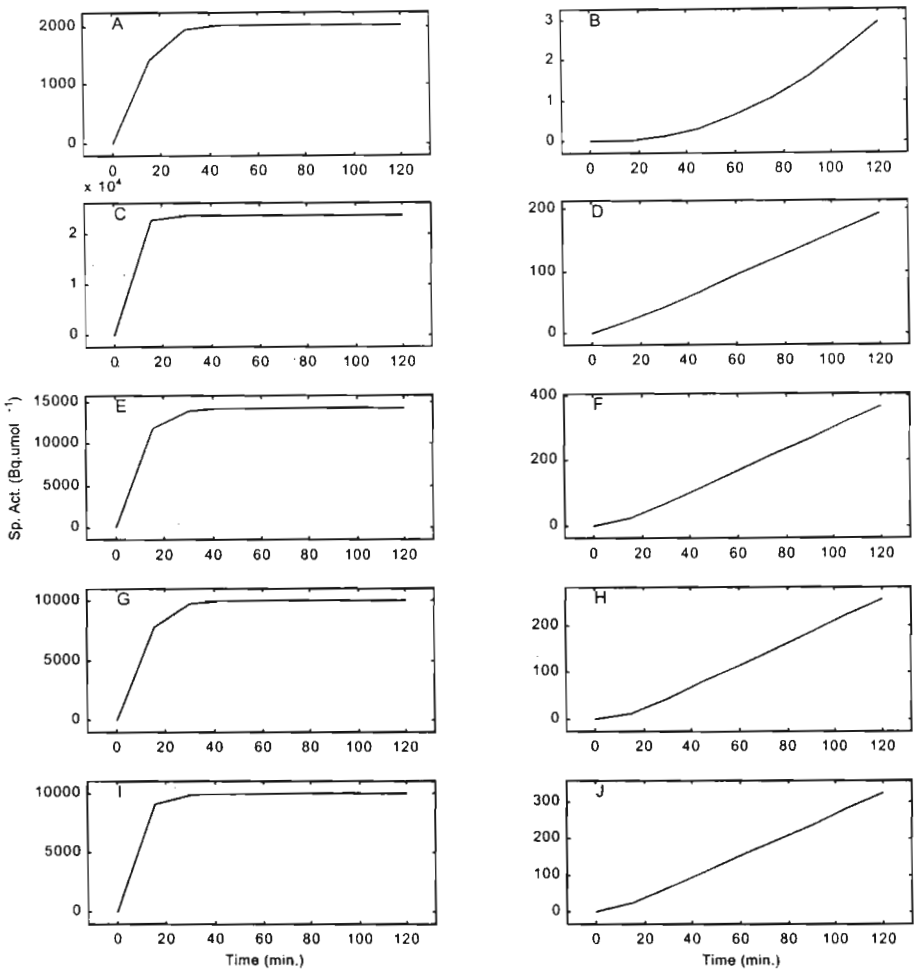

Figure 6.6. Flux model simulation of the changes in the specific activity of individual pools in internode three tissue after feeding labelled fructose. Glc_{cyt} [y_1] (A), Glc_{vac} [y_8] (B), Fru_{cyt} [y_2] (C), Fru_{vac} [y_9] (D), Suc-Fru_{cyt} [y_4] (E), Suc-Fru_{vac} [y_5] (F), Suc-Glc_{cyt} [y_6] (G), Suc-Glc_{vac} [y_7] (H), sugar phosphates [y_3] (I) and total output [y_{10}] (J).

6.3.2 Internode Three

The flow of label through the system can be seen in the specific activities of the individual pools (Fig. 6.4, 6.6). The cytosolic source hexose pool has the highest specific activity (Fig. 6.4A, 6.6C). The sugar phosphate pool label (Fig. 6.4I, 6.6I) is derived from the source hexose or the glucose moiety of the cytosolic sucrose. Due to the relatively small pool size (Table 6.3), the sugar phosphate pool will turn over rapidly and follow the specific activity of the source label hexose. The corresponding hexose moiety of the cytosolic sucrose is derived either solely from the sugar phosphates (glucose) or from the sugar phosphates and the cytosolic hexose pool (fructose). This pool shows the next highest specific activity (Fig. 6.4G, 6.6E). As would be expected, the hexose moiety of the vacuolar sucrose that has the highest specific activity is that of the source label hexose (Fig. 6.4H, 6.6F). Similarly, the vacuolar source label hexose (Fig. 6.4B, 6.6D) has a higher specific activity than the non-source hexose (Fig. 6.4D, 6.6B). The vacuolar hexoses also have a much lower specific activity than the cytosolic counterparts. This is due to the vacuolar hexoses being mainly derived from the lower specific activity vacuolar sucrose and the presence of a larger vacuolar hexose pool.

The total output (Fig. 6.4J, 6.6J) is the sink representing respiratory output and other pools that do not have a significant return rate. An important feature of the sink pool (m_{10}) is that it has no output flux. The increase in specific activity of this pool (y_{10}) represents the total label input to the pool during the simulation. The specific activity plotted is a model artefact of convenience for interpretation. The pool size has been set at an arbitrary value. The important feature of the plots, is the change in the slope of the curve with time. A constant slope indicates that the rate of label input to the pool is constant. An increase in the slope of the curve indicates that the label input rate is increasing, while the opposite is true for the case of a decreasing slope. The rate of change of the slope will indicate the rate of increase or decrease of the label input rate to this pool. The slope of the increase in label of this pool is influenced by the increase in specific activity of its source pool (y_3), the sugar

phosphates. The specific activity of the sugar phosphates rapidly attains an apparent isotopic equilibrium (Fig. 6.4I, 6.6I). This is reflected in the output pool activity (y_3), which shows an initial increase in slope after which a constant slope indicates a constant rate of label input (Fig. 6.4J, 6.6J).

The release of $^{14}CO_2$ is a constant component of the input to pool m_3; assuming metabolic steady state during the experimental time period. Theoretical calculations for the attainment of isotopic equilibrium for the sucrose pool based on maximum extractable invertase activities can be made. The time required to hydrolyse the entire sucrose pool in internode three by the combined extractable invertase activities would be approximately 3.6 hrs (Table 3.3). With the assumptions of a single compartment system and a direct source label input into the total sucrose; the time required to reach a specific activity of approximately 99% of the source would be approximately 24 hrs. The label data (Table 5.1, Table 6.4) also supports the hypothesis that it would take a significant period to reach isotopic equilibrium.

An interesting observation can be made for the model simulation output for pool m_{10} (Fig. 6.4J, 6.6J). If the change in the slope of the curve for the high vacuolar:cytosolic sugar ratio simulations for pool m_{10} (Fig. 6.4J, 6.6J) were viewed in isolation, they could be interpreted as indicating that the system had attained isotopic equilibrium. The system is in fact far from isotopic equilibrium as indicated by the vacuolar sugar pools (Fig. 6.4 B,D,F,H; 6.6 B,D,F,H). The reason for the attainment of an apparent constant slope for the total output is the hyperbolic shape of the specific activity curve for pool m_3 (Fig. 6.4I, 6.6I). Compartmentation of the system, and the vacuolar:cytosolic ratio reduce the cytosolic pool sizes. This results in reduced turnover times for the cytosolic sugar pools. The cytosolic metabolites attain an apparent state of isotopic equilibrium, this apparent plateau will actually be increasing at a rate that may not be noticeable. The rate of specific activity increase will be influenced by the rate of increase of the vacuolar metabolite specific activities and the rate of return of that label to the cytosolic compartment. This apparent plateau of specific activity leads to the apparent constant slope of the output pool

specific activity (y_{10}). This would lead to the system rapidly reaching an apparent constant rate of $^{14}CO_2$ release. The rate of change may not be noticeable within the normal experimental time period and experimental error.

A significant feature of the internode three labelling is that the source hexose specific activity is less than the sucrose specific activity (Fig. 6.3, 6.5). By increasing the vacuolar:cytosolic ratio to 499:1 the model was able to reproduce this behaviour (Fig 6.3, 6.5). As indicated in chapter five, this observation suggests that the ratio is greater than that previously assumed. The reason for the model performing relatively poorly for the internode three source label hexose is clear when the change in specific activity of the individual metabolite pools are considered. Due to all label entering through the cytosolic source hexose pool (Fig. 6.4A, 6.6C) the total label in this pool increases rapidly. The cytosolic source hexose pool is closer to isotopic equilibrium than any of the other pools. Due to the pool approaching the specific activity of the external source hexose, it rapidly forms a large part of the total label pool (data not shown, total activity curve for the individual pool). An increased vacuolar:cytosolic ratio results in a much steeper initial slope of the curve, and it rapidly approaches an apparent specific activity plateau. This pool is the major contributor to the total activity of the source hexose. The label uptake rate is constant and therefore the total label in the source hexose pool is difficult to reduce to the levels of the experimental data. The decreased cytosolic pool size and the pool approaching isotopic equilibrium, reduces the contribution of the cytosolic source hexose pool. This improves the fit of the model specific activities to the experimental data.

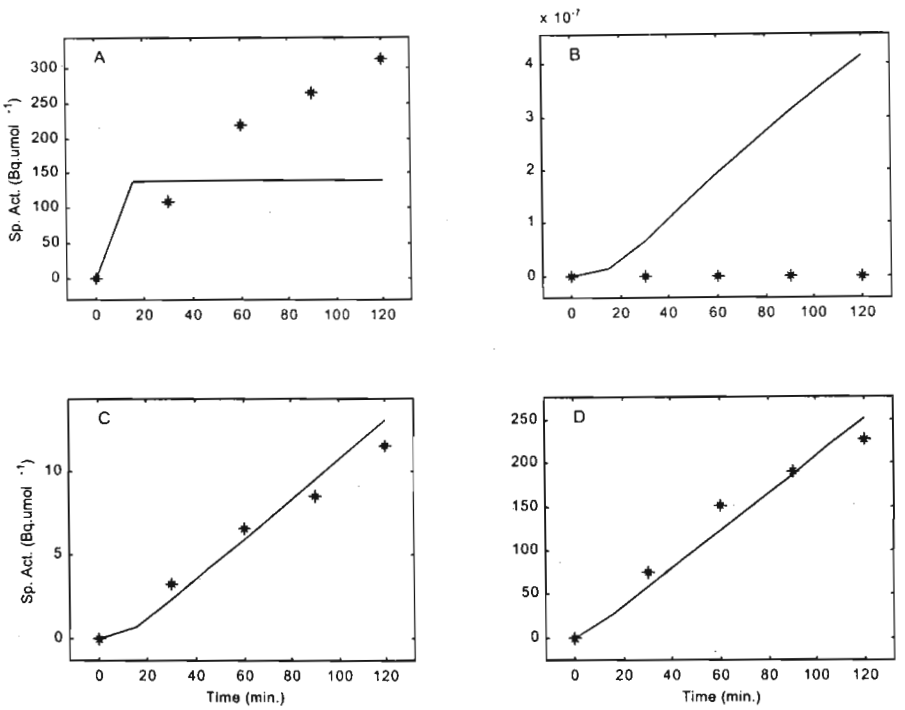

Figure 6.7. Changes in the specific activity of glucose (A), fructose (B), sucrose (C) and other components (D) in internode six tissue after feeding labelled glucose. Symbols represent experimental data and the solid line the model simulation.

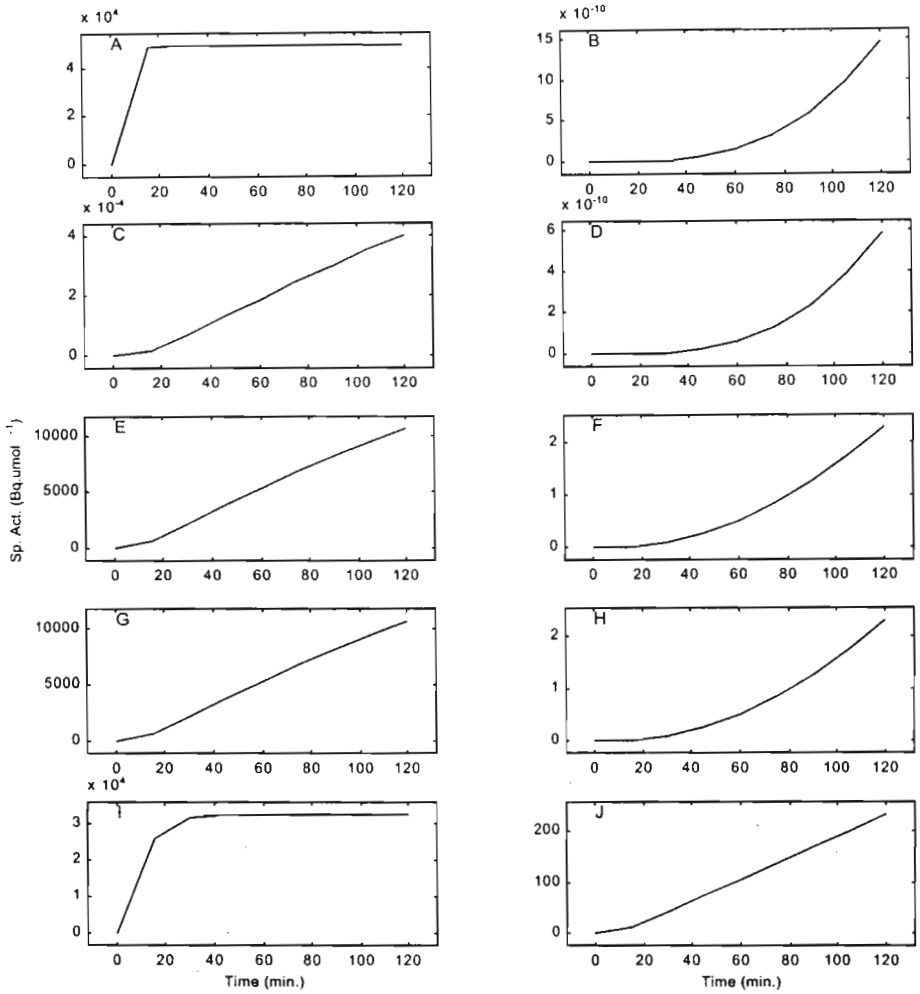

Figure 6.8. Flux model simulation of the changes in the specific activity of individual pools in internode six tissue after feeding labelled glucose. Glc_{cyt} [y_1] (A), Glc_{vac} [y_8] (B), Fru_{cyt} [y_2] (C), Fru_{vac} [y_9] (D), Suc-Fru_{cyt} [y_4] (E), Suc-Fru_{vac} [y_5] (F), Suc-Glc_{cyt} [y_6] (G), Suc-Glc_{vac} [y_7] (H), sugar phosphates [y_3] (I) and total output [y_{10}] (J).

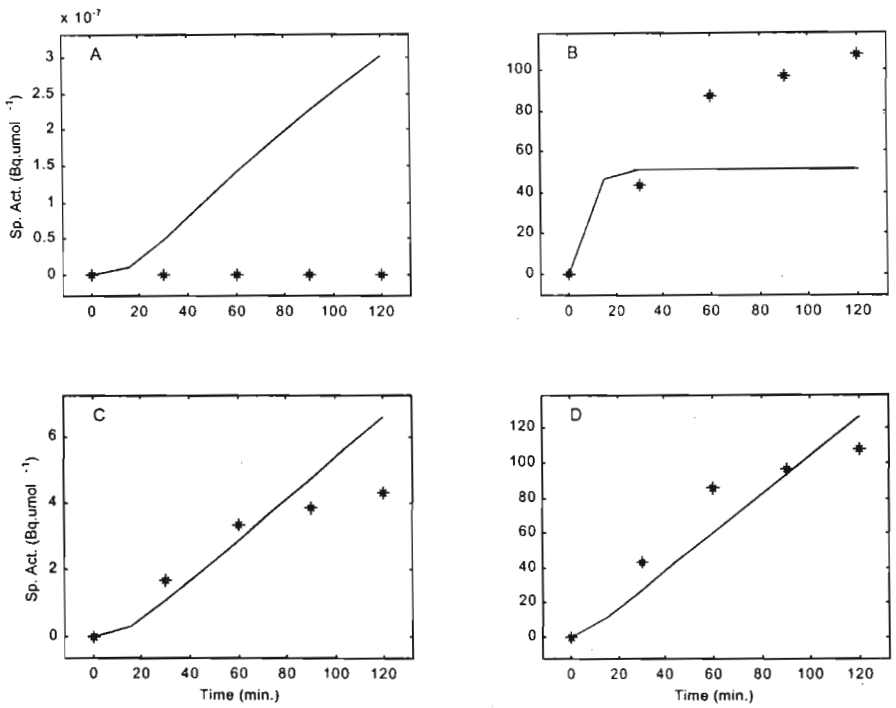

Figure 6.9. Changes in the specific activity of glucose (A), fructose (B), sucrose (C) and other components (D) in internode six tissue after feeding labelled fructose. Symbols represent experimental data and the solid line the model simulation.

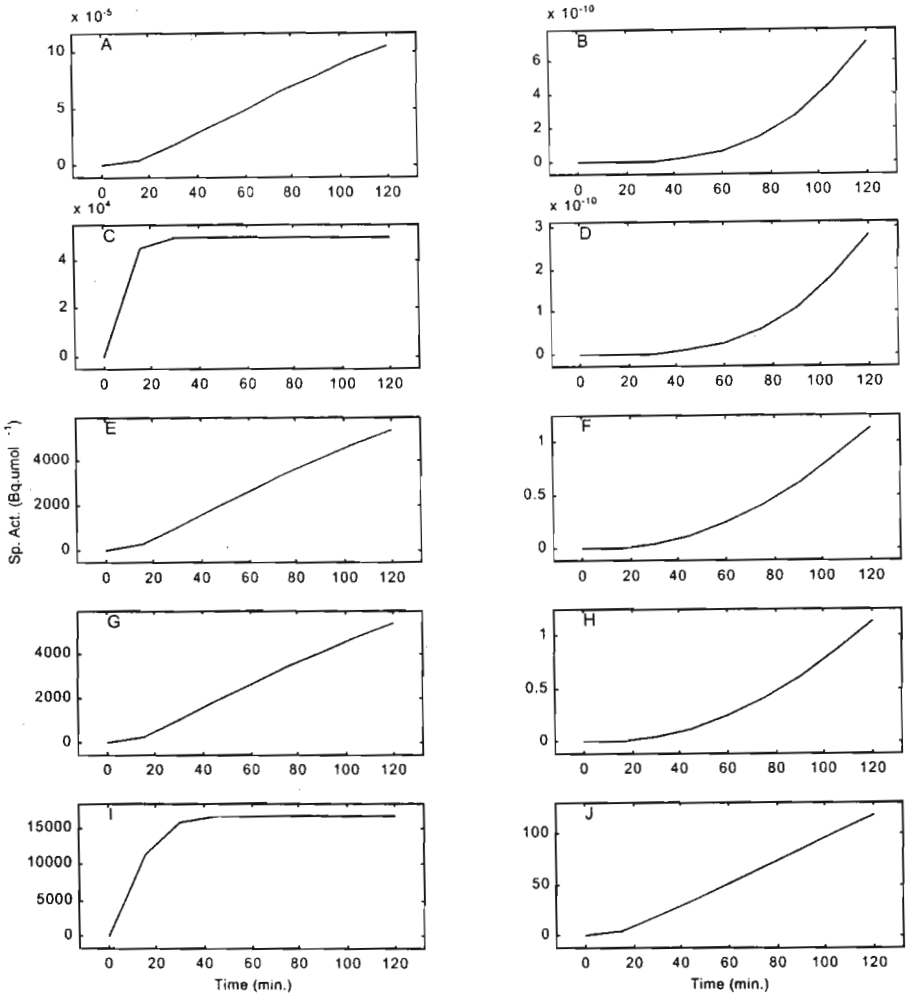

Figure 6.10. Flux model simulation of the changes in the specific activity of individual pools in internode six tissue after feeding labelled fructose. Glc_{cyt} [y_1] (A), Glc_{vac} [y_8] (B), Fru_{cyt} [y_2] (C), Fru_{vac} [y_9] (D), Suc-Fru_{cyt} [y_4] (E), Suc-Fru_{vac} [y_5] (F), Suc-Glc_{cyt} [y_6] (G), Suc-Glc_{vac} [y_7] (H), sugar phosphates [y_3] (I) and total output [y_{10}] (J).

6.3.3 Internode Six

The principles of the movement of label within the system are the same as those described for internode three. As for the internode three simulations the source hexose cytosolic pool reaches a specific activity plateau early with a high vacuolar:cytosolic ratio (Fig. 6.7A, 6.9B). This enables the rapid movement of label into the sucrose (Fig. 6.7C, 6.7D) and output pools (Fig. 6.9C, 6.9D) and the approximately linear increase in the specific activities of these pools.

The specific activities of the source and non-source hexoses are similar in the internode three experiments (Fig. 6.3, 6.5). In contrast, the internode six data shows that very little label reaches the non-source hexose (Fig. 6.7, 6.9, Table 6.4). A low rate of cytosolic and vacuolar sucrose breakdown would result in the low specific activity of the non-source hexose (Fig. 6.8B, 6.8D, 6.10B, 6.10D). The large vacuolar sucrose pool having a low specific activity for both it's hexose moieties would also contribute (Fig. 6.8F, 6.8H, 6.10F, 6.10H).

The cytosolic source hexose specific activities (Fig. 6.8A, 6.10C) are the primary contributors to the source hexose activity (Fig. 6.7A, 6.9C), which is also the case for internode three. The symmetry of the activities of the hexose moieties of sucrose (Fig. 6.8E-H, 6.10E-H) is a result of the dominant contribution of SPS to sucrose synthesis in the internode six model. The low specific activity of the vacuolar sucrose (Fig. 6.8F, 6.8H, 6.10F, 6.10H) is due to the large vacuolar sucrose pool size.

The sugar phosphate pool (m_3) is primarily derived from the cytosolic hexose pools due the low sucrose breakdown in the internode six model. The plateau of activity reached by the source hexose results in a similar hyperbolic activity curve for the sugar phosphate pool specific activity (y_3). This is due to the relatively small pool size (Table 6.3, m_3) having a short turnover time, as in internode three. The internode six

simulation also indicates that the label output rate would become linear after an initial increase (Fig. 6.8J, 6.10J). This would include $^{14}CO_2$ release.

The model optimization yielded glucose, fructose and sucrose ratios of 350:1, 962:1 and 987:1 respectively. The increased vacuolar:cytosolic hexose ratio facilitated the fit to the experimental data by reducing the average source hexose specific activity.

6.3.4 Enzyme Activities

The parameter sets obtained in the optimization for internodes three and six are shown in Table 6.5. The optimized model flux parameters (Table 6.5) can be compared to the limits and constraints that were determined experimentally (Table 6.2). All of the flux parameters were within the determined limits except one. Glucokinase ($A_{3,1}$) for internode three was significantly greater than that of the experimentally determined limit. This rate is physiologically feasible and may indicate that the *in vivo* glucokinase activity has been overestimated by the model or that the *in vitro* rate is an underestimated of the *in vivo* rate for internode three. The determination of the maximum extractable activity of an enzyme does not necessarily reflect the maximum *in vivo* rate limit of the step catalysed by the enzyme. This observation may reflect an *in vivo* rate that has previously been underestimated. However, further model refinement and investigation would provide insight into the source of this discrepancy.

The fructokinase rate (Table 6.5) is less than the extractable activity for internode three (Table 6.2). The fructokinase rate required would be lower due to the lower uptake rate of fructose (Fig. 6.2) and the low SuSy breakdown rate ($A_{3,6}$). The optimized rate for fructokinase is lower than the glucokinase rate for internode three (Table 6.5). This is also the case for internode six (Table 6.5). This is in contrast to the experimentally determined activities which show the opposite relationship (Table 6.2). It must be noted that the maximum extractable activity does not represent the *in*

vivo rate of the step catalysed by the enzyme. It does however give an indication of the feasible rate limits within the system.

NI ($A_{1,6}$) and SAI ($A_{9,5}$) contribute to sucrose hydrolysis in internode three but not internode six (Table 6.5). For the optimized data sets the NI hydrolysis rate is approximately equal to the SAI rate in internode three. The presence of significant NI activity in internode three sugarcane storage parenchyma tissue indicates that it has the capacity to contribute to sucrose hydrolysis (chapter three). Sucrose cleavage activity was purposely minimised in the internode six simulation to produce the labelling profile that agreed with the experimental data. This does not however preclude the presence of low levels of *in vivo* invertase activity that could be significant over a longer time period.

The SuSy synthesis rate ($A_{4,2}$) is within the experimental limit. The optimized parameter set has a rate of zero for the contribution of SPS ($A_{4,3}$) to sucrose synthesis in internode three. The SPS rate is dominant in internode six due to the SuSy sucrose synthesis rate being set to a low fixed rate (Table 6.5). The increase in the contribution of SPS to sucrose synthesis with tissue maturation is consistent with experimental observation (Botha *et al.*, 1996). In the glucose source label experiments the specific activity of the glucose moiety of sucrose in the cytosol (Fig. 6.4G, 6.8G) and the vacuole (Fig. 6.4H, 6.8H) is always greater than the fructose moiety of sucrose in the cytosol (Fig. 6.4E, 6.8E) and the vacuole (Fig. 6.4F, 6.8F).

The relative contributions of SPS and SuSy to sucrose synthesis can be estimated by the label ratio of the hexose moieties of sucrose where the source label hexose is glucose (Geigenberger and Stitt, 1993). The contribution of SuSy would be underestimated where the return of label to cytosolic fructose is significant. The ratio of specific activities between the hexose moieties of sucrose is approx. 1.4 for internode three (Fig. 6.4C, 6.4E, 6.4F, 6.4H). This is in close agreement with experimental observation of approx. 1.6 (Whittaker, PhD thesis 1997). Making the assumption of no significant label return to cytosolic fructose, the relative contribution

of SPS:SuSy to sucrose synthesis would be approx. 1.6. The model label ratio would result in a SPS:SuSy synthesis ratio of approx. 2.4, the actual ratio is approx. 2.21 (Table 6.5). The model is therefore in close agreement with experimental observation. The potential significance of the return of label to cytosolic fructose in this calculation should however not be ignored.

The relative contribution of SPS is dominant in internode six. The observed label ratio in the hexose moieties of sucrose is in agreement with experimental observation. Experimental observation shows that the glucose:fructose label ratio is close to one in internode six (Whittaker, PhD thesis 1997). This is also the case for the simulated data set (Fig. 6.8C, 6.8E, 6.8F, 6.8H). This is due to the large contribution of SPS to sucrose synthesis in the parameter set used. The model data for the internode six sucrose hexose moieties label ratio should be able to be used to accurately predict the SPS:SuSy synthesis ratio. This is due to there being a very low return of label to the cytosolic fructose pool in the glucose labelling experiment (Fig. 6.8C). The glucose:fructose label ratio of sucrose for internode six glucose is approx. 1. This ratio would be achieved as the SPS:SuSy sucrose synthesis ratio approaches infinity. This is the case in the internode six model where the SPS:SuSy sucrose synthesis ratio is high. The sucrose hexose moiety label ratio could be considered as a model constraint in further investigations.

Sugarcane storage parenchyma is a tissue in which sucrose concentration increases with maturation (Moore, 1995). One would therefore expect the net sucrose synthesis rate to exceed that of sucrose breakdown. Sucrose synthesis is catalysed in the cytosol by SuSy and SPS (Fig. 1.2). Sucrose breakdown is catalysed by SuSy and NI in the cytosol, and by SAI in the vacuole. Intuitively one would expect the internode three synthesis:breakdown ratio to be lower than internode six based on the labelling pattern (Table 6.4). This would also be in agreement with the experimental observation that the rate of sucrose accumulation increases with maturation and then tends toward a steady state (Moore, 1995).

The internode three ratio of sucrose synthesis:breakdown is 1.007. This indicates that the tissue is accumulating sucrose over the time frame of the experiment, with the synthesis rate only slightly exceeding the breakdown rate. The model rate of sucrose accumulation is 9.02×10^{-5} $\mu mol.min^{-1}.g^{-1}$ fw. The sucrose breakdown rate has been set to a very low level in internode six. The sucrose synthesis:breakdown ratio in internode six is 2.34×10^{6}. In the model simulation internode six is definitely a sucrose accumulating tissue. This is in agreement with what would be expected with sugarcane culm tissue maturation. The model sucrose accumulation rate for internode six is 4.69×10^{-4} $\mu mol.min^{-1}.g^{-1}$ fw. It must be noted that the high sucrose pool size buffers the return of label to the non-source hexose making it difficult to assess sucrose breakdown over the normal time frame of a labelling experiment. The internode six sucrose accumulation rate is however five times that of internode three which represents a significant increase. Further investigation may enable the sucrose synthesis:breakdown ratio to be included as a non-linear constraint.

SuSy catalyses a reversible reaction (Avigad, 1982), the net rate of sucrose synthesis or degradation will be influenced by the concentrations of its substrates and products. Immature sugarcane culm has a much lower concentration of sucrose than the mature culm. Assuming approximately equal extractable activities of SuSy, it would be expected that the rate of sucrose degradation catalysed by SuSy in the immature sugarcane culm would be lower than that catalysed in the mature culm. This is the case when comparing the SuSy sucrose breakdown rate of internode three and six (Table 6.5, $A_{3,6}$) This is in agreement with the previously reported lower SuSy sucrose cleavage activity in immature vs mature sugarcane culm tissue (Komor *et al.*, 1996).

6.3.5 General Conclusion

Models of complex natural systems are always an approximation of reality. This approximation is taken to a level acceptable to the requirements of the modeller. The flux model developed here has provided insight into the nature of the system studied.

The foundation and proof of concept have been developed. Specific information on the distribution of sugars and label between the cytosol and vacuole will improve the understanding of the system. This could provide insight that would lead to the adjustment of the model design to more closely approximate the system's behaviour. The implementation of the label ratio of the hexose moieties of sucrose as a constraint would refine the model. Changes in specific activities of the sugars over time in each compartment would provide data that would enable more effective model optimization.

The use of a flux model for the determination of *in vivo* flux, in conjunction with a kinetic model, will lead to a greater understanding of the metabolic control of sugarcane sucrose metabolism. This information can be used to direct the metabolic engineering of sugarcane.

Chapter 7

General Discussion

Sucrose metabolism in sugarcane has been an area of active investigation since the 1960s (for review see Moore, 1995). The topic of the distribution of the invertases in the sugarcane culm has been the subject of a number of studies. General opinion has assumed that the level of SAI declines with tissue maturation while that of NI increases. It was also assumed that high sucrose accumulating sugarcane varieties exhibit low levels of acid invertase in sucrose storing tissue implying that the decrease in acid invertase is necessary for sucrose accumulation.

This study has shown that sucrose accumulation occurs in a high sucrose accumulating sugarcane variety (NCo376) in the presence of significant invertase activity, including SAI (chapter three). Invertase mediated sucrose turnover was shown to occur at a significant rate in tissue which had reached the sucrose plateau per gram fresh weight. The rate of sucrose synthesis exceeded the rate of sucrose breakdown as would be expected in a sucrose accumulating tissue such as sugarcane. The manipulation of such a substrate cycle may provide a means of increasing the efficiency of sugarcane at accumulating sucrose.

Acid invertase has been the focus of many studies in the microbial and plant kingdom (Avigad, 1982; Hawker, 1985). However, NI is recognised as being an enzyme neglected by plant biochemists (Avigad, 1982; Hawker, 1985). The characterisation of sugarcane NI revealed many similarities to NI purified from other sources (chapter four). Significant differences were found between the results of the current study and a previous report on sugarcane NI (del Rosario and Santisopasri, 1977). In that study, sugarcane NI was shown to be glycosylated and of lower molecular weight when compared to other purified NI. In contrast, the results of this

study indicated that that NI was non-glycosylated and had a similar molecular weight to other NI. In addition, sugarcane NI was shown to possess similar kinetic properties to other NI where product inhibition could provide a mechanism of fine control. This would reduce sucrose hydrolysis in a high sucrose accumulating tissue in which the enzyme would be in substrate saturating conditions. NI may also play a role in the regulation of the expression of sugar responsive genes such as SAI by affecting the cytosolic glucose concentration (Koch, 1996). A similar temperature dependent transition to that of a sugarcane leaf sheath acid invertase was observed (Sampietro *et al.*, 1980). The differences in metal ion inhibition profiles indicated differences at the structural level.

The exact roles and importance of enzymes and transporters involved in sugarcane sucrose metabolism remain to be revealed. The advent of genetic engineering to manipulate plant enzyme levels is a relatively new tool that will enable the investigation of plant metabolism in ways not previously possible. The primary objective for commercial gain would be the metabolic engineering of sugarcane to accumulate higher levels of sucrose or to achieve these levels in a shorter crop cycle. The manipulation of the sucrose substrate cycle is a possible means to increase the rate of sucrose accumulation in sugarcane. The cloning of a cDNA displaying neutral/alkaline invertase properties will hopefully provide tools for the investigation of the enzyme at the sequence and structural level (Gallagher and Pollock, 1998). Further molecular investigations will reveal the role of NI in sugarcane development and sucrose metabolism.

The substrate cycle of sucrose synthesis and breakdown has been known to be a part of sugarcane suspension cell and immature storage parenchyma metabolism (for review see Moore, 1995). The presence of a cycle of sucrose synthesis and degradation in sugarcane tissue that has reached the sucrose concentration plateau per gram fresh weight has been demonstrated (chapter five). The sucrose synthesis rate exceeds the sucrose breakdown rate in internodes three to 12 (chapter five). This would be expected for a sucrose accumulating tissue such as sugarcane.

The lack of detailed information on the compartmentation of sugars in sugarcane storage parenchyma tissue is a major limitation to understanding the flux and control of sucrose metabolism. As has been shown previously (for review see Glasziou and Gayler, 1972), sugars occur in two compartments in sugarcane storage parenchyma cells, namely the cytosol and the vacuole. Internode three cytosolic label was shown to have a longer turnover time than internode six (chapter five). A higher vacuolar:cytosolic sugar molar ratio is indicated than is commonly assumed.

The effect of the assumptions for flux calculation was investigated. Variation of the distribution of label and sugars between the cytosolic and vacuolar compartments is shown to influence the results significantly (chapter five).

Carbon allocation in sugarcane storage parenchyma has been investigated (Whittaker and Botha, 1997). In chapter five, carbon allocation in sugarcane storage parenchyma discs was observed over time. As has previously been shown, younger tissue allocated a greater percentage of label to insoluble matter, which consisted mainly of structural polysaccharides. The hyperbolic shape of the fractions of the neutral component indicated that the pools were approaching a percentage steady state distribution (chapter five). In the region of the sugarcane culm spanning internodes three to 12, the greatest difference in the change of carbon allocation was observed between internodes three and six. This indicated that developmentally this would be the region to investigate in order to understand the underlying changes which occur to effect this dramatic change in carbon allocation. The tissue changes from a system geared for growth to a primarily sucrose storing tissue.

A metabolic flux model of sugarcane storage parenchyma sucrose metabolism was developed to investigate *in vivo* flux and sugar compartmentation (chapter six). Complex metabolic networks are recognised as being underdetermined. This is due to insufficient information provided by conventional experimental techniques (Bonarius *et al.*, 1997). A significant challenge was the optimization of the model.

The metabolic flux model was optimized for the best feasible flux parameters. The results produced from the flux model simulations supported the evidence that the vacuolar:cytosolic sugar molar ratio could be greater than previously assumed. Flux rates of the optimized parameter sets were physiologically meaningful and the model parameters were in agreement with experimental observation. The use of the model in investigating the label ratio in sucrose was demonstrated. The sucrose synthesis rate exceeded the sucrose breakdown rate in internodes three and six. This is in agreement with the conclusions of chapter five and is consistent with what would be expected for a sucrose accumulating tissue. The sucrose accumulation rate increased from internodes three to six as would be expected in the sugarcane culm. The model adhered to all of the experimental limits and constraints other than that of glucokinase activity. The model rate was greater than the maximum extractable activity, this indicates that the *in vivo* glucokinase rate may be underestimated as the model rate was physiologically feasible.

Future flux model development could address the inclusion of a constraint for the ratio of sucrose synthesis vs degradation. A further constraint that could be implemented for internode six is the SPS:SuSy sucrose synthesis ratio. This may only be feasible for a tissue in which the return of labelled fructose in a ^{14}C-Glucose labelling experiment is not significant. SAI and NI contributed to sucrose hydrolysis in internode three but not in internode six. This does not preclude the presence of low *in vivo* levels of SAI and NI which would be significant over a longer time period. The ability to observe the change in specific activity of individual metabolite pools within the system enhances the understanding of the dynamics of label movement in the system. A refined flux model could also be used to simulate different labelling experiment designs in order to identify experiments that would provide the most useful information.

Information on the timecourse of movement of sugars between the vacuolar and cytosolic compartments would vastly increase the understanding of the experimental

system. However, due to the limitations of current technology this information remains inaccessible.

In order to understand the metabolic regulation of the system, a kinetic model must also be developed. This, in conjunction with the flux model would give insight into the regulation of the metabolic system. Traditional biochemical methodologies used for the understanding of control in metabolic systems are recognised as being largely qualitative (Fell, 1997). The advent of metabolic control theory as originally proposed by Kacser and Burns (1973) and later Heinrich and Rapoport (1974) has led to the development of a quantitative theory for the study of control in metabolic systems. Other less popular approaches have been developed for the study of the control of metabolism, namely: Biochemical Systems Theory (Savageau, 1971) and Flux-Oriented Theory (Crabtree and Newsholme, 1987). Metabolic control theory has largely been applied to microbial and animal systems (Fell, 1997). Of the theories proposed, metabolic control theory has found the widest application to plant metabolism (Kruckeberg *et al.*, 1989; Stitt, 1989; Smith *et al.*, 1990 and Jenner *et al.*, 1993). The application of metabolic control theory to plant metabolism has been reviewed (ap Rees and Hill, 1994) and the specific requirements pertaining to plant metabolism have been identified. Of those, one of the areas lacking is that of measuring *in vivo* flux. This is largely due to the highly compartmented nature of plant metabolism rendering it inaccessible to current methods for the analysis of *in vivo* flux (ap Rees and Hill, 1994).

Plant metabolism is also characterised by redundancy, sucrose metabolism in sugarcane is no exception (Fig. 1.1). Redundancy and the concept of shared control in metabolic pathways (Fell, 1997), indicate that the manipulation of the cycle of sucrose synthesis and degradation in either the biosynthetic or degradative direction will require altering the levels of multiple enzymes and/or transporters. Altering this cycle significantly may require a combinatorial search for the optimum levels of combinations of enzymes and/or transporters.

Information required for MCA is derived from classical enzymology and the analysis of *in vivo* metabolic flux. A possible reason for the slow adoption of metabolic control theory is the large amount and presently inaccessible information required to explicitly satisfy the requirements. The acknowledgement of the need for new approaches to understanding biological organisms that incorporate levels of complexity and information created at each level is being recognised (Strohman, 1997a; Bains, 1997; Strohman, 1997b; Streelman and Karl, 1997). The advent of genetic engineering in plants and the development of techniques for the analysis of *in vivo* metabolic flux will provide essential information. The use of metabolic control theory for the quantitative analysis of the metabolic networks will result in a more efficient and directed approach to the improvement of sugarcane as a commercial crop.

Further development of a metabolic flux model will aid in the understanding of *in vivo* flux and the compartmentation of metabolites. The measurement of *in vivo* flux aids in the validation, assessment and development of a kinetic model. A kinetic model based on metabolic control theory, developed for the analysis of sugarcane cytosolic carbohydrate metabolism will aid in the directed metabolic engineering of sugarcane.

Literature Cited

Akazawa, T., and K. Okamoto. 1980. Biosynthesis and metabolism of sucrose. p. 199-220. *In*: Stumpf, P.K., E.E. Kohn (ed.) The Biochemistry of Plants. A Comprehensive Treatise, vol 3. Academic Press, London.

Anon. 1998. An overview of the South African Sugar Industry and its Experiment Station's partnership with the University of Stellenbosch Plant Biotechnology Institute. Presentation to the Institute of Plant Biotechnology University of Stellenbosch, 6 March 1998.

Asthir, B., and R. Singh. 1997. Purification and characterisation of neutral invertase from chickpea nodules. Indian Journal of Biochemistry and Biophysics 34:529-534.

Avigad, G. 1982. Sucrose and other disaccharides. p. 217-347. In: Loewus, F. A. and Tanner, W., (ed.) Encyclopedia of Plant Physiology, New Series, vol. 13A, Springer-Verlag, Berlin and New York.

Bains, W. 1997. Should you hire an epistemologist? Nature Biotechnology 15:396.

Ball, K.L., and T. ap Rees. 1988. Fructose 2,6-bisphosphate and the climacteric in bananas. Eur. J. Biochem. 177:637-641.

Batta, S.K., and R. Singh. 1986. Sucrose metabolism in sugar cane grown under varying climatic conditions: synthesis and storage of sucrose in relation to the activities of sucrose synthase, sucrose-phosphate synthase and invertase. Phytochem. 25:2431-2437.

Bergmeyer, H.U., and E. Bernt 1974. p.1176-1179. *In*: H.U. Bergmeyer (ed.), Methods of Enzymatic Analysis, 2nd ed., vol. 3, Verlag Chemie Weinheim, Academic Press, Inc., New York and London.

Bergner, P. E. 1964. Tracer dynamics and the determination of pool-sizes and turnover factors in metabolic systems. J. Theor. Biol. 6:137-158.

Bielski, R.L. 1962. The physiology of sugar cane. V. Kinetics of sugar accumulation. Aust. J. Biol. Sci. 15:429-444.

Blake, M.S., K.H. Johnston, G.J. Russel-Jones, and E.C.A. Gotschlich. 1984. A rapid sensitive method for detection of alkaline phosphate-conjugated anti-body on Western blots. Anal. Biochem. 136:175-179.

Blum, J.J., and R.B. Stein. 1982. On the analysis of metabolic networks. p. 99-125. *In*: R.F. Goldberger and K.R. Yamamoto (ed.) Biological Regulation and Development. Plenum Press, New York and London.

Bonarius, H.P.J., G. Schmid, and J. Tramper. 1997. Flux analysis of underdetermined metabolic networks: The quest for the missing constraints. Trends in Biotechnology 15:308-314.

Borowitz, M.J., R.B. Stein, and J.J Blum. 1977. Quantitative analysis of the change of metabolic fluxes along the pentose phosphate and glycolytic pathways in *Tetrahymena* in response to carbohydrates. J. Biol. Chem. 252:1589-1605.

Botha, F.C., A. Whittaker, D.J. Vorster, and K.G. Black. 1996. Sucrose accumulation rate, carbon partitioning and expression of key enzyme activities in sugarcane stem tissue. p. 98-101. *In*: Wilson, J.R., D.M. Hogarth, J.A. Campbell, and A.L. Garside (ed.) Sugarcane: Research Towards Efficient and Sustainable Production. CSIRO Division of Tropical Crops and Pastures, Brisbane, Australia.

Bowen, J.E. 1972. Sugar transport in immature internodal tissue of sugarcane. I. Mechanism and kinetics of accumulation. Plant Physiol. 49:82-86.

Bowen, J.E. and , J.E. Hunter. 1972. Sugar transport in immature internodal tissue of sugarcane. II. Mechanism of sucrose transport. Plant Physiol. 49:789-793.

Bracho, G.E., and J.R. Whitaker. 1990. Characteristics of the inhibition of potato (*Solanum tuberosum*) invertase by an endogenous proteinaceous inhibitor in potatoes. Plant Physiol. 92:381-385.

Bradford, M.M. 1976. A rapid and sensitive method for the quantitation of microgram quantities of protein utilizing the principle of protein-dye binding. Anal. Biochem. 72:248-254.

Buczynski, S.R., M. Thom, P. Chourney, and A. Maretzki. 1993. Tissue distribution and characterization of sucrose synthase isozymes in sugarcane. J. Plant Physiol. 142:641-646.

Carson, E.R., C. Cobelli, and L. Finkelstein. 1983. The mathematical modelling of metabolic and endocrine systems. John Wiley and Sons, NY.

Chen, J.Q., and C.C. Black. 1992. Biochemical and immunological properties of alkaline invertase isolated from sprouting soybean hypocotyls. Arch. Biochem. Biophys. 295:61-69.

Cornish-Bowden, A. 1979. Fundamentals of Enzyme Kinetics. Butterworths, London.

Crabtree, B., and E.A. Newsholme. 1987. A systemic approach to describing and analysing metabolic control systems. Trends in Biochemical Sciences 12:4-12.

Cullen, M.R. 1985. Linear models in biology. Linear systems analysis with biological applications. Ellis Horwood Ltd, England.

Dendsay, J.P.S., P. Singh, A.K. Dhawan, and H.L. Sehtiya. 1995. Activities of internodal invertases during maturation of sugarcane stalks. Sugar Cane 6:17-19.

Dickson, R.E. 1979. Analytical procedures for the sequential extraction of ^{14}C-labelled constituents from leaves, bark and wood of cottonwood plants. Physiol. Plant. 45:480-488.

Dieuaide-Noubhani. M., G. Raffard, P. Canioni, A. Pradet, and P. Raymond. 1995. Quantification of compartmented metabolic fluxes in maize root tips using isotope distribution from ^{13}C- or ^{14}C-labelled glucose. J. Biol. Chem. 270:13147-13159.

Doehlert, D.C., and S.C. Huber. 1983. Regulation of spinach leaf sucrose-phosphate synthase by Glc6P, inorganic phosphate and pH. Plant Physiol. 73:989-994.

Echeverria, E. and J.K. Burns. 1989. Vacuolar acid hydrolysis as a physiological mechanism for sucrose breakdown. Plant Physiol. 90:530-533.

Echeverria, E., and G. Salerno. 1994. Properties of sucrose-phosphate phosphatase from rice (*Oryza sativa*) leaves. Plant Science 96:15-19.

Eschrich, W. 1989. Phloem unloading of photoassimilates. p.206-263. *In:* Baker, D.A. and, J.A. Milburn (eds). Longman, New York.

Fell, D. 1997. Understanding the control of metabolism. p.213-225. Portland Press, London and Miami.

Gadian, D.G., and G.K. Radda. 1981. NMR studies of tissue metabolism. Annu. Rev. Biochem. 50:69-83.

Gallagher, J.A., and C.J. Pollock. 1998. Isolation and characterisation of a cDNA clone from *Lolium temulentum* L. encoding for a sucrose hydrolytic enzyme which shows alkaline/neutral invertase activity. J. Exp. Bot. 49:789-795.

Gayler, K.R., and K.T. Glasziou. 1972a. Physiological functions of acid and neutral invertases in growth and sugar storage in sugar cane. Physiol. Plant. 27:25-31.

Gayler, K.R., and K.T. Glasziou. 1972b. Sugar accumulation in sugarcane. Carrier mediated active transport of glucose. Plant Physiol. 49:563-568.

Geigenberger, P., and Stitt, M. 1993. Sucrose synthase catalyses a readily reversible reaction in vivo in developing potato tubers and other plant tissues. Planta. 189:329-339.

Gifford, R.M., J.H. Thorne, W.D. Hitz and R.T. Giaquinta. 1984. Crop productivity and photoassimilate partitioning. Science 225:801-808.

Glasziou, K.T. 1960. Accumulation and transformation of sugars in sugar cane stalks. Plant Physiol. 35:895-901.

Glasziou, K.T. 1961. Accumulation & transformation of sugars in stalks of sugar cane. Origin of glucose & fructose in the inner space. Plant Physiol. 36:175-179.

Glasziou, 1962. Accumulation and transformation of sugars in sugarcane stalks: mechanism of inversion of sucrose in the inner space. Nature 193:1100.

Glasziou, K.T., and K.R. Gayler. 1972. Storage of sugars in stalks of sugar cane. Bot. Rev. 38:471-490.

Glasziou, K.T., and J.C. Waldron. 1964a. Regulation of acid invertase-levels in sugar cane stalks by auxin- and metabolite- mediated control systems. Nature 203:541-542.

Glasziou, K.T., and J.C. Waldron. 1964b. The regulation of invertase synthesis in sugar-cane: effects of sugars, sugar derivatives, and polyhydric alcohols. Aust. J. Biol. Sci. 17:609-618.

Goldner W., M. Thom, and A. Maretzki. 1991. Sucrose metabolism in sugarcane cell suspension cultures. Plant. Sci. 73:143-147.

Haefner, J.W. 1996. Modelling biological systems. Principles and applications. Chapman and Hall, NY.

Hartt, C.E. 1943. The synthesis of sucrose in the sugarcane plant. Hawaiian Planter's Record 47:155-170.

Hatch, M.D. 1963. A uridine diphosphatase from sugar cane. Biochem. J. 88:423-427.

Hatch, M.D. 1964. Sugar accumulation by sugar-cane storage tissue: the role of sucrose phosphate. Biochem. J. 93:521-526.

Hatch, M.D., and K.T. Glasziou. 1963. Sugar accumulation cycle in sugar cane. II. Relationship of invertase activity to sugar content & growth rate in storage tissue of plants grown in controlled environments. Plant Physiol. 38:344-348.

Hatch, M.D. and, Glasziou, K.T. 1964. Direct evidence for translocation of sucrose in sugarcane stems. Plant Physiol. 39:180-184.

Hatch, M.D., J.A. Sacher, and K.T. Glasziou. 1963. Sugar accumulation cycle in sugar cane. I. Studies on enzymes of the cycle. Plant Physiol. 38:338-343.

Hawker, J.S. 1966. Studies on the location of sucrose phosphatase in plant tissues. Phytochem. 5:1191-1199.

Hawker, J.S. 1967. Inhibition of sucrose phosphatase by sucrose. Biochem. J. 102:401-406.

Hawker, J.S. 1985. Sucrose. p.1-51. *In*: P. M. Dey and R. A. Dixon (ed.) Biochemistry of Storage Carbohydrates in Green Plants. Academic Press, New York.

Hawker, J.S. and M.D. Hatch. 1965. Mechanism of sugar storage by mature stem tissue of sugarcane. Physiol. Plant. 18:444-453.

Hawker, J.S. and M.D. Hatch. 1966. A specific sucrose phosphatase from plant tissues. Biochem. J. 99:102-107.

Hawker, J.S., C.F. Jenner, and C.M. Niemietz. 1991. Sugar metabolism and compartmentation. Aust. J. Plant Physiol. 18:227-237.

Hawker, J.S., and G.M. Smith. 1984. Occurrence of sucrose phosphatase in vascular and non-vascular plants. Phytochem. 23:245-249.

Hawker, J.S., G.M. Smith, H. Phillips, and J.T. Wiskich. 1987. Sucrose phosphatase associated with vacuole preparations from red beet, sugar beet, and immature sugarcane. Plant Physiol. 84:1281-1285.

Heinrich, R., and T.A. Rapoport. 1974. A linear steady-state treatment of enzymatic chains. General properties, control and effector strength. Eur. J. Biochem. 42:89-95.

Hill, S.A., and T. ap Rees. 1994. Fluxes of carbohydrate metabolism in ripening bananas. Planta. 192:52-60.

Huber, S.C., and T.A. Akazawa. 1986. A novel sucrose synthase pathway for sucrose degradation in cultured sycamore cells. Plant. Physiol. 81:1008-1013.

Jacobsen, K.R., D.G. Fischer, A. Maretzki and P.H. Moore. 1992. Developmental changes in the anatomy of the sugarcane stem in relation to phloem unloading and sucrose storage. Bot. Acta 105:70-80.

Jaynes, T.A., and O.E. Nelson. 1971. An invertase inactivator in maize endosperm and factors affecting inactivation. Plant Physiol. 47:629-634.

Jenner, C.F., K. Siwek, and J.S. Hawker. 1993. The synthesis of [^{14}C]starch from [^{14}C]sucrose in isolated wheat grains is dependent upon the activity of soluble starch synthase. Aust. J. Plant Physiol. 20:329-335.

Jones, D. R. 1999. DIRECT. Encyclopedia of Optimization, Kluwer Academic Publishers.

Kacser, H., and J.A. Burns. 1973. The control of flux. Symposia of the Society for Experimental Biology 28:65-104.

Karuppiah, N., B. Vadlamudi, and P.B. Kaufman. 1989. Purification and characterization of soluble (cytosolic) and bound (cell wall) isoforms of invertases in barley (*Hordeum Vulgare*) elongating stem tissue. Plant Physiol. 91:993-998.

Katz, J. 1979. Use of isotopes for the study of glucose metabolism *in vivo*. Techn. Metab. Res. 207:1-22.

Kelly, P.J., J.K. Kelleher, and B.E. Wright. 1979. The tricarboxylic acid cycle in *Dictyostelium discoideum*. A model of the cycle at preculmination and aggregation. Biochem. J. 184:589-597.

Knott, G. 1975. MLAB, an on-line modelling laboratory, 5th edn (Division of Computer Research and Technology, NIH).

Koch, K. E., Y. Wu, and J. Xu. 1996. Sugar and metabolic regulation of genes for sucrose metabolism: potential influence of maize sucrose synthase and soluble invertase response on carbon partitioning and sugar sensing. J. Exp. Bot. 47:1179-1185.

Komor, E., O. Zingsheim, and H. Sprugel. 1996. Cycles of sugar transport and sucrose metabolism in sugarcane tissue: quantitative determination. p. 92-94. *In*: Wilson, J.R., D.M. Hogarth, J.A. Campbell, and A.L. Garside (ed.) Sugarcane: Research Towards Efficient and Sustainable Production. CSIRO Division of Tropical Crops and Pastures, Brisbane, Australia.

Kruckeberg, A.L., H.E. Neuhaus, R. Feil, L.D. Gottleib, and M. Stitt. 1989. Decreased-activity mutants of phosphoglucose isomerase in the cytosol and chloroplast of *Clarkia xantiana*. Biochem. J. 261:457-467.

Kruger, N.J. 1997. Carbohydrate synthesis and degradation. p. 83-104. *In:* Dennis, D.T., D.B. Layzell, D.D. Lefebvre and D.H. Turpin (ed.) Plant Metabolism. Addison Wesley Longman Limited, Essex, England.

Laemmli, U.K. 1970. Cleavage of structural proteins during the assembly of the head of bacteriophage T4. Nature. 227:680-685.

Lee, H., and A. Sturm. 1996. Purification and characterisation of neutral and alkaline invertase from carrot. Plant Physiol. 112:1513-1522.

Leloir, L.F., and C.E. Cardini. 1955. The biosynthesis of sucrose phosphate. J. Biol. Chem. 214:157-165.

Lingle, S.E. 1989. Evidence for the uptake of sucrose intact into sugarcane internodes. Plant Physiol. 90:6-8.

Lingle, S.E. 1996. Rates of sugar accumulation in sugarcane in relation to sucrose synthase activity. p. 95-97. *In*: Wilson, J.R., D.M. Hogarth, J.A. Campbell, and A.L. Garside (ed.) Sugarcane: Research Towards Efficient and Sustainable Production. CSIRO Division of Tropical Crops and Pastures, Brisbane, Australia.

Lingle, S.E. 1997. Seasonal internode development and sugar metabolism in sugarcane. Crop Sci. 37:1222-1227.

Lingle, S.E., and J.E. Irvine. 1994. Sucrose synthase and natural ripening in sugarcane. Crop Sci. 34:1279-1283.

Lingle, S.E., and R.C. Smith. 1991. Sucrose metabolism related to growth and ripening in sugarcane internodes. Crop Sci. 31:172-177.

Longacre, A., J.M. Reimers, J.E. Gannon, and B.E. Wright. 1997. Flux analysis of glucose metabolism in *Rhizopus oryzae* for the purpose of increasing lactate yields. Fungal Genetics and Biology 21:30-39.

Maretzki, A. and, M. Thom. 1972a. Membrane transport of sugars in cell suspensions of sugarcane I. Evidence of sites and specificity. Plant Physiol. 49:172-182.

Maretzki, A. and, M. Thom. 1972b. The existence of two membrane transport systems for glucose in suspensions of sugarcane cells. Biochem. Biophys. Res. Comm. 47:44-50.

Maretzki, M. and, M. Thom. 1986. A group translocator for sucrose assimilation in tonoplast vesicles of sugarcane cells. Plant Physiol. 80:34-37.

Maretzki, M. and, M. Thom. 1988. High performance liquid chromatography-based reevaluation of disaccharides produced upon incubation of sugarcane vacuoles with UDP-Glucose. Plant Physiol. 88:266-269.

Masuda, H., T. Takahashi, and S. Sugawara. 1988. Acid and alkaline invertases in suspension cultures of sugar beet cells. Plant Physiol. 86:312-317.

Miller, E.M. and, P.S. Chourey. 1992. The maize invertase-deficient miniature-1 seed mutation is associated with aberrant pedicel and endosperm development. Plant Cell 4:297-305.

Milling, R.J., J.L. Hall, and R.A. Leigh. 1993. Purification of an acid invertase from washed discs of storage roots of red beet (*Beta vulgaris* L.) J. Exp. Bot. 44:1679-1686.

Moore, P.H. 1995. Temporal and spatial regulation of sucrose accumulation in the sugarcane stem. Aust. J. Plant Physiol. 22:661-679.

Morris, D.A. 1982. Hormonal regulation of sink invertase activity: implications for the control of assimilate partitioning. p.659-688. *In*: Plant growth substances. Waering, P.F. (ed.) Academic Press, London.

Northrop, P. 1981. The expression of isotope effects on enzyme-catalyzed reactions. Annu. Rev. Biochem. 50:103-131.

Preisser, J. and E. Komor. 1988. Analysis of the reaction products from incubation of sugarcane vacuoles with uridine-diphosphate-glucose: No evidence for the group translocator. Plant Physiol. 88:259-265.

Preisser, J. and E. Komor. 1991. Sucrose uptake into vacuoles of sugarcane suspension cells. Planta 186:109-114.

Preisser, J., H. Sprugel, and E. Komor. 1992. Solute distribution between vacuole and cytosol of sugarcane suspension cells: Sucrose is not accumulated in the vacuole. Planta 186:203-211.

Pressey, R. 1968. Invertase inhibitors from red beet, sugar beet, and sweet potato roots. Plant Physiol. 43:1430-1434.

Pressey, R. 1994. Invertase inhibitor in tomato fruit. Phytochem. 36:543-546.

ap Rees, T. 1974. Pathways of carbohydrate breakdown in higher plants. p. 89-127. *In*: Northcote, D.H. (ed.) Int Rev Biochem, vol XI. Butterworth, London.

ap Rees, T., and S.A. Hill. 1994. Metabolic control analysis of plant metabolism. Plant, Cell and Environment 17:587-599.

Ricardo, C.P.P. 1974. Alkaline β-fructofuranosidases of tuberous roots: possible physiological function. Planta 118:333-343.

del Rosario, E.J., and V. Santisopasri. 1977. Characterization and inhibition of invertases in sugar cane juice. Phytochem. 16:443-445.

Ross, H.A., D. McRae, and H.V. Davies. 1996. Sucrolytic enzyme activities in cotyledons of the faba bean. Plant Physiol. 111:329-338.

Sacher, J.A., and K.T. Glasziou. 1962. Regulation of invertase levels in sugar cane by an auxin-carbohydrate mediated control system. Biochem. Biophys. Res. Commun. 8:280-282.

Sacher, J.A., M.D. Hatch, and K.T. Glasziou. 1963a. Sugar accumulation cycle in sugar cane. III. Physical and metabolic aspects of cycle in immature storage tissues. Plant Physiol. 38:348-354.

Sacher, J.A., M.D. Hatch, and K.T. Glasziou. 1963b. Regulation of invertase synthesis in sugar cane by an auxin- and sugar-mediated control system. Physiol. Plant. 16:836-842.

Salon, C., and P. Raymond. 1988. Quantification of metabolic fluxes in cyclic pathways by labelling experiments and modelization. Plant Physiol. Biochem. 26:187-195.

Salon, C., P. Raymond, and A. Pradet. 1988. Quantification of carbon fluxes through the tricarboxylic acid cycle in early germinating lettuce embryos. J. Biol. Chem. 263:12278-12287.

Salvucci, M.E., F. J. van de Loo, and R.R. Klein. 1995. The structure of sucrose-phosphate synthase. *In*: Pontis, H.G., G.L. Salerno, and E.J. Echeverria (ed.) International Symposium on Sucrose Metabolism. American Society of Plant Physiologists.

Sampietro, A.R. 1995. The plant invertases. *In*: Pontis, H.G., G.L. Salerno, and E.J. Echeverria (ed.) International Symposium on Sucrose Metabolism. American Society of Plant Physiologists.

Sampietro, A.R., M.A. Vattuone, and F.E. Prado. 1980. A regulatory invertase from sugar cane leaf-sheaths. Phytochem. 19:1637-1642.

Savageau, M.A. 1971. Parameter sensitivity as a criterion for evaluating and comparing the performance of biochemical systems. Nature 229:542-544.

Savinell, J.M., and Palsson, B.O. 1992a. Network analysis of intermediary metabolism using linear optimization. I. Development of mathematical formalism. J. Theor. Biol. 154:421-454.

Savinell, J.M., and Palsson, B.O. 1992b. Network analysis of intermediary metabolism using linear optimization. II. Interpretation of hybridoma cell metabolism. J. Theor. Biol. 154:455-473.

Savinell, J.M., and Palsson, B.O. 1992c. Optimal selection of metabolic fluxes for *in vivo* measurement. I. Development of mathematical methods. J. Theor. Biol. 155:201-214.

Savinell, J.M., and Palsson, B.O. 1992d. Optimal selection of metabolic fluxes for *in vivo* measurement. II. Application to *Escherichia coli* and hybridoma cell metabolism. J. Theor. Biol. 155:215-242.

Sherwood, P., P. Kelly, J.K. Kelleher and B. Wright. (1979). TFLUX: A general purpose program for the interpretation of radioactive tracer experiments. Computer Programs in Biomedicine. 10:66-74.

Singh, O., and R.S. Kanwar. 1991. Enzymes in ripening of sugar cane at low temperatures. Sugar Cane 4:2-4.

Slack, C.R. 1965. The physiology of sugar cane. VIII. Diurnal fluctuations in the activity of soluble invertase in elongating internodes. Aust. J. Biol. Sci. 18:781-788.

Slack, C.R. 1966. Inhibition of UDP glucose:D-fructose 2-glucosyltransferase from sugar cane stem tissue by phenol oxidation products. Phytochem. 5:397-403.

Smith, A.M., H.E. Neuhaus, and M. Stitt. 1990. The impact of decreased activity of starch-branching enzyme on photosynthetic starch synthesis in leaves of wrinkled-seeded peas. Planta 181:310-315.

Stitt, M. 1989. Control analysis of photosynthetic sucrose synthesis: assignment of elasticity coefficients and flux control coefficients to cytosolic fructose-1,6-bisphosphatase and sucrose phosphate synthase. Philosophical Transactions of the Royal Society of London, Series B 323:327-338.

Stitt, M. 1990. Fructose-2,6-bisphosphate as a regulatory molecule in plants. Annu. Rev. Plant Physiol. Plant Mol. Biol. 41:153-185.

Streelman, J.T., and S.A. Karl. 1997. Paradigms and the rise (or fall?) of molecular biology. Nature Biotechnology 15:696-697.

Strohman, R.C. 1997a. The coming Kuhnian revolution in biology. Nature Biotechnology 15:194-200.

Strohman, R.C. 1997b. Profit margins and epistemology. Nature Biotechnology 15:1224-1225.

Sturm, A. 1999. Invertases: Primary Structures, Functions, and Roles in Plant Development and Sucrose Partitioning. Plant Physiol. 121: 1-7.

Sturm, A. and M. Chrispeels. 1990. cDNA cloning of carrot extracellular â-fructosidase and its expression in response to wounding and bacterial infection. Plant Cell 2:1107-1119.

Sturm, A., D. Hess, H. Lee, and S. Lienhard. 1999. Neutral invertase is a novel sucrose-cleaving enzyme. Physiol. Plant. 107: 159-165.

Sturm, A. and G. Tang. 1999. The sucrose-cleaving enzymes of plants are crucial for development, growth and carbon partitioning. Trends in Plant Science 4: 401-407.

Thom, M., A. Maretzki, and E. Komor. 1982a. Vacuoles from sugarcane suspension cultures. I. Isolation and partial characterization. Plant Physiol. 69:1315-1319.

Thom, M., E. Komor, and A. Maretzki. 1982b. Vacuoles from sugarcane suspension cultures. II. Charaterization of sugar uptake. Plant Physiol. 69:1320-1325.

Thom, M. and A. Maretzki. 1985. Group translocation as a mechanism for sucrose transfer into vacuoles from sugarcane cells. Proc. Natl. Acad. Sci. USA 82:4697-4701.

Thom, M. and, A. Maretzki. 1992. Evidence for direct uptake of sucrose by sugarcane stalk tissue. J. Plant Physiol. 139:555-559.

Tymowska-Lalanne, Z. and, M. Kreis. 1998. The plant invertases: physiology, biochemistry and molecular biology. Advances in Botanical Research 28:71-117.

Unger, C., M. Hardegger, S. Lienhard and, A. Sturm. 1994. cDNA cloning of carrot (*Daucus carota*) soluble acid â-fructofuranosidase and comparison with the cell wall isoenzyme. Plant Physiol. 104: 1351-1357.

Van den Ende, W., and A. Van Laere. 1995. Purification and properties of a neutral invertase from the roots of *Cichorium intybus*. Physiol. Plant. 93:241-248.

Varma, A., and O. Palsson. 1994. Metabolic flux balancing: basic concepts, scientific and practical uses. Bio/Technology 12:994-998.

Veith, R., and E. Komor. 1993. Regulation of growth, sucrose storage and ion content in sugarcane cells, measured with suspension cells in continuous culture grown under nitrogen, phosphorous or carbon limitation. J Plant Phys. 142:414-424.

Venkataramana, S., and M. Mohan Naidu. 1993. Invertase-sucrose relationship in young and mature stem of sugarcane. Phytochem. 32:821-822.

Viola, R. 1996. Hexose metabolism in discs excised from developing potato (*Solanum tuberosum* L.) tubers II. Estimations of fluxes in vivo and evidence that fructokinase catalyses a near rate-limiting reaction. Planta 198:186-196.

Vorster, D.J., and F.C. Botha. 1998. Partial purification and characterisation of sugarcane neutral invertase. Phytochem. 49:651-655.

Vorster, D.J., and F.C. Botha. 1999. Sugarcane internodal invertases and tissue maturity. J Plant Physiol. 155:470-476.

Walsh, K.B., R.C. Sky, and S.M. Brown. 1996. Pathway of sucrose unloading from the phloem sugarcane stalk. p. 105-107. *In*: Wilson, J.R., D.M. Hogarth, J.A. Campbell, and A.L. Garside (ed.) Sugarcane: Research Towards Efficient and Sustainable Production. CSIRO Division of Tropical Crops and Pastures, Brisbane, Australia.

Walker, R.P., and C.J. Pollock. 1993. The purification and characterization of soluble acid invertase from coleoptiles of wheat (*Triticum aestivum* L. cv. Avalon). J. Exp. Bot. 44:1029-1037.

Weber, H. and T. Roitsch. 2000. Invertases and life beyond sucrose cleavage. Trends in Plant Sciences. 5: 47-48.

Weis, M.F. 1974. SAAM25, simulation, modelling and data fitting program - user's guide. National Cancer Institute, NIH.

Welbaum, G.E., and F.C. Meinzer. 1990. Compartmentation of solutes and water in developing sugarcane stalk tissue. Plant Physiol. 93:1147-1153.

Welbaum, G.E., F.C. Meinzer, R.L. Grayson and K.T. Thornham. 1992. Evidence for and consequences of a barrier to solute diffusion between the apoplast and vascular bundles in sugarcane stalk tissue. Aust. J. Plant Physiol. 19:611-623.

Wendler, R., R. Veith, J. Dancer, M. Stitt, and E. Komor. 1990. Sucrose storage in cell suspension cultures of *Saccharum* sp. (sugarcane) is regulated by a cycle of synthesis and degradation. Planta. 183:31-39.

Whittaker, A. 1997. Pyrophosphate dependent phosphofructokinase (PFP) activity and other aspects of sucrose metabolism in sugarcane internodal tissue. PhD thesis, University of Natal, Durban, South Africa.

Whittaker, A., and F.C. Botha. 1997. Carbon partitioning during sucrose accumulation in sugarcane internodal tissue. Plant Physiol. 115:1651-1659.

Wiechert, W., and A.A. de Graaf. 1997. Bidirectional reaction steps in metabolic networks: I. Modelling and simulation of carbon isotope labelling experiments. Biotechnology and Bioengineering 55:101-117.

Wiechert, W., C. Siefke, A.A. de Graaf, and A. Marx. 1997. Bidirectional reaction steps in metabolic networks: II. Flux estimation and statistical analysis. Biotechnology and Bioengineering 55:101-117.

Wright, B.E., and J.M. Reimers. 1988. Steady-state models of glucose-perturbed *Dictyosteum discoideum*. J. Biol. Chem. 263:14906-14912.

Wright, B.E., A. Longacre, and J. Reimers. 1996. Models of metabolism in *Rhizopus oryzae*. J. Theor. Biol. 182:453-457.

Zellner, M.G. 1970. DSS, distributed system simulator. PhD thesis, Lehigh University.

Zhu, Y. J., E. Komor, and P. H. Moore. 1997. Sucrose accumulation in the sugarcane stem is regulated by the difference between the activities of soluble acid invertase and sucrose phosphate synthase. Plant Physiol. 115:609-616.

Appendix A: Flux model MatLab M files

main.m

```
function main()
%main control file used to initialise simulations
%file main.m
%batch run of all simulations

%-------------------------------------------------------
%SUGARCANE CARBOHYDRATE METABOLISM FLUX SIMULATOR
%Author: Darren Vorster
%Created: 01/1999
%Last Updated: 06/2000
%MatLab version 5 compatible
%-------------------------------------------------------

%display a title
'SUGARCANE CARBOHYDRATE METABOLISM FLUX SIMULATOR by Darren Vorster'

%internode 3 or 6 simulation
intnd = input('Internode 3 or 6: ');
%cast to a string
intnd = int2str(intnd);

%will this be a simulation or a graphical output of the simulation
results
optimisedata = input('Optimisation [1] or simulation output [0]: ');

%get the no. of function evaluations for the global optimisation
a = input('Input the no. of optimisation function evaluations: ');

cntr = 0;

%assign the no. of max evaluations
mevals = a;
%-------------------------------------------------------------------------
---
if optimisedata == 1
   %NORMAL OPTIMISATION
   main_min(intnd,mevals)
else
   %-------------------------------------------------------------------
------
   %CHART OUTPUT IS GENERATED
   %chart each hexose
   for lblcntr = 1:2
      if lblcntr == 1
         lbl = 'Glc'
      else
         lbl = 'Fru'
      end
      for row=1:1
         cntr=cntr+1;
         simout(intnd,lbl,cntr,row,mevals);
      end
```

```
    end
end
    %-------------------------------------------------------------------------
------

%release resources
clear all;
```

main_min.m

```
function X = main_min(intrnd,maxevals)
% function main_min('internode',maxevals)
% file main_min.m
% main control file that calls the optimisation algorithm
% with the simulation file as a parameter

global F;
global Am;

global Al;
global X_L;
global X_U;
global b_L;
global b_U;
global c_L;
global c_U;

global m;
global E;
global y;
global internode;
global label;
global rsquare;
global FID;
global X;

tic;

%initialise matrices and vectors
Am = zeros(10);
F = zeros(10,1);
E = zeros(10,1);
m = zeros(10,1);

%assign the input values to global variables
internode = intrnd;

%set the global external flux parameters
if internode == '3'
    F(1) = 0.019019;
    F(2) = 0.009884;
elseif internode == '6'
    F(1) = 0.004952;
    F(2) = 0.002551;
end

%convert and set filename
extension = '.csv';

%set the file name
```

```
outputfile = [internode '_' int2str(maxevals) extension];

%open a file as write text for output from stat
[FID, MESSAGE] = fopen(outputfile,'wt')

%=================================================================
%OPTIMIZATION ALGORITHM
%=================================================================
%-----------------------------------------------------------------------
------------
%OPTIMIZATION TOOLBOX TOMLAB 2.0 GCLSOLVE 'DIRECT' BOUNDED CONSTRAINED
MINIMIZATION
%-----------------------------------------------------------------------
------------
%call the optimization function gclSolve.m

%initialise all of the constraints
constraints(internode);

%set up the file field names
res1 = header(FID,X_L);

%call the optimization algorithm
GLOBAL.MaxEval=maxevals;
if internode == '3'
   X = gclSolve('main_sim',[],X_L,X_U,Al,b_L,b_U,[],[],[],GLOBAL);
elseif internode == '6'
   X = gclSolve('main_sim',[],X_L,X_U,[],[],[],[],[],[],GLOBAL);
   %X = gclSolve('main_sim',[],X_L,X_U,Al,b_L,b_U,[],[],[],GLOBAL);
   %X =
gclSolve('main_sim','nonlinconst',X_L,X_U,Al,b_L,b_U,c_L,c_U,[],GLOBAL);
end

%-------------------------------------------------------
%display the model optimization results
X.f_k

%output the results to a file if the result is feasible
if not(isinf(X.f_k))
   %display the result
   X.x_k
   %generate all of the flux parameters
   fluxdep(X.x_k,internode);
   %output the results
   result_out(Am,F);
   fprintf(FID,'%-17.10g ,',X.x_k);
   fprintf(FID,'%-17.10g \n',X.f_k);
else
   %write to file of the result is not feasible
   fprintf(FID,'%s \n','NOT FEASIBLE');
end

%-------------------------------------------------------
%end of the DIRECT optimization conditional
%-----------------------------------------------------------------
%=================================================================

%close output file
ST = fclose(FID);
toc
```

constraints.m

```
function constraints(internode)
%function that initialise all of the global variables used for the
constraints
%in the gclsolve optimisation

global Al;
global X_L;
global X_U;
global b_L;
global b_U;
global c_L;
global c_U;
global F;

%set the finetune flag
finetune = 1;

if internode == '3'

      %WITH SUSY BOX BOUNDS
      %min and max within feasible bounds
      X_L = [0    ;0    ;0    ;0    ;0    ;0    ;0    ]
      X_U = [0.05;0.05;0.05;0.05;0.05;0.05;0.05]

      if finetune == 1
         %X_M = [0.03395160516      ;1.411257317e-07    ;0.02222179885
;0.01111096999      ;0.0277779189       ;0.01358038804
;0.01666680779];
         X_M = [0.03136138348      ;1.411257317e-07    ;0.02037022924
;0.00555541443      ;0.01666680779      ;0.008313857982
;0.007727621693];

         %set the new bounds
         X_L = X_M - 0.005;
         X_L = uptozero(X_L);
         X_U = X_M + 0.005;
      end

      %WITH SUSY LINEAR CONSTRAINT BOUNDS
      %lower bound forces positive parameter space optimization
      b_L = [-0.009884;0      ;-0.009135;0.009884;0.009135;-
0.009135;0.009884;0    ;-0.009884;-0.009884;0    ]
      b_U = [0.05      ;0.05  ;0.05      ;0.05     ;0.05     ;0.05      ;0.05
;0.05;0.05      ;0.05      ;0.05]

      %limits using vector F
      %b_L = [-F(2)     ;0      ;-(F(1)-F(2));F(2)     ;(F(1)-F(2)) ;-
(F(1)-F(2));F(2) ;0     ;-F(2)  ;-F(2)     ;0    ]
      %b_U = [0.05      ;0.05  ;0.05         ;0.05     ;0.05         ;0.05
;0.05 ;0.05 ;0.05    ;0.05      ;0.05]

elseif internode == '6'
   %Box bounds for independent parameters
   X_L = [0    ; 10   ; 10   ; 10   ];
   X_U = [0.01; 1000; 1000; 1000];

end

%-------------------------------------------------
```

```
%non-linear constraint bounds
c_L = [1e-20;1e-20];
c_U = [1e20;1e20];
%-------------------------------------------------

%linear constraint matrix
%coefficients taken from the dependent parameter equations in fluxdep.m
%parameter equations Am(7,6), Am(8,7) and Am(5,4) are redundant
%this leads to a system of linear constraint equations represented by
the coefficient matrix Al
%the bounds for the inequalities are represented by vectors b_L and b_U
Al = [0  0 -1 -1  0  1  1; %A(9,2)
      0  0  0 -1  1  0  0; %A(4,3)
      0  0  2  2 -2  0  0; %A(10,3) (F1 + F2)>= dm10/dt >= 0
      0  0  1  1  0 -1  0; %A(9,5)
      1  0 -1 -1  0  1  0; %A(1,6)
     -1  0  1  1  0  0  0; %A(3,6)
      0  1  1  1  0 -1  0; %A(1,8)
      0  0  0  0  1 -2  0; %dm4/dt >= 0 (Suc Cyt)
      0  0 -1 -1  0  2  0; %dm5/dt >= 0 (Suc Vac)
      0  0 -1 -1 -1  4  0; %dm5/dt >= dm4/dt
      0  0  0 -2  1  0  0] %sps >= susy synthesis


function XR = uptozero(XN)
%function that converts the lower bound of each vector element to zero
if it is less than zero
sz = size(XN)
sz(1)
for i = 1:sz(1)
     if XN(i) < 0
          XN(i) = 0;
     end
end
XR = XN
```

nonlinconst.m

```
function result = nonlinconst(x)
%function that has the non linear constraints
global F;

%Suc accumulation rate (vac)/Suc accumulation rate (cyt)
result(1) = (-x(3)-x(4)+2*x(6)+F(2))/(x(5)-2*x(6));
%SPS suc synth >= susy suc synth
result(2) = (-x(4)+x(5))/x(4);

result = transpose(result)
```

header.m

```
function r = header(FID,X_L)
% function header(FID)
% header.m
% writes headers of the outputfile

%common output column headers
fprintf(FID,'%s ,','Am(3.1)');
```

```
fprintf(FID,'%s ,','Am(8.1)');
fprintf(FID,'%s ,','Am(3.2)');
fprintf(FID,'%s ,','Am(4.2)');
fprintf(FID,'%s ,','Am(9.2)');
fprintf(FID,'%s ,','Am(4.3)');
fprintf(FID,'%s ,','Am(6.3)');
fprintf(FID,'%s ,','Am(10.3)');
fprintf(FID,'%s ,','Am(2.4)');
fprintf(FID,'%s ,','Am(5.4)');
fprintf(FID,'%s ,','Am(9.5)');
fprintf(FID,'%s ,','Am(1.6)');
fprintf(FID,'%s ,','Am(3.6)');
fprintf(FID,'%s ,','Am(7.6)');
fprintf(FID,'%s ,','Am(8.7)');
fprintf(FID,'%s ,','Am(1.8)');
fprintf(FID,'%s ,','Am(2.9)');
fprintf(FID,'%s ,','F(1)');
fprintf(FID,'%s ,','F(2)');

%vector x
for i = 1 : length(X_L)
   fprintf(FID,'%s ,',['x(' int2str(i) ')']);
end
%final f_k
fprintf(FID,'%s \n','f_k');

r = 1;
```

main_sim.m

```
function rsum = main_sim(x)
% function main_sim(x)
% file main_sim.m
% main simulation function called by the optimization algorithm
% returns the error statistic to the optimization algorithm

global Am;
global F;
global y;
global label;
global sucratio;
global internode;
global FID;

rsum = 0;

% Calculate fluxes depending on internode by calling fluxdep
% Define global variables Am and F
fluxdep(x,internode);

%assign the sucrose and hexose vacuolar:cytosolic ratio
if internode == '3'
   glcratio = 500;
   fruratio = 500;
   sucratio = 500;
elseif internode == '6'
   glcratio = x(2);
   fruratio = x(3);
   sucratio = x(4);
end
```

```
%loop through both label sources
for lblcntr = 1:2
   %set the label
   if lblcntr == 1
      label = 'Glc';
   else
      label = 'Fru';
   end

   %set the external specific activities
   ext_activities(label);

   %initialise all of the parameters from main_sim for double simulation
   %set up the input data arrays
   pool_size(internode,glcratio,fruratio,sucratio);
   activities(internode,label);

   % Call the ode solver ode45 if massbalance criteria passed
   % which calls the model definition file modelm.m
   % output time points

   tspan = [0 30 60 90 120];

   % y is the equivalent of X the 10 dimensional vector of compartment
specific activities

   % Vector of initial conditions
   y0 = [0 0 0 0 0 0 0 0 0 0];

   % Call the ode solver
   [t,y] = ode45('modelmmatrix',tspan,y0);

   %plot(t,y)

   %-------------------------------------------------------------------------
----------
   %MODEL STATISTICS
   %-------------------------------------------------------------------------
----------
   %run statistical comparison and return results in an array
   %CALCULATE THE ERROR STATISTIC
   r = stat(y);

   %keep the sum of the error for the model
   rsum = rsum + r;

end

%OBSERVE THE OPTIMIZATION VECTOR X
x'
```

fluxdep.m

```
function fluxdep(x,internode)
% function fluxdep(x)
% file fluxdep.m
% assigns the indepedent flux parameters to the global flux matrix Am
% assigns the dependent flux parameters to the global flux matrix Am
% and sets the external specific activities
```

```
% Declare global variables
global Am; % 10x10 matrix of linear coefficients for differential
equation
global F; % 10 dimensional vector of input functions, constants

%calculate the dependent flux constants
%external input flux constants (F1,F2)
if internode == '3'
   F(1) = 0.019019;
   F(2) = 0.009884;

   %Assign the independent flux parameters
   Am(3,1) = x(1);
   Am(8,1) = x(2);
   Am(3,2) = x(3);
   Am(4,2) = x(4);
   Am(6,3) = x(5);
   Am(2,4) = x(6);
   Am(2,9) = x(7);

   Am(9,2) = -x(3)-x(4)+x(6)+x(7)+F(2);
   Am(4,3) = -x(4)+x(5);
   Am(10,3) = 2*x(3)+2*x(4)-2*x(5)+(F(1)-F(2));
   Am(9,5) = x(3)+x(4)-x(6)-F(2);
   Am(1,6) = x(1)-x(3)-x(4)+x(6)-(F(1)-F(2));
   Am(3,6) = -x(1)+x(3)+x(4)+(F(1)-F(2));
   Am(7,6) = x(6);
   Am(8,7) = x(3)+x(4)-x(6)-F(2);
   Am(1,8) = x(2)+x(3)+x(4)-x(6)-F(2);
   Am(5,4) = x(6);
elseif internode == '6'
   F(1) = 0.004952;
   F(2) = 0.002551;

   Am(3,1) = F(1);
   Am(8,1) = 0;
   Am(3,2) = F(2);
   Am(4,2) = 0;
   Am(9,2) = 0;
   Am(4,3) = x(1);
   Am(6,3) = x(1);
   Am(10,3) = (Am(3,1) + Am(3,2)) - (Am(6,3)+Am(4,3));
   Am(2,4) = 1E-10;
   Am(5,4) = Am(4,3);
   Am(9,5) = 1E-10;
   Am(1,6) = 1E-10;
   Am(3,6) = 0;
   Am(7,6) = Am(6,3);
   Am(8,7) = 1E-10;
   Am(1,8) = 0;
   Am(2,9) = 0;

end
```

ext_activities.m

```
function ext_activities(label)
%function that sets the external activities
```

```
global E;

% Define constants depending on labelled sugar
% constant y (specific activity) Bq/umol
% E for external source of label
if label == 'Glc'
   %glucose
   E(1) = 49333;
   %fructose
   E(2) = 0;
elseif label == 'Fru'
   %glucose
   E(1) = 0;
   %fructose
   E(2) = 49333;
end
```

pool_size.m

```
function pool_size(internode,glcratio,fruratio,sucratio)
% function pool_size(hexratio,internode)
% file pool_size.m
% initialisation of the pool sizes uses cyt:vac ratio in calculations
% pool size units in umols/g fw

%declare global variables
global m;

%ratios of metabolites vacuole:cytosol
ratio18 = glcratio;
ratio29 = fruratio;
ratio4567 = sucratio;

%input metabolite pool sizes to m array
if internode == '3'
   %internode 3
   %internode 3 totals
   m1m8 = 31;
   m2m9 = 27;
   m4m5 = 27.5;
   m6m7 = 27.5;

   m(1) = m1m8/ratio18;
   m(2) = m2m9/ratio29;
   m(3) = 0.08;
   m(4) = m4m5/ratio4567;
   m(5) = m4m5/ratio4567*(ratio4567-1);
   m(6) = m4m5/ratio4567;
   m(7) = m4m5/ratio4567*(ratio4567-1);
   m(8) = m1m8/ratio18*(ratio18-1);
   m(9) = m2m9/ratio29*(ratio29-1);
   m(10) = 100;

elseif internode == '6'
   %internode 6
   %internode 6 totals
   m1m8 = 6;
   m2m9 = 15;
   m4m5 = 128;
   m6m7 = 128;
```

```
    m(1) = m1m8/ratio18;
    m(2) = m2m9/ratio29;
    m(3) = 0.05;
    m(4) = m4m5/ratio4567;
    m(5) = m4m5/ratio4567*(ratio4567-1);
    m(6) = m4m5/ratio4567;
    m(7) = m4m5/ratio4567*(ratio4567-1);
    m(8) = m1m8/ratio18*(ratio18-1);
    m(9) = m2m9/ratio29*(ratio29-1);
    m(10) = 100;

end
```

activities.m

```
function activities(internode,label)
% function activities(internode,label)
% file activities.m
% initialisation total label per pool

%declare global variables
global expdata;

if internode == '3' & label == 'Glc'
    %internode 3 glucose [Glc Fru Suc Tot_out]
    expdata = [0          0         0         0    ,
        500.261   270.833   3275.78   19776.1 ,
        1000.521  541.6667  6551.563  39552.28,
        1115.1    611.719   11046.9   69509   ,
        1229.688  681.7708  15542.19  99465.67];

elseif internode == '3' & label == 'Fru'
    %internode 3 fructose [Glc Fru Suc Tot_out]
    expdata = [0          0         0         0   ,
        117.448   344.792   2249.48   11893.3,
        234.8958  689.5833  4498.958  23786.66,
        342.708   1106.51   6382.03   36042.8,
        450.5208  1523.438  8265.104  48298.94];

elseif internode == '6' & label == 'Glc'
    %internode 6 glucose [Glc Fru Suc Tot_out]
    expdata = [0          0       0         0    ,
        650         5E-10   845       7500    ,
        1314.583    1E-9    1689.063  15152.95,
        1595        1.5E-9  2190      18939   ,
        1876.042    2E-9    2960.417  22726.86];

elseif internode == '6' & label == 'Fru'
    %internode 6 fructose [Glc Fru Suc Tot_out]
    expdata = [0          0         0         0    ,
        5E-10     653       432       4283    ,
        1E-9      1307.813  864.5833  8566.776,
        1.5E-9    1459      989       9674    ,
        2E-9      1611.458  1113.021  10782.6];
end
```

modelmmatrix.m

```
function dy = modelmmatrix(t,y)
% function modelmmatrix(t,y)
% file modelmmatrix.m
% the function called by the numerical integrator which describes the
% change in specific activities of metabolic pools in the system

%global variables
global Am F E m;

%initialise the change in specific activity vector
dy = zeros(10,1);
%differential equations for specific activities
%fluxes into each compartment by: Am*y + F.*E
%the fluxes out of each compartment: - sum(Am)'.*y)
dy = (Am*y-sum(Am)'.*y+F.*E)./m;
```

stat.m

```
function fx = stat(y)
% function stat(y)
% file stat.m
% the main error function, calculates the sum of the squares of the
deviation
% from the experimental data

%declare global variables
global m;
global expdata;
global mdat;

%Glucose (y1 and y8)
g1 = m(1)*y(:,1)+m(8)*y(:,8);
%Fructose (y2 and y9)
f1 = m(2)*y(:,2)+m(9)*y(:,9);
%Sucrose (y4,y6 and y5,y7)
s1 = m(4)*y(:,4)+m(5)*y(:,5)+m(6)*y(:,6)+m(7)*y(:,7);
%Total Out (y3 and y10)
t1 = m(3)*y(:,3)+m(10)*y(:,10);

%TOTAL MODEL
Yt = [g1;f1;s1;t1];
mdat = [g1 f1 s1 t1];
%output all of the single pool data as well
%mdat = [g1 f1 s1 t1 m(1)*y(:,1) m(8)*y(:,8) m(2)*y(:,2) m(9)*y(:,9)
m(4)*y(:,4) m(5)*y(:,5) m(6)*y(:,6) m(7)*y(:,7) m(3)*y(:,3)];

%set the normalisation flag
norm = 0;

if norm == 0
%-------------------------------------------------------------------------
-----
%ORIGINAL NON-NORMALISED
%-------------------------------------------------------------------------
-----

% Residuals. The deviation between data and models. Now unweighted.
%TOTAL MODEL
```

```
%Yt
%expdata
rx = Yt - expdata(:);

% Function value, sum of squares of deviation
fx = rx'*rx;
%-------------------------------------------------------------------------
-----

elseif norm == 1

%-------------------------------------------------------------------------
-----
%NORMALISED
%-------------------------------------------------------------------------
-----

% Residuals. The deviation between data and models. Unweighted.
%TOTAL MODEL
%Yt
%expdata
%normalise to the highest experimental data value and then muliply by 10

Yt = [g1(2);g1(3);f1(2);f1(3);s1(2);s1(3);t1(2);t1(3)];
expdataM = [expdata(2,:);expdata(3,:)];

YtN = Yt ./ expdataM(:);
expdataN = expdataM ./ expdataM;

%get the difference
rx = YtN - expdataN(:);
%multiply by a factor
rx = rx*10;

% Function value, sum of squares of deviation
fx = rx'*rx;

%-------------------------------------------------------------------------
-----

elseif norm == 2
%-------------------------------------------------------------------------
-----
%WEIGHTED TOTAL OUTPUT TO IMPROVE I6 PERFORMANCE
%-------------------------------------------------------------------------
-----

% Residuals. The deviation between data and models. Now unweighted.
%TOTAL MODEL
%Yt
%expdata

%weight the data
Yt(7:9) = Yt(7:9)*1000;
expdata(:,3) = expdata(:,3)*1000;
Yt(10:12) = Yt(10:12)*1000;
expdata(:,4) = expdata(:,4)*1000;

rx = Yt - expdata(:);

% Function value, sum of squares of deviation
```

```
fx = rx'*rx;

%-------------------------------------------------------------------------
-----
end
```

result_out.m

```
function result_out(Am,F)
% function result_out
% file result_out.m
% function that outputs all of the simulation data to file

global FID;

%output data to file
fprintf(FID,'%-17.10g ,',Am(3,1));
fprintf(FID,'%-17.10g ,',Am(8,1));
fprintf(FID,'%-17.10g ,',Am(3,2));
fprintf(FID,'%-17.10g ,',Am(4,2));
fprintf(FID,'%-17.10g ,',Am(9,2));
fprintf(FID,'%-17.10g ,',Am(4,3));
fprintf(FID,'%-17.10g ,',Am(6,3));
fprintf(FID,'%-17.10g ,',Am(10,3));
fprintf(FID,'%-17.10g ,',Am(2,4));
fprintf(FID,'%-17.10g ,',Am(5,4));
fprintf(FID,'%-17.10g ,',Am(9,5));
fprintf(FID,'%-17.10g ,',Am(1,6));
fprintf(FID,'%-17.10g ,',Am(3,6));
fprintf(FID,'%-17.10g ,',Am(7,6));
fprintf(FID,'%-17.10g ,',Am(8,7));
fprintf(FID,'%-17.10g ,',Am(1,8));
fprintf(FID,'%-17.10g ,',Am(2,9));
fprintf(FID,'%-17.10g ,',F(1));
fprintf(FID,'%-17.10g ,',F(2));
```

simout.m

```
function simout(internode,label,simcnt,row,iters)
%simout.m
%output the simulation points for selected f parameter sets

%dbstop 39

%define global variables
global F;
global Am;
global m;
global E;
global y;
global expdata;

%initialise matrices and vectors
Am = zeros(10);
F = zeros(10,1);
E = zeros(10,1);
m = zeros(10,1);

%open a file to read in the f parameters
```

```
%convert the values to strings
striters = int2str(iters);

optype = [striters];
main = [internode '_' optype];
extension = '.csv';
filename = [main extension]
filename2 = [main '_res.csv']

%open a file as write text for output from stat
[FID, MESSAGE] = fopen(filename2,'wt')

if internode == '3'

   %read a file saved in csv format
   RNG = [1 0 1 25]

   A = dlmread(filename,',',1,0,RNG)

   %assign the independent variables
   x(1) = A(row,1);  %Am(3,1)
   x(2) = A(row,2);  %Am(8,1)
   x(3) = A(row,3);  %Am(3,2)
   x(4) = A(row,4);  %Am(4,2)
   x(5) = A(row,7);  %Am(6,3)
   x(6) = A(row,9);  %Am(2,4)
   x(7) = A(row,17)  %Am(2,9)

   %assign the fluxes
   Am(3,1) = A(row,1);
   Am(8,1) = A(row,2);
   Am(3,2) = A(row,3);
   Am(4,2) = A(row,4);
   Am(9,2) = A(row,5);
   Am(4,3) = A(row,6);
   Am(6,3) = A(row,7);
   Am(10,3) = A(row,8);
   Am(2,4) = A(row,9);
   Am(5,4) = A(row,10);
   Am(9,5) = A(row,11);
   Am(1,6) = A(row,12);
   Am(3,6) = A(row,13);
   Am(7,6) = A(row,14);
   Am(8,7) = A(row,15);
   Am(1,8) = A(row,16);
   Am(2,9) = A(row,17);
   F(1) = A(row,18);
   F(2) = A(row,19);

   %assign the ratios
   glcratio = 500;
   fruratio = 500;
   sucratio = 500;

   %call fluxdep to calculate the dependent parameters
   %fluxdep(x,internode);
   %Am

elseif internode =='6'

   %read a file saved in csv format
```

```
    RNG = [1 0 1 23]
    A = dlmread(filename,',',1,0,RNG)

    %assign the independent variables
    x(1) = A(row,6);
    x(2) = A(row,21);
    x(3) = A(row,22);
    x(4) = A(row,23);

    %assign the fluxes
    Am(3,1) = A(row,1);
    Am(8,1) = A(row,2);
    Am(3,2) = A(row,3);
    Am(4,2) = A(row,4);
    Am(9,2) = A(row,5);
    Am(4,3) = A(row,6);
    Am(6,3) = A(row,7);
    Am(10,3) = A(row,8);
    Am(2,4) = A(row,9);
    Am(5,4) = A(row,10);
    Am(9,5) = A(row,11);
    Am(1,6) = A(row,12);
    Am(3,6) = A(row,13);
    Am(7,6) = A(row,14);
    Am(8,7) = A(row,15);
    Am(1,8) = A(row,16);
    Am(2,9) = A(row,17);
    F(1) = A(row,18);
    F(2) = A(row,19);

    %assign the ratios
    glcratio = A(row,21);
    fruratio = A(row,22);
    sucratio = A(row,23);
end

%set up the input data arrays
pool_size(internode,glcratio,fruratio,sucratio);
activities(internode,label);
ext_activities(label);

%call the function that outputs the interesting flux ratios and
differences
modelstatout(x,internode,Am,FID,glcratio,fruratio,sucratio);

%output time points
tspan = [0 15 30 45 60 75 90 105 120];

%vector of initial conditions
y0 = [0 0 0 0 0 0 0 0 0];

%call the ode solver with the differential equations defined in modelm.m
[t,y] = ode45('modelmmatrix',tspan,y0);
%plot(t,y)

%initialise the time point variable
tm = 0;

%calculate the specific activities of the pools
%Glucose (y1 and y8)
sg1 = (m(1)*y(:,1)+m(8)*y(:,8))/(m(1)+m(8));
```

```
%Fructose (y2 and y9)
sf1 = (m(2)*y(:,2)+m(9)*y(:,9))/(m(2)+m(9));
%Sucrose (y4,y6 and y5,y7)
ss1 = (m(4)*y(:,4)+m(5)*y(:,5)+
m(6)*y(:,6)+m(7)*y(:,7))/(m(4)+m(5)+m(6)+m(7));
%Total Out (y3 and y10)
st1 = (m(3)*y(:,3)+m(10)*y(:,10))/(m(3)+m(10));

%output the total activities for plotting
%Glucose (y1 and y8)
g1 = m(1)*y(:,1)+m(8)*y(:,8);
%Fructose (y2 and y9)
f1 = m(2)*y(:,2)+m(9)*y(:,9);
%Sucrose (y4,y6 and y5,y7)
s1 = m(4)*y(:,4)+m(5)*y(:,5)+m(6)*y(:,6)+m(7)*y(:,7);
%Total Out (y3 and y10)
t1 = m(3)*y(:,3)+m(10)*y(:,10);

%add the activity data to an array for output, spactcall = 0
simdata1 = [g1 f1 s1 t1];
%output all of the single pool activity data as well, spactcall = 0
simdata2 = [g1 f1 s1 t1 m(1)*y(:,1) m(8)*y(:,8) m(2)*y(:,2) m(9)*y(:,9)
m(4)*y(:,4) m(5)*y(:,5) m(6)*y(:,6) m(7)*y(:,7) m(3)*y(:,3)
m(10)*y(:,10)];
%output all of the data as specific activities, spactcall = 1
simdata3 = [sg1 sf1 ss1 st1 y(:,1) y(:,8) y(:,2) y(:,9) y(:,4) y(:,5)
y(:,6) y(:,7) y(:,3) y(:,10)];
%calculate the experimental data specific activities
sexpdata = [expdata(:,1)./(m(1)+m(8)) expdata(:,2)./(m(2)+m(9))
expdata(:,3)./sum(m([4 5 6 7])) expdata(:,4)./(m(3)+m(10))];

%set the output file name
fileout = [internode '_' label '_' optype '_out' extension]

%set the data set to be used
simdataout = simdata2;
%output the sim results to a lotus file
csvwrite(fileout,simdataout)

%initialise the time vectors
xexp = [0;30;60;90;120];
xsim = transpose(tspan);
yexp = expdata;
syexp = sexpdata;
ysim = simdata1;
sysim = simdata3;

%plot each data set individually
totfig = (simcnt-1)*2+1
figure(totfig);

%initialise the label variables
xlbl='';
ylbl='';

for ncnt = 1:4
   rc=rowcol(ncnt,2,2)
   %set the label variables to be displayed for the last row and first
column
   if rc(1) == 2
      xlbl='Time (min.)';
```

```
   else
      xlbl=('');
   end
   if rc(2) == 1
      %have both label types
      ylbl = 'Activity (Bq.g^-^1 fw)';
      y2lbl = 'Sp. Act. (Bq.umol^-^1.g^-^1 fw)';
   else
      ylbl = '';
      y2lbl = '';
   end

   subplot(2,2,ncnt);
   %Plot the total activity

%plot_chart(xexp,xsim,yexp(:,ncnt),ysim(:,ncnt),char(64+ncnt),xlbl,ylbl)
;
   %Plot the specific activity

plot_chart(xexp,xsim,syexp(:,ncnt),sysim(:,ncnt),char(64+ncnt),xlbl,y2lb
l);

%plot_chartyy(xexp,xsim,yexp(:,ncnt),ysim(:,ncnt),syexp(:,ncnt),sysim(:,
ncnt),char(64+ncnt),xlbl,ylbl,y2lbl);
   set(gcf,'position',[0 0 700 500]);
end

%control the generation of the individual pool plots
ipool = 1;
if ipool == 1
   figure(totfig+1);
   %plot all of the individual pools
   for icnt = 5:14
      rc=rowcol(icnt-4,5,2);
      %set the label variables to be displayed for the last row and
first column
      if rc(1) == 5
         xlbl=('Time (min.)');
      else
         xlbl=('');
      end

      if rc(2) == 1 & rc(1) == 3
         %have both label types
         ylbl = 'Activity (Bq.g^-^1 fw)';
         y2lbl = 'Sp. Act. (Bq.umol^-^1)';
      else
         ylbl = '';
         y2lbl = '';
      end

      subplot(5,2,icnt-4);
      yexpempty = [];
      %plot_chart(xexp,xsim,yexpempty,ysim(:,icnt),char(64+icnt-
4),xlbl,ylbl);
      plot_chart(xexp,xsim,yexpempty,sysim(:,icnt),char(64+icnt-
4),xlbl,y2lbl);

%plot_chart(xexp,xsim,yexpempty,ysim(:,icnt),yexpempty,sysim(:,icnt),cha
r(64+icnt-4),xlbl,ylbl,y2lbl);
   end
```

```
   set(gcf,'position',[0 0 700 750]);
end

%close the file
ST = fclose(FID);


function rc = rowcol(pos,rows,cols)
%function that returns an array with the row and column
rc=[];
rc(1)=ceil(pos/cols);
rc(2)=pos-((rc(1)-1)*cols);


function modelstatout(x,internode,Am,FID,glcratio,fruratio,sucratio)
%function that generates model stats

global F;
global Al;
global b_L;

if internode == '3'
   %initialise the constraints used for the optimisation
   constraints(internode);
   x = transpose(x)
   %calculate the result of the matrix vector multiplication and
subtraction of the lower bound
   %Vr = Al*x-b_L

   %calculate the interesting ratios
   spssusy = Am(4,3)/Am(4,2)
   sucacc = (-x(3)-x(4)+2*x(6)+F(2))/(x(5)-2*x(6))
   synthhydrol = (Am(4,2)+Am(4,3))/(Am(3,6)+Am(1,6)+Am(9,5))
   sucacc2 = (Am(4,2)+Am(4,3))-(Am(3,6)+Am(1,6)+Am(9,5))

   %output data to file
   fprintf(FID,'VECTOR X:\n');
   fprintf(FID,'%-17.10g \n',x);
   %fprintf(FID,'VECTOR Vr:\n');
   %fprintf(FID,'%-17.10g \n',Vr);
   fprintf(FID,'SPS:SuSy \n %-17.10g \n',spssusy);
   fprintf(FID,'Suc Acc: \n %-17.10g \n',sucacc);
   fprintf(FID,'Suc Synth:Hydrol: \n %-17.10g \n',synthhydrol);
   fprintf(FID,'Suc Acc2: \n %-17.10g \n',sucacc2);
   fprintf(FID,'Glc Ratio: \n %-17.10g \n',glcratio);
   fprintf(FID,'Fru Ratio: \n %-17.10g \n',fruratio);
   fprintf(FID,'Suc Ratio: \n %-17.10g \n',sucratio);

elseif internode == '6'

   %calculate the interesting ratios
   spssusy = Am(4,3)/Am(4,2)
   sucacc = Am(4,3)
   synthhydrol = (Am(4,2)+Am(4,3))/(Am(3,6)+Am(1,6)+Am(9,5))
   sucacc2 = (Am(4,2)+Am(4,3))-(Am(3,6)+Am(1,6)+Am(9,5))

   %output data to file
   fprintf(FID,'VECTOR X:\n');
   fprintf(FID,'%-17.10g \n',x);
   fprintf(FID,'SPS:SuSy \n %-17.10g \n',spssusy);
   fprintf(FID,'Suc Acc: \n %-17.10g \n',sucacc);
```

```
    fprintf(FID,'Suc Synth:Hydrol \n %-17.10g \n',synthhydrol);
    fprintf(FID,'Suc Acc2: \n %-17.10g \n',sucacc2);
    fprintf(FID,'Glc Ratio: \n %-17.10g \n',glcratio);
    fprintf(FID,'Fru Ratio: \n %-17.10g \n',fruratio);
    fprintf(FID,'Suc Ratio: \n %-17.10g \n',sucratio);

end
```

plot_chart.m

```
function z = plot_chart(x1,x2,y1,y2,chtlabel,xlbl,ylbl)
%Plot function for chart generation
%accepts two x arrays and two multirow y arrays
%x1,y1 are experimental data
%x2,y2 are model data

%set the array of point styles
arrPts = ['*' 's' 'd' '^'];
arrLn = ['-' ':' '-.' '--'];

for i = 1:size(y1,2)
    %set the subplot
    %subplot(2,2,i);
    strPt = ['k' arrPts(i)];
    %add the experimental data set
    plot(x1,y1(:,i),strPt);
    if ishold == 0
        hold on;
    end
end
for j = 1:size(y2,2)
    %set the subplot
    %subplot(2,2,i+j);
    strPt = ['k' arrLn(j)];
    %add the model data set
    plot(x2,y2(:,j),strPt);
end

%conditional for the chart axis titles
g = 1;
if g == 1
%get the min and max of the x and y
xmin = min(x1(:));
xmax = max(x1(:));
y1min = min(y1(:));
y1max = max(y1(:));
y2min = min(y2(:));
y2max = max(y2(:));

%get the min and max of the ranges
if y1min < y2min
    ymin = y1min;
else
    ymin = y2min;
end
if y1max > y2max
    ymax = y1max;
else
    ymax = y2max;
```

```
end

%set the range to incrment or decrement as 10%
rx = xmax - xmin;
ry = ymax - ymin;
xminnew = xmin-(rx*0.1);
xmaxnew = xmax+(rx*0.1);
yminnew = ymin-(ry*0.1);
ymaxnew = ymax+(ry*0.1);

%set the axis ranges
axis([xminnew xmaxnew yminnew ymaxnew]);

%set the font properties
set(gca,'fontname','Arial');
set(gca,'fontsize',8);

%set the axis labels
xlabel(xlbl);
ylabel(ylbl);
text(xmin,ymax,chtlabel);


end

hold off;
z = 1;



function z = plot_chartyy(x1,x2,y1,y2,sy1,sy2,chtlabel,xlbl,ylbl,ylbl2)
%Plot function for chart generation
%accepts two x arrays and two multirow y arrays
%x1,y1 are experimental data
%x2,y2 are model data

%set the array of point styles
arrPts = ['*' 's' 'd' '^'];
arrLn = ['-' ':' '-.' '--'];

for i = 1:size(y1,2)
   %set the subplot
   %subplot(2,2,i);
   strPt = ['k' arrPts(i)];
   %add the experimental data set
   %plot(x1,y1(:,i),strPt);
   [xh h1 h2] = plotyy(x1,y1(:,i),x1,sy1(:,i));
   if ishold == 0
      hold on;
   end
end
for j = 1:size(y2,2)
   %set the subplot
   %subplot(2,2,i+j);
   strPt = ['k' arrLn(j)];
   %add the model data set
   %plot(x2,y2(:,j),strPt);
   [xh h1 h2] = plotyy(x2,y2(:,j),x2,sy2(:,j))
end

%get(h1,'Factory')
```

```
g = 0;
if g == 1
%get the min and max of the x and y
xmin = min(x1(:));
xmax = max(x1(:));
y1min = min(y1(:));
y1max = max(y1(:));
y2min = min(y2(:));
y2max = max(y2(:));
sy1min = min(sy1(:));
sy1max = max(sy1(:));
sy2min = min(sy2(:));
sy2max = max(sy2(:));

%get the min and max of the ranges
if y1min < y2min
   ymin = y1min;
else
   ymin = y2min;
end
if y1max > y2max
   ymax = y1max;
else
   ymax = y2max;
end

if sy1min < sy2min
   symin = sy1min;
else
   symin = sy2min;
end
if sy1max > sy2max
   symax = sy1max;
else
   symax = sy2max;
end

%set the range to incrment or decrement as 10%
rx = xmax - xmin;
ry = ymax - ymin;
xminnew = xmin-(rx*0.1);
xmaxnew = xmax+(rx*0.1);
yminnew = ymin-(ry*0.1);
ymaxnew = ymax+(ry*0.1);

%set the axis ranges
%axis([xminnew xmaxnew yminnew ymaxnew]);

%sry = symax - symin;
%syminnew = symin-(sry*0.1);
%symaxnew = symax+(sry*0.1);


%add the axis labels and text id
set(h1,'fontname','Arial');
set(h1,'fontsize',8);
set(h1,'Title',text('String',ylbl,'Color','k'))
%set(xh(I),'Title',ylbl)

xlabel(xlbl);
```

```
%ylabel(ylbl);
%text(xmin,ymax,chtlabel);

end

hold off;
z = 1;
```

solve_params.m

```
function solve_params(internode)
%mfile for the solution of the mass balance equations and other
constraints
%Z = solve('(A1,6+A1,8+F1+A1,3)-(A3,1+A8,1)',%MB1
%'(A2,4+A2,9+F2+A2,3)-(A3,2+A4,2+A9,2)',%MB2
%'(A3,1+A3,2+A3,6)-(A4,3+A6,3+A10,3+A1,3+A2,3)',%MB3

%'(A4,2+A4,3)-(A2,4+A5,4)',
%'(A5,4)-(A9,5)',
%'(A6,3)-(A1,6+A3,6+A7,6)',
%'(A7,6)-(A8,7)',
%'(A8,1+A8,7)-(A1,8)',%MB8
%'(A9,2+A9,5)-(A2,9)',%MB9



%'A9,5-A8,7',%Vacuolar Suc breakdown, hexose rates =
%'A5,4-A7,6',%Cyt to Vac Suc transport, hexose rates =
%'A6,3-(A4,3+A4,2)',%Cyt Suc synthesis SuSy & SPS rate equality
%'A2,4-(A3,6+A1,6)',%Cyt Suc breakdown SuSy & NI rate equality
%'F1=Glc IN',%Glc input rate
%'F2=Fru IN')%Fru input rate

if internode == 3
%internode three
Z = solve('l + p + r + t - (a + b) = 0',... %MB1
'i + q + s + u - (c + d + e) = 0',... %MB2
'a + c + m - (f + g + h + t + u) = 0',... %MB3
'(b + o) - p = 0',... %MB8
'(e + k) - q = 0',... %MB9
'k - o = 0',... %Vacuolar Suc breakdown, hexose rates =
'j - n = 0',... %Cyt to Vac Suc transport, hexose rates =
'g - (f + d) = 0',... %Cyt Suc synthesis SuSy & SPS rate equality
'i - (m + l) = 0',... %Cyt Suc breakdown SuSy & NI rate equality
'd + f - (i + j) - (g - (l + m + n)) = 0'    ,... %MB4 - MB6
'j - k -(n - o) = 0',... %MB5 -MB7
'r = 0.016114',... %Glc input rate
's = 0.008134') %Fru input rate

elseif internode == 6

%internode six
Z = solve('l + p + r + t  - (a + b) = 0',... %MB1
'i + q + s + u - (c + d + e) = 0',... %MB2
'a + c + m - (f + g + h + t + u) = 0',... %MB3
'(b + o) - p = 0',... %MB8
'(e + k) - q = 0',... % MB9
'k - o = 0',... %Vacuolar Suc breakdown, hexose rates =
'j - n = 0',... %Cyt to Vac Suc transport, hexose rates =
'g - (f + d) = 0',... %Cyt Suc synthesis SuSy & SPS rate equality
```

```
'i - (m + l) = 0',... %Cyt Suc breakdown SuSy & NI rate equality
'd + f - (i + j) - (g - (l + m + n)) = 0'     ,... %MB4 - MB6
'j - k -(n - o) = 0',... %MB5 - MB7
'r = 0.004095',... %Glc input rate
's = 0.002036') %Fru input rate

end

%display the results
Z.g,Z.h,Z.k,Z.l,Z.m,Z.n,Z.o,Z.p,Z.q,Z.r,Z.s,Z.t,Z.u

%verify that all of the parameters solved for are displayed
Z

%For the sucrose accumulation model these mass balances are > 0
%Also the output flux A10,3 < F1+F2
%'d + f - (i + j) = 0',... %MB4
%'j - k = 0',... %MB5
%'g - (l + m + n) = 0',... %MB6
%'n - o = 0',... %MB7
```

Publications

1. Botha, F.C., A. Whittaker, D.J. Vorster and, K.G. Black. 1996. Sucrose Accumulation Rate, Carbon Partitioning and Expression of Key Enzyme Activities in Sugarcane Stem Tissue. *In* "Sugarcane: Research Towards Efficient and Sustainable Production." Wilson, J.R. et al. (Eds). CSIRO Division of Tropical Crops and Pastures, Brisbane, 92-94.

2. Vorster, D.J. and F.C. Botha. 1997 Sugarcane internodal invertases: Changes during tissue maturation and properties of neutral invertase. International Plant Biology meeting, Vancouver, Canada. Plant Physiol. 114:82.

3. Vorster, D.J., and F.C. Botha. 1998. Partial Purification and Characterisation of Sugarcane Neutral Invertase. Phytochem. 49:651-655.

4. Vorster, D.J., and F.C. Botha. 1999. Sugarcane internodal invertases and tissue maturity. J Plant Physiol. 155:470-476.

Presentations

1. Vorster, D.J. 1996. Kinetic Constants of Sugarcane Neutral Invertase and the Possible Metabolic Implications. South African Association of Botanists 22nd Annual Congress. University of Stellenbosch, South Africa.

2. Vorster, D.J., and F.C. Botha. 1997. Sugarcane invertases (β-fructofuranosidase, E.C. 3.2.1.26): distribution in the culm, involvement in sucrose cycling, and kinetic properties of neutral invertase. Phytochemical Society of Europe International Symposium on "Regulation of Primary Metabolic Pathways in Plants", St Hugh's College, Oxford, United Kingdom.

3. Vorster, D.J., and F.C. Botha. 1997. Sugarcane Internodal Invertases: Changes During Tissue Maturation and Properties of Neutral Invertase. Plant Biology '97, Vancouver, Canada.

4. Botha, F.C., and D.J. Vorster. 1999. "Futile" cycling of carbon during sucrose accumulation in sugarcane. South African Association of Botanists 25th Annual Congress. UNITRA, Umtata, South Africa.

5. Botha, F.C., and D.J. Vorster. 1999. Analysis of carbon partitioning to identify metabolic steps limiting sucrose accumulation. International Society of Sugar Cane Technologists, XXIII ISSCT Congress. New Delhi, India.